The Institute of Paper Chemistry

Appleton, Wisconsin

Doctor's Dissertation

The Role of Polyelectrolyte Charge Density in the Mechanism of Hydrodynamic Shear-Induced Restabilization of a Flocculated Colloidal Dispersion

Martin D. Sikora

June, 1978

THE ROLE OF POLYELECTROLYTE CHARGE DENSITY IN THE MECHANISM OF HYDRODYNAMIC SHEAR-INDUCED RESTABILIZATION OF A FLOCCULATED COLLOIDAL DISPERSION

A thesis submitted by

Martin D. Sikora

B.S. 1972, Wittenberg University

M.S. 1975, Lawrence University

in partial fulfillment of the requirements
of The Institute of Paper Chemistry
for the degree of Doctor of Philosophy
from Lawrence University,
Appleton, Wisconsin

June, 1978

TABLE OF CONTENTS

SUMMARY

Previous studies have shown that the mechanism by which anionic colloidal particles are flocculated by cationic polyelectrolytes depends on the charge densities of the components. With low electrostatic interactions between colloidal particles and flocculating polymer, bridging may be the dominant mechanism of destabilization. Polyion patches have been suggested to play an important role in the flocculation of colloids which form strong electrostatic interactions with oppositely charged polymers.

It was the intent of this investigation to elucidate the mechanisms involved in the mechanical degradation of aggregates of colloidal polystyrene latices (PSL) formed with optimum flocculation concentrations of polyvinylamine (PVAm) of various charge densities in water. The investigation was conducted by monitoring both molecular weight distributions of the PVAm and the available anionic surface sites of the PSL.

Potentiometric titrations were used to determine that the charge density of PSL remains constant above pH 2, while the charge density of PVAm decreases with increasing pH. Experiments were conducted at pH's 3, 9, and 10 to provide evidence for flocs formed by patches, some intermediate mechanism, and bridges, respectively.

Together, the investigation of molecular weight distributions of PVAm after hydrodynamic shear and measurements of available anionic surface sites on PSL under various conditions provide strong evidence for describing how the flocs are constructed with PVAm at different charge densities.

At pH 10 about 3% of the available nitrogens on PVAm are protonated. Flocculation most likely occurs by polymeric bridging, with the adsorbed configuration of PVAm resembling that of the unadsorbed molecule in solution. Subjecting these flocs to hydrodynamic shear produced extensive molecular

degradation of PVAm, as would be expected if the polymer were adsorbed in an extended, bridgelike configuration. Restabilization of the colloid occurred with shearing; reaggregation of these particles was slow and incomplete when compared to the initial process. In addition to degradation of the flocculating polymer, separation occurred at the polyion-particle interface.

At pH 3 nearly all of the nitrogens on PVAm have been protonated, providing a strong electrostatic interaction with anionic PSL surfaces. The solution configuration of PVAm is very extended, while the adsorbed configuration is that of a flat electrostatic patch with a high positive charge. The extension of the polyion between negative charges on the PSL surface was found to be very close to the theoretical minimum predicted from average bond lengths. Subjecting these flocs to sufficient hydrodynamic shear causes PSL resuspension to some extent, but reflocculation occurs more quickly and as completely as initial aggregation. There is no molecular degradation of PVAm when adsorbed, as would be expected from a flat patchlike configuration. Monitoring available PSL surface sites indicated that floc disruption must occur only by polyion-particle separation.

At pH 9 only 13% of the nitrogens of PVAm are protonated, but the adsorption configuration is still very much characteristic of an electrostatic patch. Loops on the PSL surface are again only as large as the theoretical minimum size necessary to associate with PSL negative site spacings on two particles. While larger than the polyion loops at pH 3, loop size at pH 9 is still only a fraction of the thickness of the particle's double layer. While the flexibility of the uncharged portion of the PVAm chain lends itself to deformation by external hydrodynamic forces, no molecular degradation takes place while in an adsorbed configuration. Resuspension of the PSL occurs as the result of hydrodynamic shear, but reflocculation does take place. Floc disruption is proposed to occur only by polyion-particle separation.

INTRODUCTION

The use of polyelectrolytes in the flocculation of colloidal dispersions has been growing in industrial application since a dewatering process for Florida phosphate rock slimes was investigated by the Atomic Energy Commission between 1950 and 1956. Cationic polyelectrolytes are now extensively employed in water clarification, sewage treatment, sugar purification, industrial ore recovery, and paper manufacturing.

Papermakers utilize cationic polyelectrolytes of various molecular weights and molecular structures to improve retention, drainage rates, sheet strength, chemical recovery, and effluent clarification. Volumes of work have been published in attempts to improve the understanding of the phenomena of colloid stability and polymer-colloid interactions. Several workers (1-9) noted that degradation of flocs produced by polymers often occurs when flocs are subjected to high rates of shear. It is now well-known that under certain conditions these flocs will reform if the shearing is reduced or stopped, while in other instances the colloidal system will be essentially restabilized. While documentation of these phenomena is abundant, the actual mechanisms involved in either restabilization or reflocculation have not yet been investigated.

The mechanism of aggregation of negatively charged particles by cationic polymers has been the focal point of a great deal of research. From such work, three major postulates have emerged to explain the phenomena: (1) Charge neutralization by inorganic electrolytes and low molecular weight polymers, (2) bridging by high molecular weight polymers, and (3) electrostatic patch formation by polymers with high charge densities. The applicability of each postulate varies with differences in ionic strength, effective electrolyte concentration, polymer molecular weight, and polymer molecular structure. LaMer

and Healy (10) distinguish mechanisms involving charge neutralization from those involving polymeric bridging, labeling the former as coagulation and the latter as flocculation. Kasper (11) has proposed an electrostatic patch mechanism in lieu of the polymer bridging theory for systems of oppositely charged components. The work of Lindquist (12) suggests that the mechanism of destabilization is dependent on the charge densities of the components of the system.

The actual manner in which aggregation takes place most likely plays a dominant role in the strength of the floc. The mechanism of formation would therefore be expected to be of direct consequence to the mechanism of aggregate degradation in a shear field, and thus have an effect on system restabilization. In the same manner, a study of aggregate degradation in a shear field should yield some insight into the preferred mechanism of aggregation of a given system. Such knowledge would be useful in optimization of systems designs and polymer usage.

THEORETICAL CONSIDERATIONS

To investigate a problem concerned with the hydrodynamic restabilization of a flocculated colloidal dispersion and the role played by polyelectrolyte charge density, it is necessary to understand the concepts involved with colloid stability, the manner in which the charge density of polyelectrolyte may affect colloid destabilization, and the behavior of various particles in a medium subjected to fluid flow.

COLLOID STABILITY

The dispersed state of a solid colloidal suspension is characterized by large free surface energies. The lower total free energy of the aggregated state thus dictates that such a colloidal dispersion should coagulate. Systems which resist this tendency to coagulate are composed of particles held apart by one or more of the following phenomena: (1) electrostatic repulsion barriers between the double layers of two similarly charged particles, (2) steric stabilization, and (3) hydration of the particle surface, which physically hinders approach. Because the adsorbed layer of water on a hydrated surface is only a few molecules thick (13), minimizing the distance of closest approach is probably important only when extremely short-range particle interactions are to be considered. For the particles to remain in at least a metastable dispersed state then, they must be sterically stabilized, or the electrostatic repulsive barrier between particles must be large compared to the total free energy of the particles.

Electrical charges may develop in essentially three ways on solid surfaces in contact with a liquid: (1) direct ionization of the substance, (2) preferential adsorption of a particular type of ion, or (3) isomorphous lattice substitution. The acquisition of charge produces an electrical double layer about all such charged surfaces.

Historical development of the electrical double-layer theory has been presented by many, including Delahay (14) and Matijevic (15), and no attempt will be made here to reiterate. The Gouy-Chapman-Stern model of the double layer consists of an inner layer of hydrated ions (Stern layer) and a diffuse layer of counterions (Gouy-Chapman layer). Figure 1 is an illustration of the Gouy-Chapman-Stern model of the double layer. The ions in the Stern layer are very strongly adsorbed and considered to be immobile. The mobile ions of the diffuse layer are distributed according to the sum of their characteristic thermal energy and their electrostatic attraction to the surface. The resulting reduction in net charge away from the surface causes the electrical potential to decrease exponentially with increasing distance from the surface of the particle. The outer boundary of the diffuse layer exists at the region in which ionic electroneutrality is reestablished. The potential at the hydrodynamic plane of shear is commonly referred to as the zeta-potential, ζ. Its value is equal to or slightly less than the potential at the Stern layer.

The direct consequence of the electrical double layer is an energy barrier that must be overcome before two particles can collide. The interaction energies between charged particles in aqueous solution are described by the Derjaguin-Landau, Verwey-Overbeek (DLVO) theory of colloid stability. A detailed discussion of the DLVO theory may be found in presentations by Verwey and Overbeek (16), Derjaguin and Landau (17), or Adamson (18).

The thickness of the double layer may be approximated as the reciprocal of the Debye-Huckel parameter, κ,

$$\kappa = eZ \sqrt{(8\pi n)/(\varepsilon kT)} , \qquad (1)$$

where e = elementary charge

Z = valence of the ions

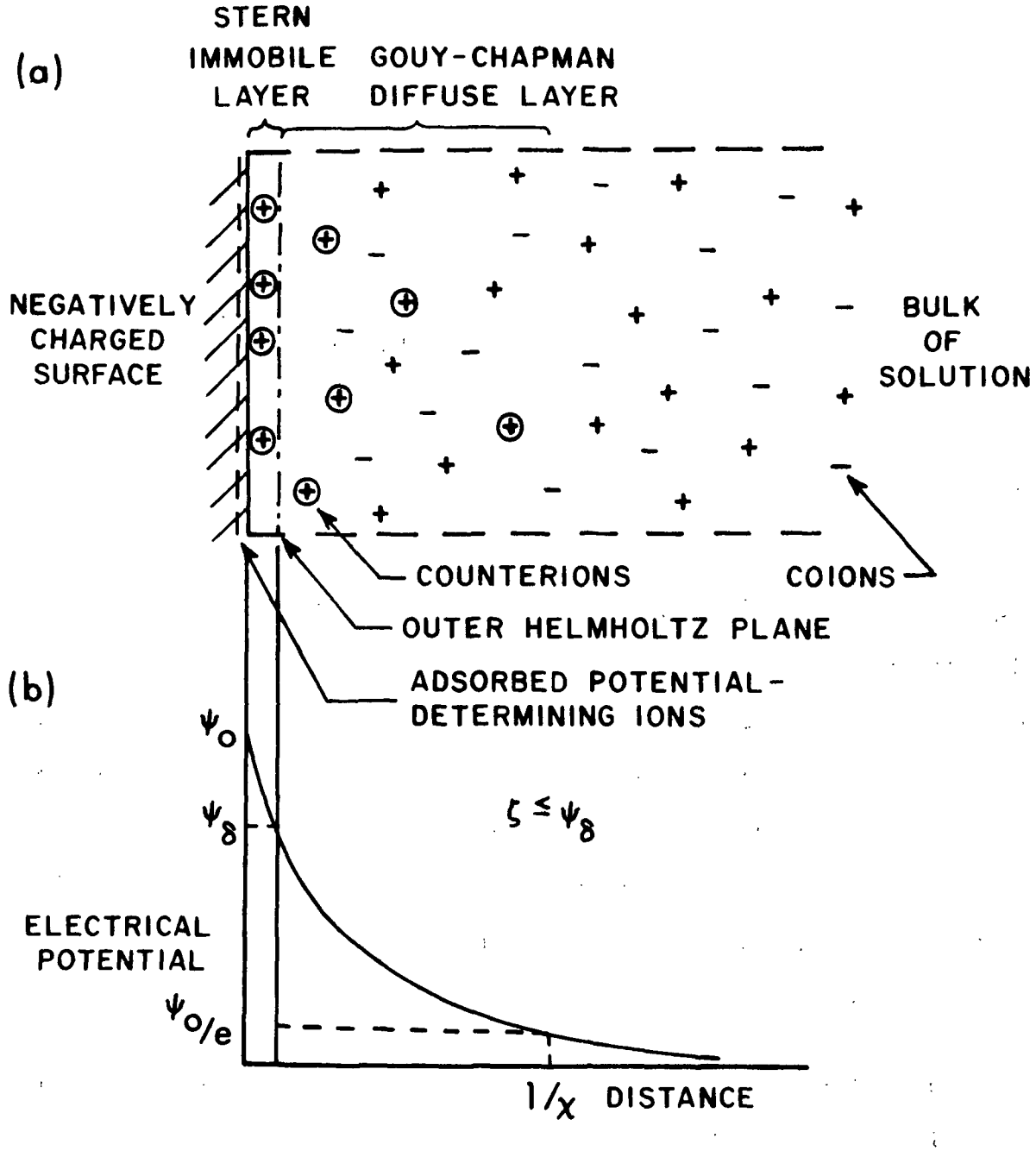

Figure 1. (a) Model of the Electric Double Layer. The Marked Counterions represent the Ions in Excess Compared to the Bulk Phase.
(b) Potential Distribution in the Electric Double Layer

n = solution ion concentration (ions/mL)

ε = dielectric constant of the bulk solution (farads/cm)

k = Boltzmann constant

T = absolute temperature

For the special case of a 1:1 electrolyte in aqueous solution at 25°C,

$$\kappa = (3.27 \times 10^7) \sqrt{C} \ \text{cm}^{-1}, \tag{2}$$

where C is the solution ion concentration in moles per liter.

The DLVO theory states that the total interaction energy between two colloidal particles is equal to the sum of the energy of repulsion and the attractive energy:

$$V_T = V_A + V_R \tag{3}$$

Figure 2 illustrates the dependence of the total interaction energy on the distance between particles for stable sols, slowly and rapidly coagulating sols. Brownian motion imparts an average energy of 3/2 kT to collidal particles. Since coagulation is prevented only if the repulsive barriers are insurmountable by all particles, interaction barriers of several kT are necessary to insure suspension stability. A barrier of 10 kT is usually sufficient to provide enough stability to prevent detectable coagulation for a period of several years (16).

While attractive energies remain constant with variations of solution composition and particle surface potential, repulsive forces can be regulated by both factors. The addition of electrolyte causes a compression of the diffuse layer and subsequent shifting of counterions from the diffuse layer to the Stern layer. This increased concentration of ions in the Stern layer

reduces the Stern potential and thus the height of the energy barrier. The attractive forces between particles may then operate to aggregate the system.

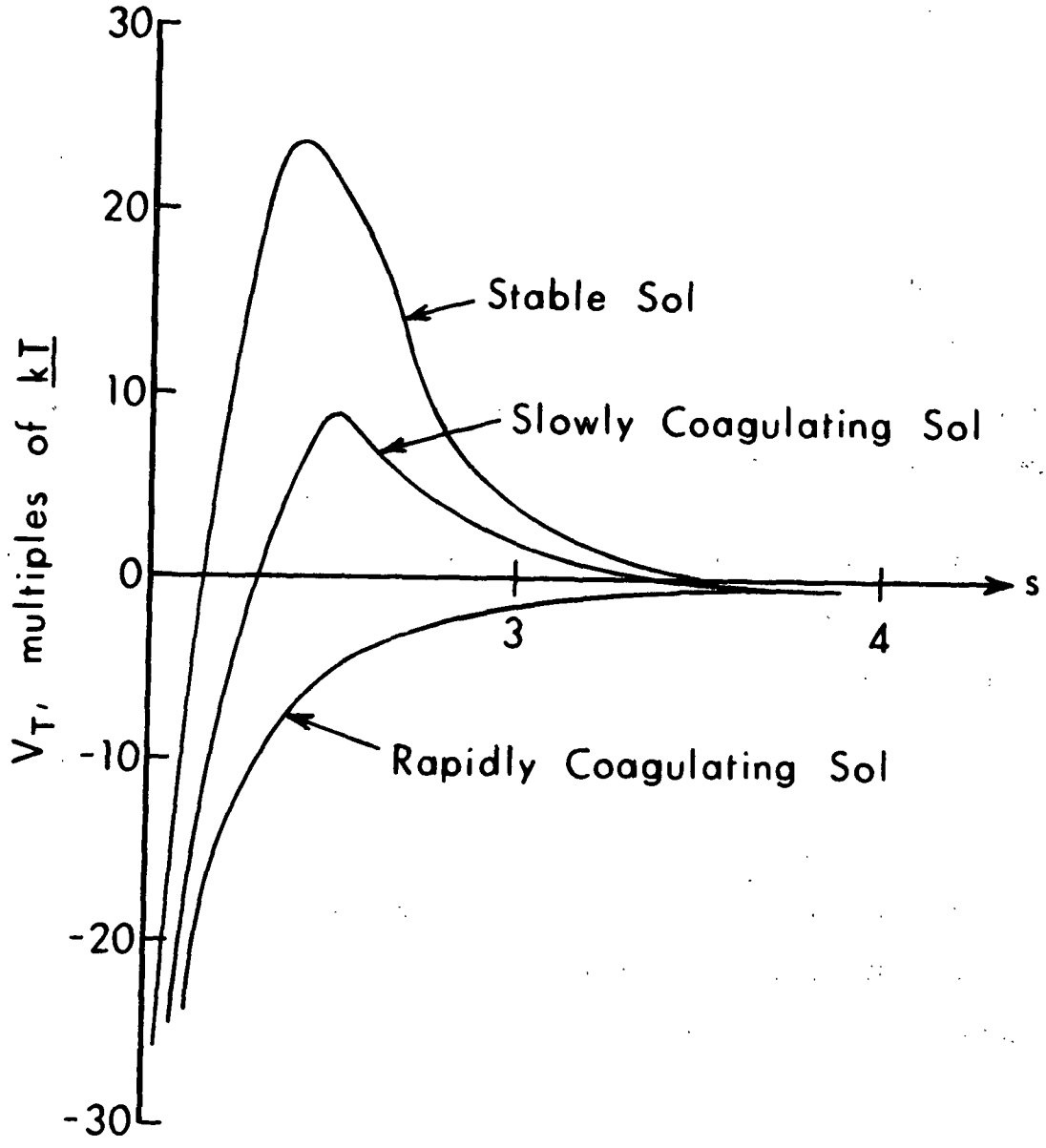

Figure 2. Total Potential Energy of Interaction Versus Unitless Distance

POLYELECTROLYTES IN SOLUTION

Polyelectrolytes are generally defined as macromolecular substances carrying a large number of ionic charges. The properties of aqueous solutions of polyelectrolytes are obviously affected by the addition of simple salts, which increases the counterion concentration.

The degree of ionization, α, is the fraction of ionizable groups which are dissociated. It is determined by the ionization constant of the individual functional groups, the dielectric constant of the solvent, and the electrostatic free energy of the molecule. The charge density of the polyelectrolyte is usually expressed as the number of ionized groups per monomer unit, and is synonymous with α if such a group exists on each repeating unit.

The radius of gyration, $\langle \underline{s}^2 \rangle^{\frac{1}{2}}$, of a macromolecule is defined as the root-mean-square distance between a segment and the center of mass. From random-flight statistics,

$$\langle s^2 \rangle = 1/6 \langle r^2 \rangle, \tag{4}$$

where $\langle \underline{r}^2 \rangle^{\frac{1}{2}}$ is the root-mean-square end-to-end displacement of the chain. When ionized groups are attached to chain segments of the macromolecule, the electrostatic forces between the charges are much larger than the London dispersion forces or the dipole-dipole interactions between uncharged groups. Because these forces act over relatively long distances, the freedom of movement of neighboring segments becomes restricted. Random flight statistical applications are no longer valid. All configurations compatible with its bond flexibility are still possible, but the repulsive interactions between charges cause the free energy to vary for different configurations. Configurations which place large numbers of charges close to one another will have a much smaller statistical weight than extended configurations which tend to maximize

the distance between charges. Lifson and Katchalsky (19) have used a calculation of the electrostatic free energy of rodlike, ionized polyelectrolyte molecules in salt-free solutions to deduce that

$$G_{el}(r) = Q^2/\epsilon r \ln [1 + 6r/\kappa \langle r_0^2 \rangle] \quad (5)$$

where $G_{el}(r)$ is the electrostatic free energy, Q is the total charge of the polyion, equal to the product of the number of ionized groups and e. In a solution having a high dielectric constant, then, polyelectrolytes will favor an extended configuration.

The magnitude of the extension is dependent on the effective charge density of the polyion and the ionic strength of the solution. This dependence is the result of a diffuse layer of counterions around the polyion. The treatment of the double layer for polyelectrolytes is analogous to that invoked for colloidal particles (16). The counterions produce a shielding effect which reduces the effective range of the repulsive interactions between neighboring charged segments. Contractile forces arise from segmental Brownian elasticity and hydrophobic interactions. As long as the ionization repulsive field is insufficient to overcome the major part of the intramolecular hydrophobic forces, the molecule will remain in a coiled state. Katchalsky (20) has shown that not until about 10% ionization do most molecules begin to open up, with the stretching of the chain then closely following the increase in α.

The intrinsic viscosity, $[\eta]$, of solvated molecules is often employed to estimate dimensions of a macromolecular coil. The most important factors to consider are the extent to which the molecular coil is permeated by the fluid and the extent to which the coil is being deformed by the velocity gradient.

The best estimation of this relationship available to date is provided by Flory (21), and Flory and Fox (22). Substituting a hydrodynamically equivalent sphere of molar volume V and radius R for the polymer coil, it was predicted that

$$[\eta] = 5V/2M = \frac{\phi \langle s^2 \rangle^{3/2}}{M}, \qquad (6)$$

where M is the molecular weight and ϕ was proposed to be a universal constant independent of the nature of the molecule and solvent. Emperically, the value of ϕ was found to be 3.67×10^{22}.

Krigbaum and Carpenter (23) compared intrinsic viscosities to the radius of gyration obtained from light scattering, and showed that the ratio of the radius of the hydrodynamically equivalent sphere to the radius of gyration of the coil tends to decrease with an increase in the excluded volume effect.

MECHANISMS OF FLOCCULATION

The aggregation of suspended particles is dependent on two separable phenomena: (1) the transport of particles to the proximity of other particles, and (2) the permanent joining of the particles. Particles are transported by velocity gradients in the solution (orthokinetic motion) and by Brownian movement (perikinetic motion). The magnitude of the velocity gradient, particle size, particle concentration, and temperature are the major influences on the rate of collision. Destabilization, viz., successful sticking together, is affected by the chemical and electrical parameters of the system that have been previously discussed.

A thorough review of the literature on flocculation has been conducted by others (10-12) and will not be presented here. The actual mechanisms of destabilization are classically divided into three categories: charge neutralization, polymer bridging, and electrostatic patch formation.

CHARGE NEUTRALIZATION

The addition of electrolyte to a colloidal suspension causes a compression of the diffuse layer and subsequent shifting of counterions from the diffuse layer to the Stern layer. This increased concentration of ions in the Stern layer lowers the Stern potential. As the height of the repulsive energy barrier is reduced, the attractive forces between particles can operate to aggregate the system.

The Schulze-Hardy Rule (24,25) predicts that in systems of simple non-adsorbable ions the coagulation ability of an ionic species should vary as the inverse sixth power of its charge. Although the assumptions that are made to arrive at the inverse sixth power rule are not applicable in real systems containing adsorbable counterionic species (26) there is a good deal of evidence that a linear relationship exists between the logarithm of the critical coagulation concentration value and the corresponding charge of the ionic species (12,26,27).

POLYMER BRIDGING

The bridging mechanism of colloidal aggregation, first postulated by Ruehrwein and Ward (28), has become a widely accepted explanation for flocculation of colloidal particles by high molecular weight polymers. LaMer, et al. (10,29-32) suggest that the polymer molecules adsorb on the particle surface at one or more sites, leaving segments extending out into the bulk solution. These extended segments are then free to adsorb onto another particle surface with vacant adsorption sites, producing a three-dimensional network. The network size will be affected by the shear gradient resulting from imposed system agitation and by the amount of polymer initially adsorbed on the particle surface.

The bridging theory is based on interactions between colloid particles and polymer in which chemical and electrostatic interactions have been ignored. Slater and Kitchener (33) have listed the following evidence in support of bridging:

(1) Polymers produce larger, "tougher" flocs than do simple electrolyte coagulants.

(2) Effectiveness of polymers of a given chemical type increases greatly with increasing molecular weight.

(3) Highly branched macromolecules are less effective than linear polymers of the same molecular weight and chemical type.

It is obvious that the feasibility of bridging is determined by the configuration of the polymer after adsorption on the particle surface has taken place. Loops and dangling ends of the polymer are capable of adsorbing on another particle only if they are longer than the average distance of closest approach of the particles. The distance of closest approach, in turn, depends on the thickness of the diffuse layer around each particle. The configuration of the adsorbed polymer will be greatly affected by the ratio of polymer size to particle size and the interaction energy between particle surface and polymer.

Lindquist (12) concluded that for systems having moderately low charges, the dominant flocculating mechanism was polymer bridging, but that in highly charged systems the electrostatic patch mechanism predominated.

ELECTROSTATIC PATCH FORMATION

The electrostatic patch mechanism for polymer flocculation was first proposed by Kasper (11). He theorized that when the interaction forces between

colloid and polyion are large, the polyelectrolyte molecules adsorb in the form of patches on the adsorption surface.

The average spacing of charges on most particulate matter found in natural aqueous suspensions is not always similar to the ionic spacing found on typical polyelectrolytes used as flocculating aids. One-to-one association between the ionized groups of the cationic polyelectrolyte and the anionic charge sites on the adsorbent does not necessarily occur. The result of the difference in charge densities is that the polyelectrolyte patch on the negatively charged particle has a net positive charge. The size of the patch depends on the molecular weight of the macromolecule and on the solution composition.

In the proposed model it was assumed that the actual distances between patches are normally distributed about some average value. This assumption is based on the fact that between like-charged patches electrostatic repulsion causes some degree of symmetry in distribution.

The effects of polyelectrolyte molecular weight and solution ionic strength on the amount of polymer required for flocculation have been mathematically modeled by Kasper. A comparison of his experimental data and the predictions of the model is shown in Fig. 3.

In the proposed patch model, particle aggregation is attributed to electrostatic attractions between positively charged polymer patches and negatively charged surfaces of other particles. For aggregation to occur, the total net charge of the particle need not be zero because the net interaction force is weighted heavily by the localized "patch" charges. The fact that particle mobility need not be zero for flocculation to occur has been shown experimentally (9,34-36).

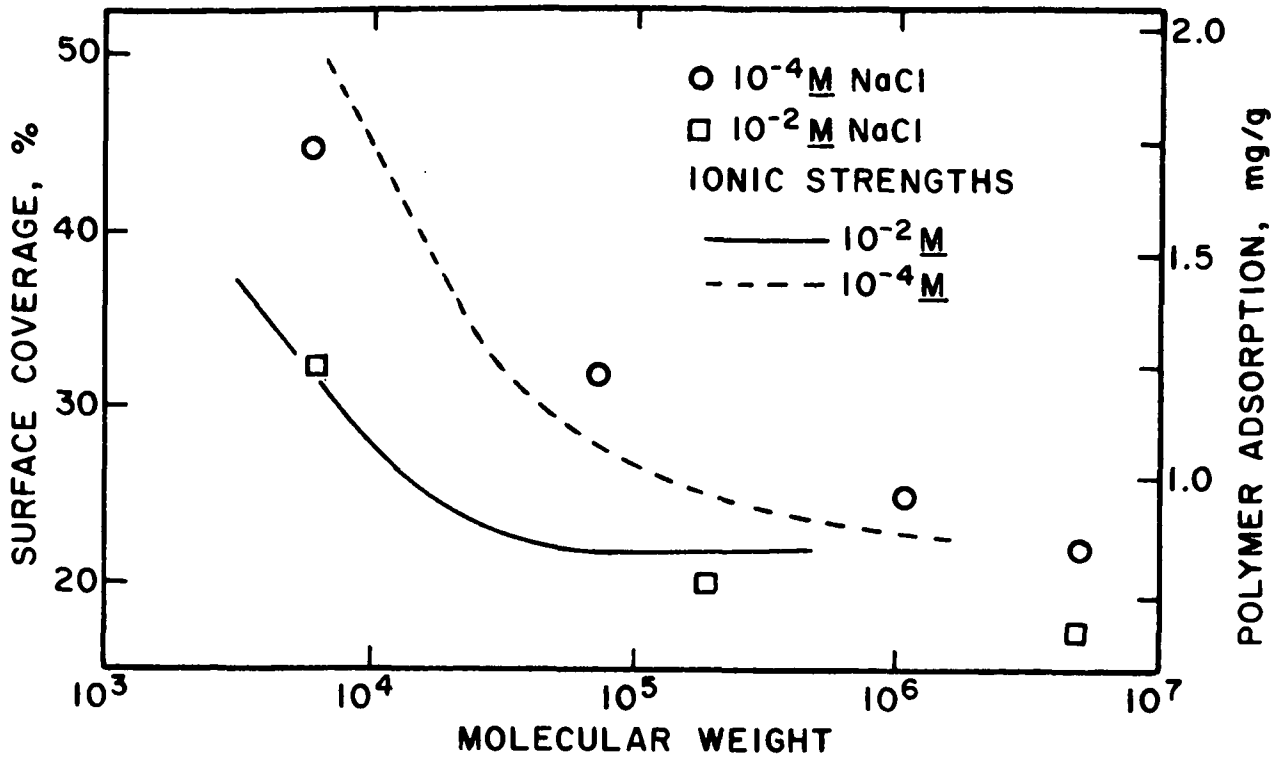

Figure 3. Comparison of PSL Experimental Optimum Flocculation Density Surface Coverage Data (Points) with Theoretical Patch Model Results (Solid and Dashed Lines) (11)

Evidence supporting Kasper's theory has been presented by Lindquist (12), Gregory (37,38), and Eggert (39).

RESPONSE OF AGGREGATES TO FLUID FLOW

The shear-induced degradation of a floc, consisting of both lyophobic particles and soluble polymer, occurs when the hydrodynamic forces acting on the aggregate overcome the mechanical strength of the floc. A purpose of this thesis was to quantify the relative importance of polymer-particle adhesion and polymer intramolecular bond strength.

Published work that is relevant to this topic can be categorized in the following manner:

a) Research related to the study of forces exerted by a shear field on suspended particles. Most of this work has been devoted to the imposed stresses and resulting motions of individual particles of well defined shapes.

b) Research related to the mechanical degradation of macromolecules by shear fields.

Of primary importance is the perception of the motion of particles suspended in a liquid medium in laminar flow. The second area of intrinsic significance is that of the mechanical degradation of macromolecules. By combining the fundamental concepts from each of these areas, conceptualization of the phenomena involved in floc degradation should be possible.

PARTICLE MOTIONS

Einstein was the first to use theoretical hydrodynamics to describe the flow-behavior of suspensions (40). His papers, involving the determination of the viscosity of a suspension of nonattracting rigid spheres of uniform size, gave rise to many experimental researches on the viscosity of fluids containing solid particles. Theoretical investigations at this time revolved around the solution of the equations of motion for the fluid around the particles.

The motion of the particle itself in a moving suspension was first investigated by Jeffrey (41). His treatment considered the motion of an ellipsoid, and the corresponding equations for the torque acting on the particle suspended in a liquid undergoing flow with arbitrary components of rotation and dilatation. Jeffrey's work revealed two specific tendencies concerning the forces acting on the particle as a whole. One effect was that the particle tends to adopt the same rotation as the surrounding fluid. The other tendency of the particle is to align with its axes parallel to the principal axes of distortion of the surrounding fluid. Experimental validation of Jeffrey's theories has been supplied by Taylor (42) and Eirich, et al. (43), among others.

At approximately this same time, Bairstow, et al. (44) made an initial attempt at a theoretical calculation of the resistance of a cylinder moving through a viscous fluid. Because it had been shown by Stokes (45) that the solution to even the most simple case (that of a circular right cylinder moving with uniform velocity in a two-dimensional field) was impossible when terms describing the inertia are omitted from the calculations, the calculations of Bairstow, et al. were the first to actually include estimations of the inertial effects in their calculations.

It should be noted that all the work to this point had started with the assumption of rigid particles. Taylor (46) deviated from this custom by describing the theoretical viscosity of a fluid containing small drops of another fluid. As his calculations allowed for some deformation of the particle, they were understandably much more complex than others to that point.

In 1926 Stimson and Jeffrey (47) discussed the motion of two spheres in a viscous fluid. The prominent outcome of this work was the determination of the forces necessary to maintain the motion of the spheres when moving with equally small, constant velocities parallel to their lines of center.

Eisenschitz (48) produced a purely hydrodynamic treatment of a modification of Einstein's work for the case of ellipsoidal particles. However, in this treatment, he became the first to consider the effects of an overwhelmingly intense Brownian motion. Because shear rates were low, the effect of this incorporation proved to be a tendency for the particles to assume a random orientation. This, of course, was contrary to the tendency of the particles to adopt those motions which, of all motions possible under the approximated equations used, corresponded to the least dissipation of energy. Guth (49) considered in greater detail the problem of the superposition of

the hydrodynamic orientating and the Brownian distorting effects. Unfortunately, his efforts also did not produce an exact solution to the problem. A thorough discussion of this problem has been presented by Sadron (50). His review includes an analysis of pertinent experimental data. As it turns out, the relative dominance of one contrary effect over the other depends on particle size, shape, the shear rate, and the temperature.

Although most of the reported work on particle behavior has been done with particles of well-defined geometry, which are rarely encountered in a practical system, it will be shown later that the resultant generalized conclusions are of significant value.

The possible variation in the geometry of aggregates of spherical particles is demonstrated in Fig. 4.

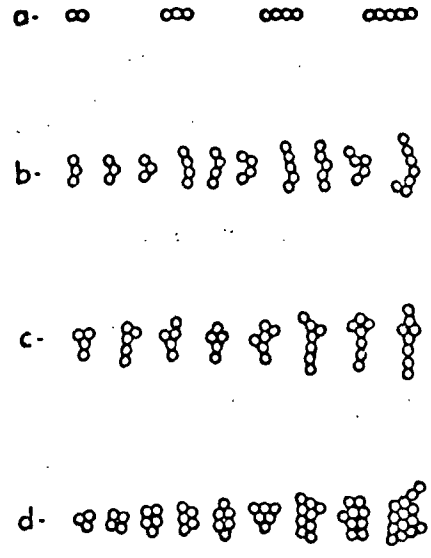

Figure 4. Photomicrographs of Polyvinyl Toluene Latex Spheres Showing Variations in the Geometry of Aggregates: (a) Straight Chains, (b) Bent Chains, (c) Branched Chains, and (d) Clusters (51)

From this evidence it becomes apparent that the most useful models to consider for the purposes of this study are the sphere, ellipse, and rod or

filament. Discussions of spheres will be omitted, as the case of a sphere can be simply obtained as the treatment of an ellipse of axis ratio $r_e = 1$. A suitable treatment of forces acting on rigid particles in Couette flow has been presented by Goldsmith and Mason (52). Portions of the following development have been paraphrased from their discussion.

When a particle of any shape is placed in a field of simple shear flow, the motion of the fluid in the vicinity of the particle becomes disturbed (46,53). This disturbance generates a system of stresses acting at the surface of the particle, which cause it to rotate and translate, as shown in Fig. 5.

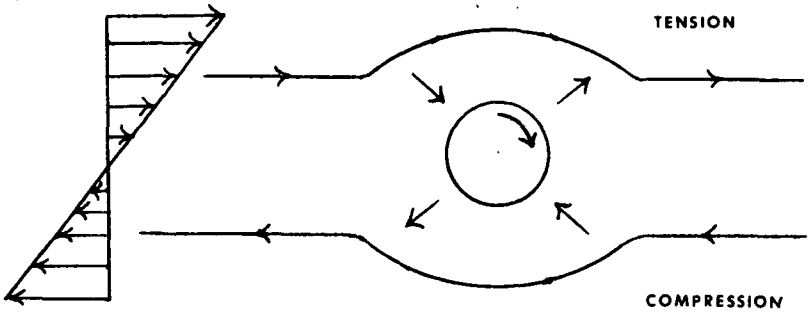

Figure 5. Laminar Shear Flow of a Newtonian Fluid Containing a Rigid Sphere

There exists no theory based on creeping flow equations which can predict the translational and rotational motions of the components of a disperse phase while they interact and collide with each other. Goldsmith and Mason (52), however, have constructed from experimental results a semiempirical and geometrical theory of the flow behavior of particles in simple shear flow.

For the simple case of a sphere, the particle will roll in the direction of motion at a constant angular velocity,

$$\omega = \dot{\gamma}/2, \tag{7}$$

with a period of rotation,

$$T_r = (4\pi/\dot{\gamma}) \tag{8}$$

Equation (8) has been verified experimentally with glass and plastic spheres by Mason and coworkers (54-56).

For a single prolate spheroid with its center at the origin of the field of fluid motion, Jeffrey's equations predict the velocity of the particle to be

$$\omega = \tfrac{1}{2}\dot{\gamma}\cos\theta, \tag{9}$$

where θ is the angle of orientation of the major axis of the particle to the direction of flow. Jeffrey's equations indicate that the angular velocity of the particle is at a maximum when the particle is at right angles to the direction of fluid motion and at a nonzero minimum when it is oriented in the direction of motion.

The rotation of the axis of revolution of an ellipsoidal particle is periodic with a period of rotation,

$$T_r = 2\pi(a^2 + b^2)/\dot{\gamma}ab \tag{10}$$

Several investigations by Mason and coworkers have substantiated Jeffrey's equations with experimental evidence (57-59).

To summarize, it may be said that in a field of undisturbed flow, viz., where all portions of the fluid are moving at the same velocity, a nonsedimenting particle will move with the same velocity as the fluid. No localized disturbances of the field of motion will occur. If a velocity gradient exists in the fluid, any particle, regardless of its shape or density, will tend to

disrupt the flow pattern of the liquid. The particle will thus be subjected to a torque arising from the uneven viscous drag of the liquid.

The torque will superimpose a rotation upon the translational motion of the particle, causing the particle to undergo spinning or tumbling movement. As the particle tumbles about in the velocity gradient, it will be constantly changing its orientation relative to the line of flow in an attempt to minimize the external forces being applied to it.

The behavior of linear agglomerates of spheres has been examined (60), allowing the derivation of the forces acting on long, thin, threadlike particles. In simple shear flow the particle experiences alternating tensions and compression as it rotates. The frictional forces not only cause the coiled threadlike particle to rotate, but they also induce a periodic change in shape as a consequence of the alternating tension and compression, as shown in Fig. 6.

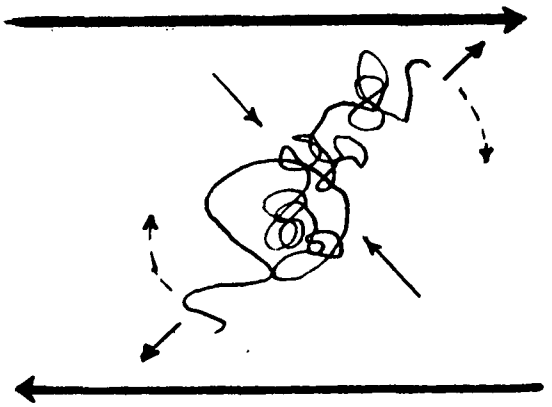

Figure 6. Tensile and Compressive Forces on a Threadlike Particle in Shear Flow. Heavy Lines Indicate Flow Lines, Light Solid Lines the Stresses on the Particle, the Dashed Lines the Direction of Rotation of the Particle

MECHANICAL DEGRADATION OF MACROMOLECULES

The response of a polymer molecule in solution to hydrodynamic shear involves a consideration of the dynamics of the molecule from two points of

reference. In the first instance the polymer molecule is treated as a discrete nonsedimenting deformable particle. In the second case the field of reference is changed to the polymer coil itself, having moveable links or segments.

The problem of polymer degradation is not a new one. Indeed, it has been studied by a myriad of investigators. Unfortunately, no one has decided conclusively what happens to a polymer molecule as it degrades under mechanical shear ... except that it will degrade.

In 1934, Staudinger and Heuer (61) reported milling polystyrene under nitrogen. Their results showed that, given identical circumstances, polymer molecules of different initial chain lengths are degraded to very similar final chain lengths. This suggested the role of a critical length, below which the polymer would not degrade due to insufficient force.

Simha and coworkers (62-64) treated the whole problem in terms of random degradation. By utilizing rate equations in their most generalized form for the degradation process, they were able to carry out a complex integration by making several simplifying assumptions. Inherent in these assumptions was the concept that all links were of equal strength and accessibility. The results were valid for the generalizations and assumptions necessary to carry out the calculations.

Several authors have tested the problem in terms of a weak link theory. Jellinek (65) carried out a series of calculations on the assumption that the weak links were distributed at random. However, the kinetics of polystyrene degradation do not support his theory (66,67).

Hess and Steurer (68) found the "critical size" for polyvinyl acetate to be 230 units. Schmid and Beuttenmuller (69) found that ultrasonic degradation

occurred to a greater extent in good solvents than in poor solvents. They also reported that degradation was more complete in dilute solution than in concentrated solution. These findings support the role of chain extension in the degradation mechanism.

Frenkel (70) calculated that if the shear stress on a polymer molecule in solution were to become sufficiently large, the tension exerted on it should actually be great enough to rupture covalent bonds. He hypothesized that the tension would be the greatest in the center of the molecule, resulting in two half-sized molecules. At that time interaction of polymer molecules with molecular oxygen was known to enhance mechanical degradation. This type of process, however was thought to involve both considerable intermolecular interactions and molecular entanglements. The rupture of a solvated molecule in dilute solution had not yet been studied.

The calculations of Morris and Schnurmann (71) demonstrated that the stretching forces on a molecule increase with the square of the length of the molecule for a given shear stress. Their experiments confirmed the calculated order of magnitude of the critical value of the rate of shear as a function of the chain length of the molecule. (They reported degrading molecular weights of 100,000 with shear rates on the order of 10^5 sec^{-1}.) Unfortunately their calculations were not demonstrated; however, they did report that the stretching forces reached their maximum for the center bond.

Using polyisobutylenes ($M \approx 10^6$) and a shear rate of 65,000 sec^{-1}, Bestul and Belcher (72) noticed that viscosity reduction leveled off at about 50% of the original value. They concluded that the molecular weight reduction can be explained on the basis of polymer chain rupture if the mechanical energy developed in a volume less than that enveloping a single polymer molecule can

be concentrated into a single polymer bond. Bestul's later experiments led him to believe that based on the energy absorbed per bond, the breakage process involved intermolecular entanglement (73).

Jellinek (74) has compiled a rather extensive review of mathematical theories of degradation involving random and weak link bases. The discussions center around the ability to predict rates of degradation for polymers in bulk and concentrated solutions, where intermolecular interactions play a significant role.

Porter, et al. (75) used a concentric cylinder device to degrade polyisobutylene and found the rate to be stress dependent. Changing the solvent had no effect on the breakage rate, and the solvent appeared not to be involved in the process. Limiting molecular weights were obtained in about 2 seconds.

The large hydrodynamic volume of DNA lends itself to the study of this phenomenon. Cavalieri (76) reported a molecular weight reduction of calf thymus DNA by passing it through an atomizer. Davison (77) demonstrated that even the shear rates generated in such common laboratory practices as shaking, pipeting and stirring were sufficient to degrade such DNA. His findings revealed that the conflicting and generally low molecular weights previously reported for a variety of native DNA molecules were the result of inadvertant degradation during sample preparation.

Hershey and Burgi (78) subjected T_2 DNA to high speed stirring. They observed an exponential decay of the whole-molecule concentration with time, using chromatographic separation techniques. An interesting finding was that the breakage rate was a function of the polymer concentration, with higher concentrations requiring greater stress to induce molecular scission (79). This phenomenon was dubbed the "self-protection effect." Hershey and Burgi

(80) studied this phenomenon more extensively, reporting that the lower concentration limit for self-protection of T_2 DNA was about 10^{-1} μg/mL. They did not find any effect of temperature on breakage. Rubenstein, et al. (81) determined the intact molecular weight of T_2 DNA to be at least 1.8×10^8 daltons.

Levinthal and Davison (82) also studied the scission of T_2 DNA using capillary flow to induce the shear. Flow through a capillary is laminar and well defined. They were therefore able to estimate the shear rate at which the DNA molecules were broken. They reported finding critical flow rates for the production of half and quarter molecules. The magnitude of these critical flow rates increased with concentration, lending support to the existence of the self-protection effect. They performed a calculation of the force exerted on the center of the model molecule. The model consisted of a rigid rod whose length was equal to a completely extended molecule. The force calculated was 1.1×10^{-3} dynes. This is comparable to the strength of C-O, C-P, and C-C bonds in vacuo (83).

Johnson and Price (84) studied the degradation of vinyl polymers by high speed stirring in the presence of iodine. Maximum degradation was reported for polymers in "poor" solvents at low temperatures and at highest shear rates. The amounts of iodine incorporated during shear were of the same order of magnitude as the number of chain scissions calculated from viscosity changes. Ott (85) also reported evidence for free radical formation during the mechanical degradation of cellulose. The mechanism proposed involved carbon-carbon bond scission.

Harrington and Zimm (86) studied polymer breakage using a variety of methods including capillary flow, stirring, flow through a sintered glass disk, and flow through the annulus of a piston and cylinder. Breakage rate

was measured as a function of shear rate. By using a calculation not requiring the choice of any particular model they arrived at a critical stress value of 2.5×10^{-5} dynes. Harrington later calculated a critical stress value of 4.3×10^{-4} dynes (87). The critical stress value found experimentally for vinyl polymers was two orders of magnitude smaller than that calculated (86).

Yew and Davidson (88) observed a strong temperature dependence for degradation in capillary flow. They also reported a self-protection effect for linear molecules, but not for circular ones.

Hlavacek and Schreiber (89) considered the response of macromolecular structures to increasing shear gradients and suggested that the coiled configuration, characteristic of the molecule at zero shear gradient, persists into the region of nonlinear viscous response. They postulated that the uncoiling of macromolecules occurs only at shear gradients approaching the onset of flow instability. Cottrell, et al. (90) found extension ratios in the direction of flow to be on the order of 30% for shear rates of 0-600 sec^{-1}.

Workers in Japan (91) found that scission in capillary flow was not a random process, and that the deviation from random scission increases on dilution. Nakano and Minoura (92) produced evidence to support a definite relation between mechanical scission of polymer chains and their hydrodynamic volume.

Adam (93) studied the shear degradation of DNA in a concentric cylinder apparatus and found no self-protection effect. He considered several scission mechanisms and postulated a base-catalyzed hydrolysis of the phosphate-ester linkage.

Many investigators have studied the degradation of macromolecules under the influence of ultrasonic waves. A complete review of their work could

indeed consume volumes. For the purposes of this discussion it will be worthwhile to contrast two major categories of investigation. Ultrasonation in the presence of various soluble gases (94-100) has produced results that differ significantly from studies using degassed solutions (101-106). The most interesting features of ultrasonic degradation investigations have been summarized collectively by Jellinek (74).

1. The decrease in molecular weight is relatively fast at first, but it slows down during the later stages of degradation and eventually stops at a definite molecular weight. Samples of different initial molecular weights reach the same final molecular weight.

2. The rate of degradation increases with the intensity of the ultrasonic waves, and the final molecular weight decreases with increasing intensity.

3. If cavitation is suppressed, ultrasonic degradation ceases or is appreciably diminished. In degassed solutions, degradation takes place only with very high molecular weight polymers. It is not clear whether this degradation is caused mainly by the mechanical agitation of the liquid due to the ultrasonic fountain or whether some "true" ultrasonic degradation is also present. This type of degradation increases with increasing intensity.

4. Increase of hydrostatic pressure decreases the rate of degradation and increases the final chain length reached. Even at fairly high hydrostatic pressures degradation still takes place especially if very high molecular weight polymers are present in the solution.

5. The rate of degradation is dependent on polymer concentrations. There are indications that the rate passes through a maximum, which means that degradation ceases in very dilute and highly concentrated solutions.

6. The rate of degradation is dependent on chain length. Under given conditions, the rate rises from zero at a certain chain length almost linearly but seems to slow down as higher chain lengths are reached.

7. The rate of degradation of polymethylmethacrylate is practically independent of frequency in the range from 300 to 10 kc/sec.

8. The same rate of degradation was found in benzene solutions saturated with air, oxygen, nitrogen, or hydrogen, but there was much less degradation in the presence of gases of appreciable solubility such as carbon dioxide, ammonia, and sulfur dioxide.

9. The degradation is not influenced by the density of solvent mixtures, as long as the solvents present are good ones. If a poor solvent is added to a good one, the rate of degradation decreases.

10. The rate of degradation seems to be dependent on the vapor pressure of the solvent. The higher the vapor pressure, the slower the degradation.

11. The molecular size distributions of degraded samples are narrower than corresponding ones obtained by ordinary random degradation.

12. Ultrasonic degradation diminishes with increasing temperatures of the polymer solutions.

13. In certain instances (polyethylacrylate) increase in molecular weight was observed on standing after irradiation.

14. A copolymer which showed weak links on thermal degradation did not indicate the presence of any abnormal links on ultrasonic degradation in vacuo.

The search for a common link between the dynamics involved in mechanically stressing a polymer solution and treating it with ultrasonic waves may provide a clue to the actual mechanism involved in polymer scission. As pointed out by Weissler (101,102), Prudhomme and Grabar (103), and Melville and Murray (104) degradation by ultrasonic cavitation is dictated by the collapse of cavities and the high fluid pressures and velocities developed. The latter are also inherently present in the other modes of mechanical shearing discussed above. If no gas nuclei are present in ultrasonic treatment, no scission occurs at ordinary intensities.

Calculations predicting a probable mechanism for molecular scission have been precluded by the inability to develop a suitable microscopic molecular model. Rather than adopt a model consisting of a rigid rod, as did Levinthal and Davison (82), it would be realistic to begin with a particle that possesses the characteristics of a deformable drop.

The limitations on the model would be that a fluid drop would have surface tension forces holding it together and working against its deformation, while a polymer coil would not have such restrictive forces. The latter, however, would have entropic forces due to Brownian motion. These tend to restore a deformed coil to a random configuration.

Taylor (106) has derived a complete set of equations for the stresses imposed on fluid drops and the resultant deformations. He observed that a drop could be drawn into a thread which remained coherent as long as it was being extended.

Rumscheidt and Mason (52) extended the work of Taylor to include fluids of several viscosity ratios. Their general observations included the fact that at low gradients, a drop was deformed into a prolate spheroid initially aligned at an angle to the flow of $\theta = \pi/4$. Both the extensional length, D, and θ increased with shear rate $\dot{\gamma}$. They also demonstrated that at high ratios of the viscosity of the drop to that of the medium it was indeed possible to deform the drop to a very long thread, as shown in Fig. 7.

Figure 7. Tracings from Photographs of Drops in Shear Flow. Shear Rate is Increasing from 1 to 4 (52)

For a case of high viscosity ratio, the normal and tangential stresses on the outside equator of the drop are (52):

$$f_n = (5/2)\ \eta_o\ \dot{\gamma}\ \sin 2\theta, \tag{11}$$

$$f_t = (5/2)\ \eta_o\ \dot{\gamma}\ \cos 2\theta \tag{12}$$

Forgacs and Mason (107) have observed the motions of threadlike particles in shear flow. Their observations are summarized in Fig. 8. When the parti-

cles were flexible, their orbits and periods of rotation differed appreciably from those of rigid cylinders. It was determined that if a particle undergoes shear-induced deformation, its shape, and hence the flow pattern around it, will depend at any instant on the deforming flocs. The measured periodic time of rotation, T_r, will vary with the particle shape and $\dot{\gamma}\,\eta_o$. For a given value of $\dot{\gamma}\,\eta_o$, there existed a critical length at which threadlike particles bent during rotation under stress imposed by the shear field. The change in shape of the projection of the coils on the plane parallel to the velocity gradient resembled the change in shape of deformed fluid drops. The filaments first uncoiled, then recoiled during each rotation. As the flexibility of the rod or filament is increased by increasing either $\dot{\gamma}\,\eta_o$ or the axis ratio a stage is reached at which the two ends appear capable of independent movement. At this point the filaments will extend completely only when aligned with the fluid flow lines.

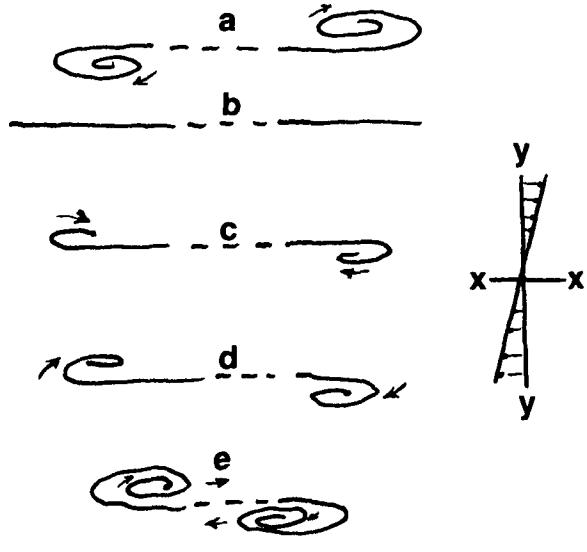

Figure 8. Tracings of Photomicrographs of the Orbits of Flexible Filaments Viewed Along the Z Axis (107)

Adam (93) argues that this "independent-end" motion is compelling evidence against the arguments of Levinthal and Davison (82) for degradation at mid-molecule due to stress intensification. However, it should be noted that

proper orientation for maximum stress will have a chance to occur many times before this critical length for independent movement is reached. The important consideration then becomes one of a play-off between the critical force necessary to cause scission and the critical particle length for "snake orbits." The path to follow starts at Frenkel's discussion of the dynamics of viscous tensions acting on the molecule (70), as presented below.

The force acting on each separate atomic group of the molecular chain is proportional to the relative velocity of the solvent with respect to the group,

$$f_i = q[V(x_i) - U_i] \tag{13}$$

For this discussion, $V(x_i)$ denotes the velocity the solvent would have at the point x_i in the absence of the macromolecule. The velocity of the ith group may be defined as $U_i = dx_i/dt$. An assumption is made that each group may be considered as a small sphere of radius r. Approximating the flow by Stoke's Law for each sphere, the proportionality constant in Equation (13) may be found as:

$$q = 6\pi \eta_o r, \tag{14}$$

where η_o is the solvent viscosity coefficient. All flow is laminar.

The macromolecule may be treated as a composite of these 2N small spheres, with slightly extensible links of length L. Consider the pull exerted on any given link, L_i, connecting the ith and $(i + 1)$th spheres. The tensile forces on the spheres, F_i and F_{i+1}, must intuitively have the same magnitude and opposite directions. F_{i+1} may be expressed as the sum of the viscous forces, $f_{i+1} + f_{i+2} + \ldots + f_k$, exerted by the relative motion of the solvent on the $(i + 1)$th sphere and all spheres following it. Similarly, F_i may be defined as the sum of the viscous forces, $f_i + f_{i+1} + \ldots + f_k$, acting on all preceding spheres.

Because the central link is subject to the resultant tension of all links lying both to the right and left of it, its position corresponds to the maximum value of F_i.

It is possible to extend these ideas to accommodate the findings of Forgacs and Mason (107) by assuming that the condition $LF_i >> kT$ is fulfilled for the next s links on either side of the center link, while for the remaining links $LF_i << kT$. When $LF_i >> kT$, the link can be assumed to be fully oriented, lying exactly in the direction of the forces F_i or F_{i+1}. If $LF_i << kT$ all its orientations can be assumed to be equally probable. Thus the molecular chain can be envisioned as consisting of a straight central portion ($2s + 1$ links), while the remaining external portions [consisting of $\frac{1}{2}(N-s)$ spheres each] are curled somewhat randomly.

The forces F_i can be determined approximately by assuming the curled portions to lie approximately at the same distance x from the chain as the sth group. The total force acting on the sth link in the direction of flow will therefore be

$$F = q \dot{\gamma} Ls(N-s), \tag{15}$$

where $(N-s)$ is the number of groups on each side. This expression reaches a maximum value for $s = N/2$.

The relation between the length of the chain ($2LN$) and the minimum value of the velocity gradient for this configuration to exist may be expressed as,

$$kT = (1/4)\, q\, \dot{\gamma}_o\, (LN)^2 \tag{16}$$

For a molecular chain where $N = 10^4$, $\dot{\gamma}_o \approx 10^3$ sec^{-1}. The maximum length of the molecules capable of resisting the extending action of the viscous flow is inversely proportional to the square root of the velocity gradient.

Earlier arguments have established that a particle of finite size will indeed rotate if placed in a velocity gradient. The existence of rotations is important for arguments of macromolecular degradation according to Frenkel's theory. Even if the initial orientation of the particle or filament is unfavorable for degradation, rotation to a favorable position can take place. The validity of Frenkel's theory is substantiated by the results of several workers mentioned here (61,68,69,71,72,75-92). It will be thus assumed that mechanical degradation of a macromolecule by hydrodynamic forces provides a reasonably possible explanation for the disruption of colloidal aggregates.

AGGREGATE RUPTURE

When an aggregated suspension is pumped, stirred, or otherwise caused to flow, the resulting velocity gradients impart shear stresses on the aggregates. It is well known that if the velocity gradient is appreciable, the aggregate may be disrupted. The resistance of the structure to these disruptive forces depends on the number of contacts between particles within the floc and on the magnitude of the molecular attraction forces.

LaMer and Healy (10) noted that the conditions of agitation of a polymer-colloid dispersion had a considerable effect on the extent of flocculation. They postulated that bridge-type flocs were broken up as the result of system agitation, and that separation occurred by a desorption of the polymer.

Albers and Overbeek (108) showed that flocculated water-in-oil emulsions can be redispersed at rates of shear greater than 10^3 sec^{-1}. They pointed out that under the influence of increasing hydrodynamic force a floc redisperses gradually. Break-up of doublets and triplets was found to be extremely difficult.

Mitin (109) measured the relative strengths of aluminum hydroxide precipitates treated with polyacrylamide. He concluded that the addition of a macromolecular flocculant to aluminum hydroxide suspensions raised the resistance to shear of the sediments formed from these suspensions. Additionally, he found an optimum polymer concentration for maximizing resistance to shear.

McKenzie (110) and Strazdins (6,111) are among the group of workers who have noted that hydrodynamic shear has a pronounced effect on the retention of particulate matter in a paper web. Higher shear rates were shown to decrease retention.

Zia, et al. (112) have examined the behavior and breakdown of chains of rigid spheres. Polystyrene spheres with a thin metal coating were aligned along a common axis by an electric field. When the field was removed and the suspension sheared, the chain rotated as a rigid rod, as predicted by creeping motion equations. Breakage occurred as the shear rate was increased to a sufficiently high value.

Argaman and Kaufman (113) suggested that the principal macroscopic mode of aggregate break-up was surface erosion of flocs by viscous drag. By intuitive and dimensional reasoning they proposed that the rate at which primary particles are stripped from a floc should be proportional to the floc surface area and the surface shearing stress.

Patterson (114) studied the degradation of agglomerates of glass beads in a matrix of polyethylene glycol. A model was proposed to calculate the size distribution as a function of time and shear stress. Results from the experimental program agreed qualitatively with the model, predicting that the size distribution of resultant particles is linearly related to time and shear

stress. The possibility of degradation due to aggregate collisions was shown to be negligible for particle concentrations less than 2% by weight.

Tomi and Bagster (115) constructed a mathematical model of idealized flocs subjected to hydrodynamic forces. Their calculations illustrated that loose flocs (viz., those formed by polymer bridges) exhibited tensions which were much more sensitive to orientation in the flow field than were compact flocs. Another difference was that the loose flocs reflected maximal tensions at or near the center of the structure, while compact flocs had maximum tensions at the periphery of the structure.

Firth and Hunter (116) have constructed a mathematical model of an "elastic" floc to describe the viscous behavior of colloidal sols. They found that most of the energy dissipation during flow could be attributed to two processes: (1) viscous flow of the suspending medium around the structures, and (2) energy involved in distorting and/or rupturing inter-particle attractive forces. They predicted a linear dependence of critical shear rate on particle radius.

Goosens and Luner (117) studied the effect of agitation on the flocculation of microcrystalline cellulose suspensions with cationic polymers. They found that with increased time of agitation, as well as degree of agitation, more polymer was needed to flocculate the suspension. They concluded that the increase in stability against flocculation with time and degree of agitation is caused by the release of Ca^{++} from the particle surface as well as by the diffusion of polymer into the pores of the particles.

Beck, et al. (118) speculated that patch-type flocs were disrupted by shear forces, but that reflocculation would take place immediately after cessation of the shear. It was also suggested that bridge-type flocs also

break up under shear forces, but that reflocculation should be much slower and less effective. No investigations of the mechanisms involved were conducted.

PRESENTATION OF THE PROBLEM

Speculations concerning the microscopic processes involved in the degradation of flocs formed by bridges and flocs formed with electrostatic patches have been presented by LaMer and Healy (10) and Beck, et al. (118). The fact that behavior under conditions of agitation varies with the type of floc is, in itself, evidence that there is a difference in the mechanisms of floc formation when polymers of low and high charge densities are used for the flocculation. The adsorption-flocculation work of Lindquist (12) was among the first performed to substantiate this view.

It was the purpose of this research to elucidate the molecular mechanisms involved in the hydrodynamic shear-induced degradation of both bridge-type and patch-type flocs. The primary objectives of this work were:

(1) To study the behavior of flocculated systems in hydrodynamic shear fields.

(2) To elucidate the manner in which aggregates of potentially different aggregate geometries are disrupted by hydrodynamic shear.

GENERAL APPROACH

The manner in which flocculated colloidal dispersions of different aggregate geometries are restabilized by hydrodynamic shear was investigated with a system of polystyrene latex (PSL) and polyvinylamine (PVAm) at various pH's. By knowing the attraction to PSL surfaces and the resultant changes in configuration of PVAm induced by shifts of pH, it was possible to produce aggregates formed by either polymer bridges or electrostatic patches. Monitoring the molecular weight distribution of the PVAm after shearing the flocs provided initial evidence for the mechanistic pathway followed. The use of a low molecular weight surface active agent as a second adsorbate produced a method for surveying the available PSL surface area throughout the shearing process. The tendency to refloc provided insight concerning the relative state of the flocculating polymer after the shearing process had ceased.

Polystyrene latex particles were chosen as a representative colloidal particle for the following reasons: (1) it is possible to obtain precise particle size and size distributions, (2) the particles are spherical and nonporous, (3) particle stability is constant over a wide pH range, and (4) the anionic surface charge classifies the particles with a large percentage of naturally-occurring colloidal material, including those found in municipal water treatment and papermaking.

For desorption of the flocculating polymer to occur, the electrostatic attraction of the polymer for the particle surface must be terminated or overcome in some manner. If the charged sites of the polymer are the result of protonation alone, extermination of all charges on the flocculating polymer will occur at sufficiently high pH's. Total desorption of the polymer from the particle surface is then possible.

In addition to satisfying the criteria for desorption, it was necessary to insure that molecular weight variation, chain branching, and chemical composition of the flocculating polymer used to produce both bridge-type and patch-type flocs would not affect interpretation of experimental results. For these reasons, it was decided that a high molecular weight, linear, primary amine was necessary for this investigation. Polyvinylamine has been prepared with high molecular weights by Hart (119) and others (120,121). In these specific preparations, 100% of the nitrogen exists as free primary amines, and the molecules have a simple, linear, and homogeneous chain structure.

The experimental program was divided into the following sections:

(1) Characterization of the polystyrene latex particles.

(2) Physical and chemical characterization of PVAm.

(3) Determination of optimum flocculation conditions for the PVAm/PSL system at various pH's.

(4) Design of the shear apparatus.

(5) Determination of the amount of shear necessary to restabilize the flocculated PSL at the various pH's, and the tendency of the resultant suspension to reaggregate with time.

(6) Monitoring the PVAm molecular weight distributions after suspension restabilization.

(7) Determination of the available PSL surface area throughout the flocculation-restabilization-reflocculation process.

EXPERIMENTAL MATERIALS AND METHODS

All water used throughout this investigation was deionized and distilled through an all-glass apparatus. The conductivity was below 2.0×10^{-6} mho/cm.

To minimize polymer adsorption on glass surfaces, all glassware was treated with a 2% solution of polyethylene glycol (122). Glassware treated in such a fashion was rinsed exhaustively with water prior to use.

CHARACTERIZATION OF POLYSTYRENE LATEX PARTICLES

Uniform latex particles were obtained from Dow Diagnostics of the Dow Chemical Company, Indianapolis, Indiana. The particles were supplied as 100 mL of a 10% slurry. The particle diameter was reported as 0.794 μm with a standard deviation of 0.0044 μm.

Ottewill and Vincent (123) have calculated surface areas for PSL from both volumetric krypton adsorption studies and geometric calculations, and found close agreement. This would suggest that the porosity of PSL is minimal. By determining the size of the PSL from electronmicrographs, then, the surface area may be easily calculated using the formula for the surface of a sphere. The surface area for PSL spheres of this size is 54.5 m^2/g. Particle density is 1.05 g/cm^3.

The Dow PSL have been shown to contain no surface carboxyl groups (124). Thus, the Dow particles are stabilized by sulfate end-groups and by adsorbed surfactants, as their preparation included the technique of emulsion polymerization. Although the layer of surfactants aids in maintaining a stable suspension, it is possible that a portion of this material would be leached off or displaced in any given experiment. The use of properly conditioned ion-exchange resins to completely desorb the emulsifiers has been used successfully

(39,125). The Dow PSL was treated according to the method of Van den Hul and Vanderhoff (125) for surfactant removal using Dowex 50W-X4 sulfonate salt resin and Dowex 1-X4 trimethylammonium salt resins. Wash water from resin conditioning was free from leached-out polyelectrolytes, as monitored by absorbance at 224 nm (126). PSL surfaces were thus free of any adsorbates after treatment (125).

DETERMINATION OF SURFACE CHARGE DENSITY

After ion-exchange treatment, the PSL suspension is stabilized only by those sulfate end groups which are located on or near the surface (127). To determine the relative abundance of these stabilizing end groups, potentiometric titrations were conducted using standardized HCl and NaOH solutions, in a manner similar to that described previously (39,128,129).

The method used consisted of two main parts. The first part involved the titration of a blank (solvent at appropriate ionic strength), where the pH was determined as a function of the quantity of titrant added. The second part includes the same procedure for a known concentration of PSL. All titrations were carried out in a Plexiglas cell, similar to that used by Clapp (130) and others (12,39), at room temperature in a CO_2-free nitrogen atmosphere. Each addition of titrant was followed by a 5-minute time interval prior to pH measurement. Determination of pH was conducted with a Corning Research pH meter, utilizing a Markson Model 808 combination electrode.

ZETA POTENTIAL

A qualitative, but much quicker, means of determining the surface charge density of the PSL particles is by microelectrophoresis. Electrophoretic mobility was determined on a Zeta-Meter (Zeta Meter, Inc.). This mobility, in turn, was converted to zeta-potential by the Helmholtz-Smoluchowski equation.

CHARACTERIZATION OF POLYVINYLAMINE

Because the synthesis of polyvinylamine is a very difficult one (131), samples were solicited from both Dr. C. J. Bloys van Treslong (University of Leiden, The Netherlands) and Dr. D. J. Dawson (Dynapol, Palo Alto, California).

Dr. Bloys van Treslong's sample of 1 g of fractionated PVAm hydrochloride was obtained as a pure and cleaned sample with a molecular weight of 250,000. Unfortunately, this sample was not of high enough molecular weight for the proposed work. However, its purity made it an excellent sample for characterization work.

Dr. Dawson was the second source contacted. The route of his synthesis (121) was significantly different than that used by Bloys van Treslong (120). Dr. Dawson was kind enough to supply 25 g of a crude reaction mixture containing approximately 5 g of polyvinylacetamide (PACE). The PACE supplied by Dawson was checked for branching by ^{13}C NMR and other techniques (132). The limit of detection methods employed was about 3%; there was no branching of this polymer noticed at these detection limits (132). It was assumed, for the purpose of this work, that the PVAm is essentially a linear molecule.

PURIFICATION AND HYDROLYSIS OF POLYVINYLACETAMIDE

Purification of the crude reaction mixture to isolate the PACE was first accomplished according to the suggestion of Dawson, et al. (121), using multiple precipitation of an ethanol solution on acetone. Diafiltration had been ruled out because of the susceptibility of polycarbonate to ethanol (133). However, it was discovered (132) that PACE will dissolve readily in water, permitting clean-up by the much more convenient diafiltration technique. Diafiltration was conducted on an Amicon ultrafiltration unit (Amicon Model 402,

Scientific Systems Division, Amicon Corporation, Lexington, Massachusetts) using membrane XM100. The process was carried out against water for a 10-volume turnover under 10 psi N_2. Lindquist (12) has shown that a 6-volume turnover is sufficient to remove 99+% of all sodium ions in a polyamine solution.

Hydrolysis was carried out in a manner similar to that outlined by Dawson, et al. (121). An aqueous solution (0.1%) of the PACE was charged to a 3-neck flask fitted with a glass/Teflon stirrer and Liebig condenser set for reflux. Sufficient concentrated HCl (12N) was added to adjust the final normality to 6N HCl. The reaction mixture was put under a purified nitrogen atmosphere, then heated to boiling. Reflux was continued for 24 hours. Sensitive titration methods, which distinguish contributions from PVAm, HCl, and acetic acid have disclosed that reflux for 24 hours is sufficient to insure 100% conversion of PACE to PVAm (132). The reaction solution was adjusted to pH 10 with KOH and then diafiltered with water for a 10-volume turnover, before concentrating.

This solution of cleaned PVAm was then freeze-dried to allow gravimetric preparation of desired solution concentrations.

GEL PERMEATION CHROMATOGRAPHY

To minimize the adverse effects of polydispersity on adsorption behavior and interpretation of shear degradation data, narrow molecular weight fractions of PVAm were prepared by gel permeation chromatography (GPC).

Several criteria are important in the selection of an appropriate gel material. It is extremely important that there be no sorption interactions between the gel and the polymer. Because the equilibrium partitioning of molecular weights due to adsorption favors the retention of higher molecular

weight species, interaction of this type would result in two partitioning mechanisms operating against one another.

Size of the gel beads and size of the pores are also important parameters. Smaller bead size provides better resolution at the expense of requiring lower flow rates. Intermediate particle size gives a good balance of resolution and flow rate.

The gel chosen as possessing the most desirable characteristics was Bio-Gel A (BioRad Laboratories), 100-200 wet mesh. This gel is made with agarose of high purity and high gel strength. The pH operating range is 4-13. Bio-Gel A is supplied as fully hydrated spherical beads, with sodium azide added as a bacteriostat. The 5 m gel provides an operating range of 10,000 to 5,000,000 daltons (based on globular molecules).

The degassed gel was supported in a precision bore, glass chromatographic tube 2.5 cm in diameter and 100 cm in height. The column was set up in a controlled-atmosphere of 22.7°C and 50% relative humidity.

The solvent used was 0.1N NaCl in 4.25×10^{-5}N NaOH. Deaerated solvent was supplied to the head of the column at a flow rate of 0.714 mL/min by a variable speed peristaltic pump (Technicon Model 1) using 0.100 inch (ID) Tygon tubing.

Eluent was passed through a comparative refractive index monitor (Pharmacia Inc.) whose signal was supplied to a Speedomax H Long Door recorder (Leeds and Northrup). The refractive index of the eluent was compared to a deaerated aliquot of the eluting solvent. All components on the eluent stream were connected by Teflon tubing (0.042 inch ID) and gum rubber sleeves (0.125 inch ID).

The polymer loading process was initiated by draining the solvent down to the level of the agarose beads. Ten milliliters of a 1.32% PVAm solution was then carefully loaded onto the gel bed by pipet. The solution was drawn into the bed by allowing the solvent to drain slowly from the outlet. The sides of the column were then washed with solvent before activating the pump.

Fractions were collected at 12-min intervals with a Technicon fraction collector.

POSTFRACTIONATION TREATMENT OF POLYVINYLAMINE

To screen any electrostatic charges on the PVAm, thus minimizing adsorption of the polymer onto the gel, fractionations were run in 0.1N NaCl with 4.25×10^{-5}N NaOH. To study the behavior of the polyelectrolyte under various charge densities, it was necessary to remove these added electrolytes. This was accomplished by diafiltration with 10 volumes of water on an Amicon Ultrafiltration System with an XM100 membrane.

MOLECULAR WEIGHT

The molecular weights of selected PVAm fractions were determined by sedimentation equilibrium techniques (134-136) using a Beckman Spinco Model E ultracentrifuge equipped with Rayleigh optics. All measurements were performed at 25.0°C in 0.10N NaCl at pH 8. Experimental details and results are provided in Appendix I.

DIFFUSION COEFFICIENT

The ultracentrifuge was also used to determine the diffusion coefficient of PVAm in 0.1N NaCl at pH 8. A discussion of the techniques involved is presented in Appendix III.

TITRATION OF POLYVINYLAMINE

PVAm is a polybase which acquires a cationic charge by accepting hydrogen ions in a manner similar to the following schematic reaction:

$$RNH_2 + H^+ \rightleftharpoons RNH_3^+ \qquad (17)$$

The extent of the cationic nature of this polymer is obviously dependent on the solution hydrogen ion concentration. If water becomes the source of hydrogen ions, the pH is shifted in an alkaline direction.

Hydrogen ion titrations were conducted according to the technique described by Kenchington (128) and Tanford (129) in a Plexiglas cell similar to that used by Clapp (130). Measurements were taken at room temperature in a CO_2-free nitrogen atmosphere. Sample size was 50 mL for all titrations.

PVAm supplied by Bloys van Treslong was studied at a concentration of 38 mg/liter. A 5.000 mL buret was used to deliver accurate (±0.005 mL) aliquots of either 0.100N NaOH or 0.100N HCl.

A Corning Research Model 12 pH meter was used with a Markson Model 808 combination electrode to determine solution pH.

Equilibrium was found to be established almost immediately after addition of titrant, although a 2-min interval was allowed between successive additions.

VISCOSITY

The intrinsic viscosity of PVAm was determined in 0.1N NaCl at pH 12, and at pH's 3, 9, and 10 without salt. Relative viscosities were measured at 25.0 ± 0.1°C using a Cannon 75 Ubbelohde dilution viscometer. Measurements were taken at a number of solution concentrations at each pH. All solutions were filtered through 2 μm Millipore filters prior to viscosity determinations.

Dilutions were made in the viscometer using a microsyringe fitted with a 10-inch stainless steel needle. A period of at least 4 hours was allowed for equilibration after each dilution. Efflux times were recorded until five successive times differed by less than 0.3 sec. Efflux times were long enough to make kinetic energy corrections unnecessary (137).

QUANTITATIVE ANALYSIS

The copper chelate formed by polyethylenimine (PEI) has been used as a reliable means of colorimetrically determining polyamine concentrations in solution (12,138). Perrine and Landis (138) tested PVAm for its copper-binding ability and found it to be very weak compared to that of PEI. Beer's Law is not obeyed for the Cu^{++}-PVAm systems (138,139).

The use of fluorescent spectroscopy for the quantitative detection of primary amines has been thoroughly reviewed (140-146). Fluorogenic reagents such as fluorescamine and o-phthalaldehyde react with the primary amines to form highly fluorescent compounds.

The concentration of polyvinylamine in solution was determined by fluorescent spectroscopy after reaction with a fluorogenic reagent containing o-phthalaldehyde (OPT) and 2-mercaptoethanol (MERC). Benson and Hare (146) have reported detection of primary amines in the picomole range using the fluorogenic reagent described by Roth (147). Conversations with L. J. Marton (University of California Medical Center, San Francisco, CA 94143) led to the use of the following procedure for reagent preparation:

a) 4 liters of KOH/boric acid buffer at pH 10.4, deaerated and equilibrated with purified nitrogen, and

b) 250 mL buffer + 0.9 mL MERC + 1.2 g KCNS + 200 mg OPT dissolved in 10 mL methanol.

Because OPT and MERC are subject to atmospheric oxidation, all reagents are stored in dark bottles under nitrogen. Solutions of the fluorogenic reagent were prepared daily.

Spectrophotometric work was conducted with an Aminco Bowman Spectrophotofluorometer, Model 4-8202. The instrument was equipped with a xenon-mercury lamp and a xenon arc stabilizer. Excitation and emission spectra were recorded on an Omnigraphic 2000 X/Y recorder (Houston Instrument Company, Division of Bausch and Lomb).

The procedure for detecting PVAm involved mixing equal portions of fluorogenic reagent and PVAm solutions. The excitation wavelength used was 340 nm, with maximum emission occurring at 450 nm. Wavelengths were not calibrated, but are close to the values (λex:340, λem:455) given by Roth (147).

The PVAm concentration of an unknown solution was determined by comparing luminescence with a standard curve. Calibration of the standard curve was done by volumetric dilution of a gravimetrically prepared solution of PVAm. Comparison of accuracy by organic nitrogen determination (e.g., Hengar technique) was not possible, due to the small amount of PVAm available.

FLOCCULATION OF POLYSTYRENE LATEX WITH POLYVINYLAMINE

A principal question to be answered by this thesis concerns the manner in which flocculated colloidal dispersions of potentially different aggregate geometries are disrupted by hydrodynamic shear. Inherent in the development of any arguments concerning aggregate response to hydrodynamic shear are assumptions that must be made concerning the configuration of adsorbed polymer molecules and the aggregate geometries, viz., polymer patches, bridges, etc. To increase the feasibility of reproduction of aggregate geometries for a given set of

experimental conditions previous methods of introducing flocculating polymer and colloid (12,39) were modified to decrease the possibility of uneven distribution of polymer in the colloidal dispersion. The ideas of Gregory and Sheiham (148) concerning the kinetics of flocculation stimulated this line of thought.

Figure 9 shows a schematic drawing of the mixing tube used to deliver premeasured aliquots of polymer and colloid to a centrifuge tube for flocculation. Flow time and mixing conditions from such a device were dependent only on the volumes delivered from each side arm; these were held equal and constant. Ten milliliters of a PSL suspension at the appropriate pH were added by volumetric pipet to arm A; 10 mL of the appropriate PVAm solution were added by volumetric pipet to arm B. Plunger C was removed quickly and the contents of both arms were emptied out port D within 0.5 sec. Mixing in this tube minimized the possibility of overdosing part of the PSL, while leaving another part untreated. Influence of the apparatus itself on polymer or colloid concentrations was assumed to be negligible, as the entire apparatus was constructed from Teflon.

The following procedure was used to determine the conditions for optimum flocculation (OFC) at a given pH:

(1) Utilizing the mixing tube, 10 mL of PSL at a concentration of 1000 mg/liter was placed into each tube of a series of 50 mL screw cap glass centrifuge tubes simultaneously with 10 mL of PVAm solution at the desired concentration.

(2) The centrifuge tubes were sealed with caps lined with polyethylene film and placed at the periphery of two 12-inch notched wheels rotating at 5 rpm in a constant temperature bath set at 25.0 ± 0.1°C. The wheels were mounted on a common axis, with the notches of one wheel advanced 15° relative to those of the

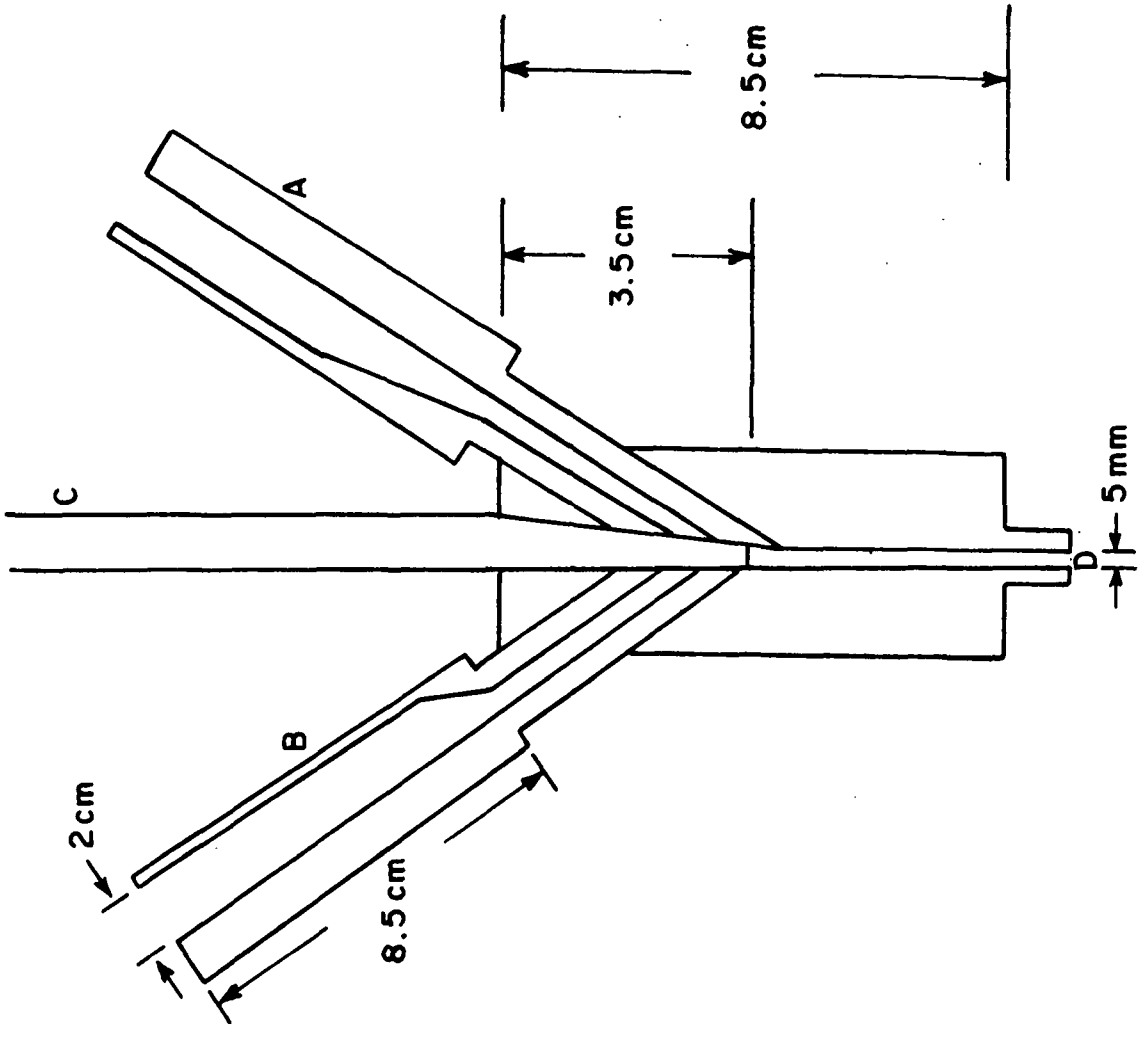

Figure 9. The Mixing Tube (Cross-sectional View)

second wheel. These conditions provided a gentle agitation, with a shear rate of approximately 1.0 sec^{-1}.

(3) After 60 min of gentle agitation, the tubes were removed from the bath and allowed to stand undisturbed for 20 min.

(4) A 0.3 mL aliquot from the same depth in each tube was diluted with 50 mL of water at pH 9, and the turbidity of the suspension measured on a Brice-Phoenix Light Scattering Photometer at a wavelength of 5460 A. The sample was held in a 24 x 24 mm cell.

(5) Electrophoretic mobility measurements were taken on the diluted samples using a Zeta Meter.

The choice of conditions used in this study was in some instances purely arbitrary. However, LaMer, et al. (149) have shown that the extent of flocculation is dependent on agitation. Using a device similar to the rotating wheel used in this work, they found flocculation to be more dependent on the total number of rotations than upon the rate of rotations. Maximum flocculation for most sols studied reached a plateau after 100-200 rotations (149). The 1-hour agitation time used in this work produced 300 rotations. Others (12,39) have shown that this number of rotations is within the flocculation plateau described by LaMer, et al. (149). The final particle concentration of 1.82×10^9 PSL/mL was chosen to minimize the possibilities of nonequilibrium flocculation while providing enough PVAm in solution (after separation from PSL) to be quantitatively detectable.

RESPONSE OF AGGREGATES TO HYDRODYNAMIC SHEAR

One prerequisite of this work was the development of an apparatus capable of producing well-defined shear flow that would induce resuspension of flocculated colloidal suspensions. Simple laminar shear is the most fundamental type of fluid flow exhibiting a velocity gradient. This type of fluid flow is

defined as that motion of a fluid between two parallel platens, one of which is at rest. An experimental apparatus which closely approximates this flow is a Couette viscometer, consisting of two vertical coaxial cylinders.

A schematic diagram of the concentric cylinder apparatus used for the shear studies is shown in Fig. 10. The basic design is a modification of a Hercules Couette-type viscometer. All components of the coaxial cylinder apparatus were constructed from polymethylmethacrylate. The volume of the shear zone annulus is 0.344 mL. Rotation rates of the inner cylinder (bob) were calibrated with a General Radio Co. Strobotac, Type 631-B. The calibration was conducted from 60 to 4400 rpm, which corresponded to shear rates of 1035 to 38,000 sec^{-1}, respectively.

Care was taken to minimize the loss of material while transferring from centrifuge tubes to the apparatus, and back. Loading was accomplished by charging an entire 20 mL test suspension into the cup portion of the apparatus. The bob was then lowered into the suspension, which was subsequently pulled into the circulating tubing by a peristaltic pump. Extensive efforts were made to eliminate large bubble formation under the bob. Any bubbles that formed were removed by quickly raising and lowering the bob in the cup before rotation was started.

A schematic diagram of the entire system used for shear experiments is illustrated in Fig. 11. The fluids to be sheared were pumped through the annulus to minimize the build up of heat. Circulation was accomplished with a Technicon Instruments Model 1 peristaltic pump at a flow rate of 2.78 mL/min. At this flow rate a volume element remained in the shear zone for 7-1/2 sec. The maximum temperature rise expected in this time, assuming all energy input was dissipated as heat, was 2.4°C. This was not deemed to be of consequence

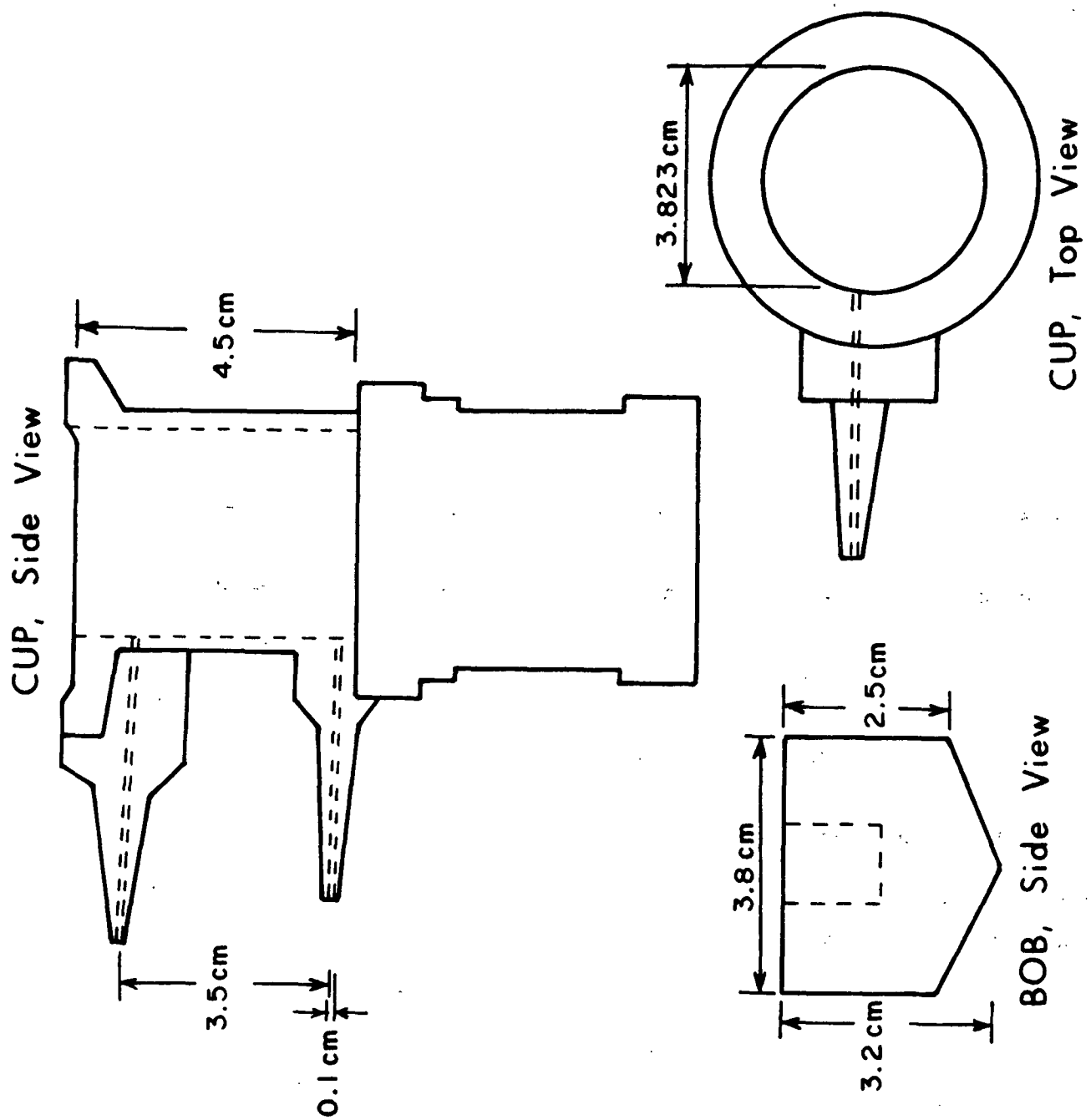

Figure 10. Schematic Diagram of Shear Apparatus

to the results of the investigation. The shear rate generated by merely pumping the fluid through the annulus (both cylinders stationary) was calculated to be on the order of 100 sec^{-1}. This was not significant enough to cause coupling between rotational and annular flows when the inner cylinder was rotating.

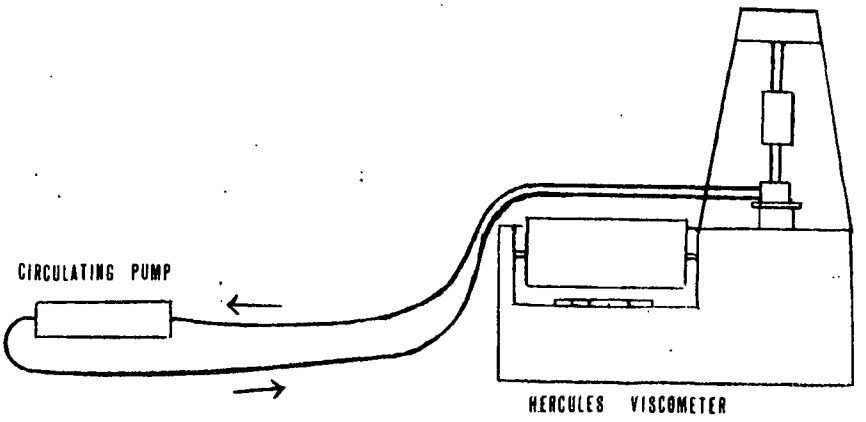

Figure 11. Schematic Diagram of the System Used for Shear Experiments

Tubing used for circulation was Thermoplastic Processes' Bev-A-Line, 3/32 inch ID. The inner contact surface of the polyvinylchloride tubing was reported to contain no vinyl chloride and no plasticizer (150), thus minimizing contamination of the test system via solvent leaching.

To obtain reliable information concerning the behavior of flocculated systems in high shear fields it was necessary to first determine the amount of energy that could be applied to a stable colloid system without inducing aggregation by mechanical impaction. PSL samples of appropriate dilution were subjected to a variety of shear stresses for several lengths of time. After shearing each sample, aliquots were taken immediately and again after 1 hour of settling time. The conditions sought by this experiment were maximum shear rate and minimal particle settling.

FLOC RESPONSE TO SHEAR

The response of flocs to shear at various pH's was investigated to quantify possible variations in the shear strength of different aggregate geometries. Aggregates at each pH were subjected to a series of shear rates for a length of time sufficiently long to allow all volume elements one pass through the shear zone. Each sample was subsequently placed on the agitation wheel in the water bath for 1 hour prior to 20 min of undisturbed settling. Aliquots were then compared by turbidity.

KINETICS OF FLOCCULATION VS. REAGGREGATION AFTER RESTABILIZING SHEAR

The tendency a restabilized colloidal dispersion displays toward reflocculation provides insight to the relative configurational state of the flocculating polymer after shear. Observing the final extents of reflocculation and comparing the kinetics involved in reaching the final reflocculation value to the respective values for initial aggregation has provided such insight.

The procedure used to study the kinetics of initial flocculation was as follows:

(1) Appropriate concentrations of PSL and PVAm were charged to screw cap centrifuge tubes through the Teflon mixing tube described previously.

(2) The tubes were placed on the agitation wheel in the water bath for designated lengths of time before removal to the stationary rack.

(3) Samples were collected from the same depth in each tube after 20 min of settling time.

(4) Relative turbidities were measured according to the previously outlined procedures.

The procedure used to study the kinetics of reaggregation after exposure to shear was as follows:

(1) Flocs were formed at the appropriate OFC according to the method outlined previously.

(2) The flocculated suspensions were charged to the shear apparatus and subjected to a designated shear rate for a standard length of time.

(3) Upon removal from the shear apparatus the suspensions were again charged to the screw top centrifuge tubes and placed on the agitation wheel in the water bath for 1 hour.

(4) Following removal from the water bath, the suspensions were allowed 20 min of undisturbed settling before aliquots were withdrawn for turbidimetric analysis.

POLYVINYLAMINE MOLECULAR WEIGHT DISTRIBUTIONS AFTER SHEAR

A measurement of the molecular weight distributions of the flocculating polymer under a variety of conditions has helped to elucidate the actual mechanism involved in restabilizing a colloidal suspension flocculated under conditions favoring either polymer bridging or electrostatic patch formation.

SEPARATION OF POLYVINYLAMINE FROM POLYSTYRENE LATICES

To monitor molecular weight distributions of PVAm used to flocculate a suspension subsequently subjected to hydrodynamic shear, total desorption of polymer from the particle surface must be possible.

Simple polyamines such as PVAm carry cationic charges as the result of an overabundance of protons, as suggested in Equation (17). By raising the pH of the solution sufficiently (viz., pH 12) all nitrogen groups will lose their associated proton, leaving no electrostatic attraction between polymer and particle surface.

Centrifuging the flocculated suspension at 75,000 g and 10°C for 2 hours removed all particles, permitting a quantitative analysis of the supernatant for PVAm concentration. Removal of PSL was monitored by light scattering and absorbance at 244 nm. Recovery of PVAm as calculated from the PVAm quantitative analysis calibration curve was within 2% (experimental error) of the amount originally added to the suspensions.

CALIBRATION OF SMALL GEL PERMEATION CHROMATOGRAPHY SYSTEM

To effectively monitor the behavior of the molecular weight distribution of the extremely small quantities of PVAm used in the flocculation systems it was necessary to set up a small scale gel permeation chromatography (GPC) system.

A 0.9 x 50 cm Bio-Rex (BioRad Laboratories) chromatography column, Type MT, was set up in a constant temperature atmosphere of 22.7°C. The column was packed with a 30 cm bed of Bio-Gel A-5M agarose beads, 100-200 mesh. The column eluent was 0.11N NaCl, adjusted to pH 8.0 with NaOH. The eluent hydrostatic head was adjusted to give a constant flow rate of 0.876 mL/min. Fractions were collected at 7 min intervals with a Technicon fraction collector. All components on the eluent stream were connected with 0.042 inch (ID) Teflon tubing and gum rubber sleeves. The system was flushed with solvent for 2 days to allow for column packing.

The polymer loading process was begun by draining off the solvent to the level of the gel packing. Two milliliters of the 10^{-3}% PVAm solution in 0.1N NaCl at pH 8.0 was loaded onto the bed with a syringe. The solution was then drawn into the bed. The sides of the column were washed with solvent and the solvent hydrostatic head applied.

The spectrophotofluorometric test for PVAm was employed to determine the concentration of PVAm in each fraction collected. In cases where the PVAm concentration in a given fraction exceeded the upper limit of the quantitative analysis calibration curve, appropriate sample dilutions were made.

POLYVINYLAMINE BEHAVIOR IN FLOCCULATED SUSPENSIONS UNDER SHEAR

After having established experimental evidence that an optimally flocculated colloid dispersion could be at least temporarily redispersed by hydrodynamic shear, a procedure was established for monitoring the behavior of PVAm molecular weight distributions by GPC. The procedure used is outlined below.

(1) Flocs at a given pH were manufactured with PVAm concentrations corresponding to those previously determined as being optimal for the respective pH.

(2) The newly-formed flocs were charged to the shear apparatus and subjected to a determined shear rate for 7 min and 12 sec. This time was calculated to be that necessary to permit each volume element one pass through the shear zone.

(3) After shearing, the suspension was removed from the shear apparatus and adjusted to pH 12.0 with 1.2N NaOH.

(4) The alkaline suspension was centrifuged at 75,000 g, 10°C for 2 hours on a Beckman Model L-2 ultracentrifuge before removing

the supernatant by syringe. Care was taken to insure that PSL was not removed with the supernatant.

(5) The pH of the alkaline PVAm solution was adjusted with 1.2N HCl to provide a pH of 8.0 when condensed to 2 mL.

(6) Rotoevaporation under vacuum to dryness was followed by dissolution in 2.00 mL distilled deionized water, yielding a solution of PVAm in 0.11N NaCl at pH 8.0.

(7) The 2 mL solution of PVAm was loaded on the GPC column as described above.

(8) The entire procedure was performed three times at each pH.

SURFACE CHARGE MEASUREMENTS

An investigation was conducted to monitor possible changes in the available surface charges of PSL due to the hydrodynamic forces exerted on the flocs. The work of Connor and Ottewill (151) on the adsorption of cationic surface active agents onto polystyrene surfaces kindled the idea that a small surfactant molecule might be useful in the examination of surface events under shear.

Connor and Ottewill showed through their work that the adsorption of surface active cations can be used to determine the number of anionic groups on the surface of PSL. They suggested that PSL has two sites for adsportion: charged sites which interact with the cationic head group of the surfactant and hydrophobic sites on which the alkyl chains adsorb. The adsorption isotherms exhibit a characteristic "knee," as shown in Fig. 12.

It is worth noting that the "knee" for all four compounds in Connor and Ottewill's work occurs at essentially identical values of Γ (amount adsorbed). Their investigation confirmed that the adsorption occurring up to the "knee" on the isotherm involves ionic interaction of the surfactant head with PSL

surface carboxyls. Adherence to Traube's Rule suggested that in this region the alkyl chains lie flat on the PSL surface.

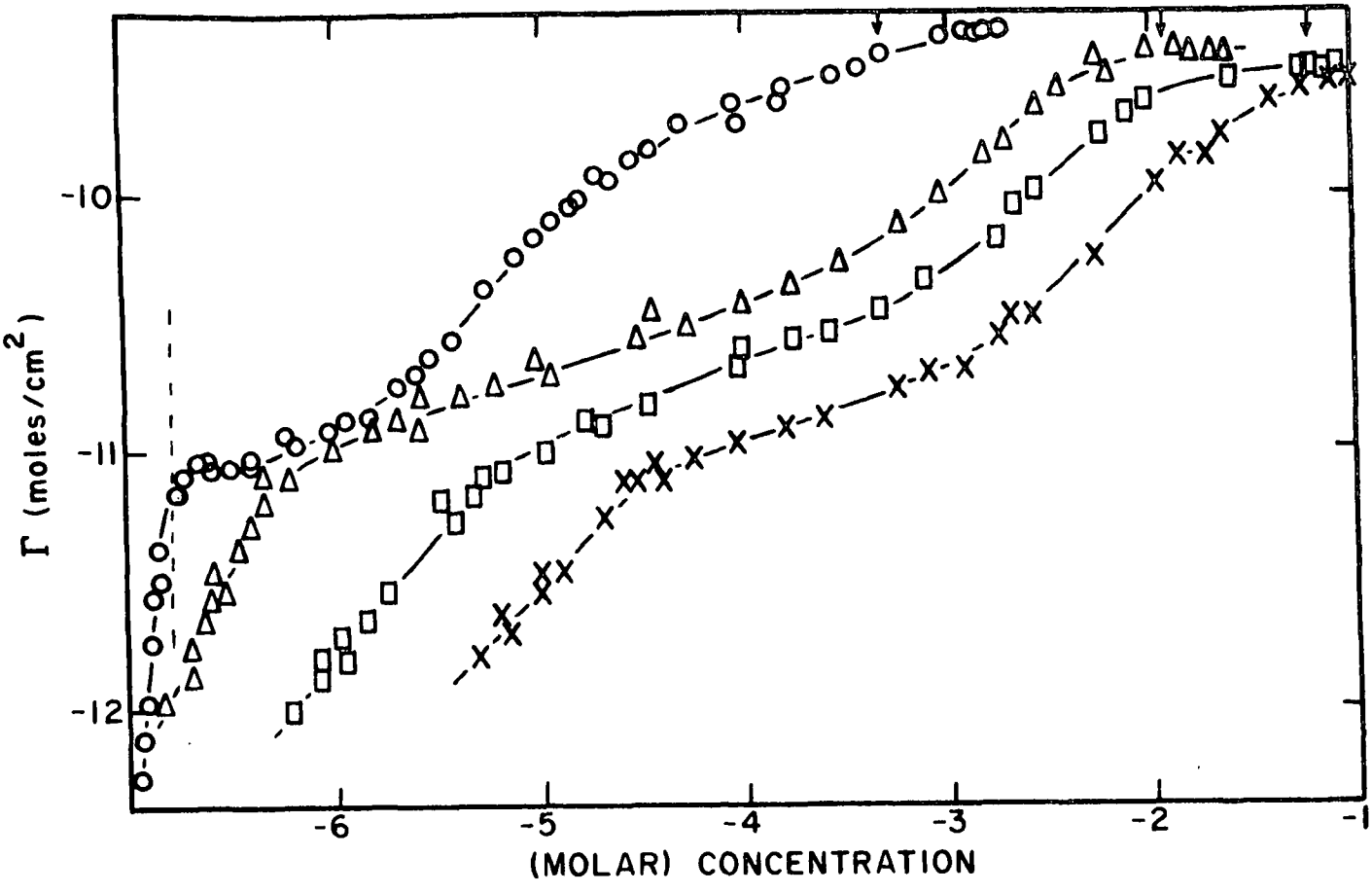

Figure 12. Adsorption Isotherms on Particles of Latex-G at pH 8.0 in 10^{-3}M KBr Solution. o = hexadecyltrimethylammonium; Δ = dodecyltrimethylammonium; □ = decyltrimethylammonium; X = octyltrimethylammonium; ↑ = c.m.c. Values; | = Reversal of Charge Concentration for the Hexadecyltrimethylammonium Ion (151)

A significant result of their research was the conclusion that the electrophoretic mobility of the PSL reversed sign at a surfactant concentration very close to the equilibrium concentration at the isotherm "knee."

To effectively monitor small concentrations and concentration changes in a manner that would not be affected by PVAm, the surface active agent used in this work was synthesized with ^{14}C-tagged methyl iodide. N,N-dimethyldodecylamine was quaternized with methyl iodide to form N,N,N-trimethyldodecylammonium iodide (TDA) in a manner similar to that outlined by Conner and Ottewill. Details of the synthesis are provided in Appendix IV.

Determination of the position of the isotherm "knee" was necessary to insure that all anionic groups on the PSL surface were neutralized by cationic surfactant groups. As adsorption above the knee is not affected by the charge density of the PSL, it was not desirable to work in that concentration range. A series of concentrations were made up from nonradioactive TDA so the expensive radiochemical tracer would be conserved. PSL was allowed to contact the TDA at 25°C on the flocculation wheel for 2 hours. The electrophoretic mobility of the particles was then measured on a Zeta Meter.

An important step to enable the attainment of reproducible results at low TDA concentrations was the treatment of all surfaces which would come into contact with the surface active agent. All such surfaces were exposed for several hours to a concentration of TDA which was a little higher than that to be used in a particular experiment. The surfaces were then rinsed twice with water.

Solution concentrations of ^{14}C-TDA were monitored by liquid scintillation counting. The procedures involved are outlined in Appendix V.

TDA adsorption of PSL was observed under the following conditions: (1) virgin PSL, (2) PSL treated with optimum flocculation concentrations of PVAm, and (3) flocs sheared in the Hercules viscometer. The latter experiment was performed under two conditions. In the first case, TDA was added before shearing, to detect loss of PVAm for PSL surfaces. In the second case, TDA was added immediately after shear, to monitor possible PVAm rearrangement on the surface.

EXPERIMENTAL RESULTS AND DISCUSSION

CHARACTERIZATION OF POLYSTYRENE LATEX PARTICLES

The uniform size and shape of the Dow PSL are illustrated by the representative transmission electron micrograph in Fig. 13.

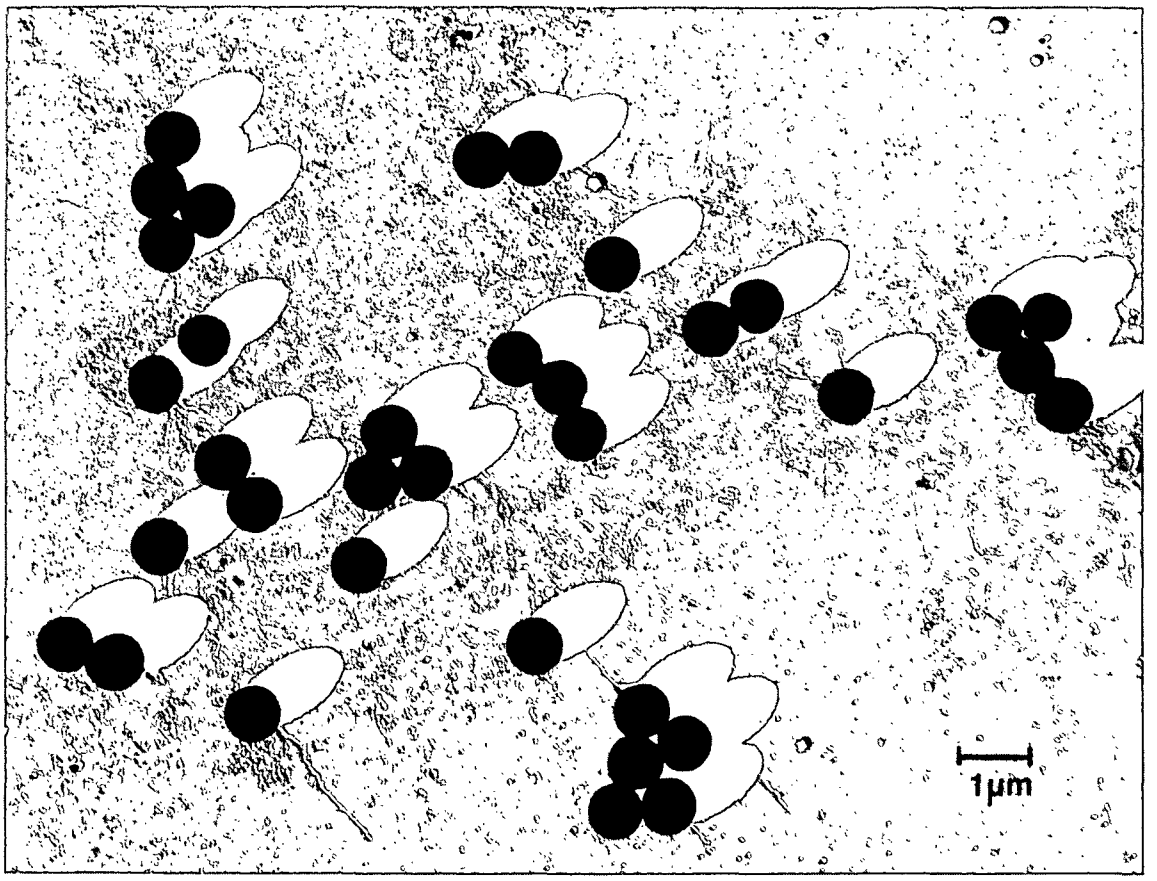

Figure 13. Dow Polystyrene Latex

SURFACE CHARGE DENSITY

The number of stabilizing negative charges on the particle surface is one of the most important parameters affecting the results of flocculation adsorption studies. The negative charges on PSL surfaces are usually the result of ionized carboxyl and/or sulfate groups (123-125,127). The extent of ionization that occurs as a function of pH can be determined by potentiometric titration (12,39,128,129).

The original titration data, pH versus milliliter of acid or base for PSL particles in water and for the blank, are shown in Fig. 14. Ionic strength of the blank was adjusted to 10^{-4}M NaCl to insure ionic equivalence with the polymer solution. The inflection near pH 6 is characteristic of the dissociation constant of sulfate groups. The presence of surface carboxyl groups would be indicated by an inflection near pH 4.2 (124,152). Absence of such an inflection point is evidence against the presence of surface carboxyls. The observation that titration equilibria were reached instantaneously supports the contention that the ionizable groups are at the particle surface, and not bedded internally (127). Only the ionized groups at the particle surface are significantly effective in electrochemically stabilizing the suspension.

The equivalence points of the potentiometric curves were determined by plotting the derivative $\Delta pH/\Delta mL$ against milliliter of acid or base. A representative plot is shown in Fig. 15.

The difference between the equivalence points of the PSL suspension and the blank sample of electrolyte constituted the amount of ions adsorbed by the surface at the given pH. The surface charge density, σ, was then calculated in terms of microcoulombs/cm^2 by utilizing the relationship

$$\sigma = (A)(F)/S \times 10^{-1}, \tag{18}$$

where σ = surface charge density expressed in μcoulombs/cm^2

A = amount of H^+ adsorbed, expressed in meq/g

S = surface area, expressed in m^2/g

F = Faraday's constant, expressed as 96,489 coulombs/eq.

The calculated surface charge density of the Dow PSL used in this study is 15.3 μcoulombs/cm^2, which is equivalent to about one charge per 105 A^2 of

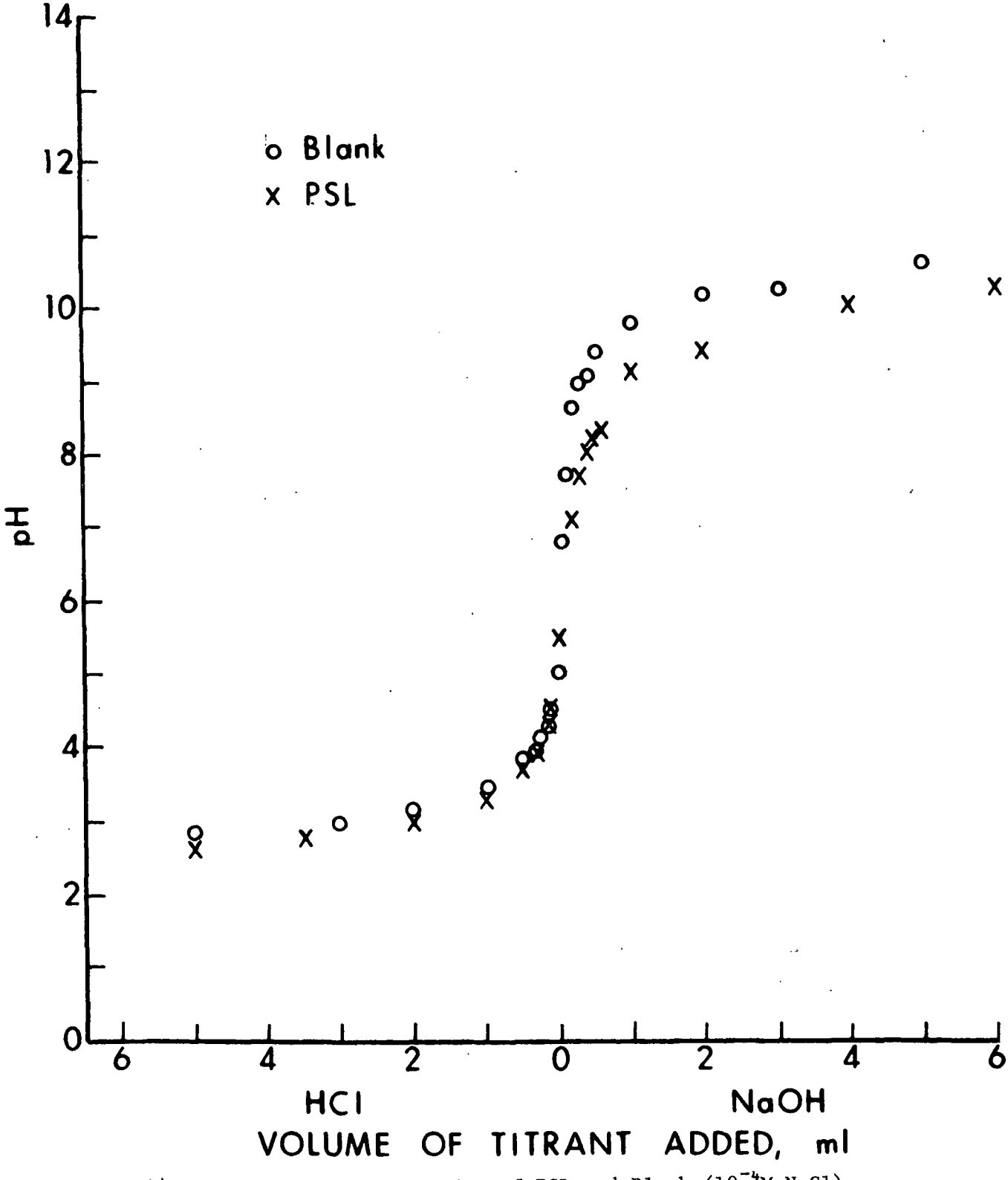

Figure 14. Potentiometric Titration of PSL and Blank (10^{-4}M NaCl)

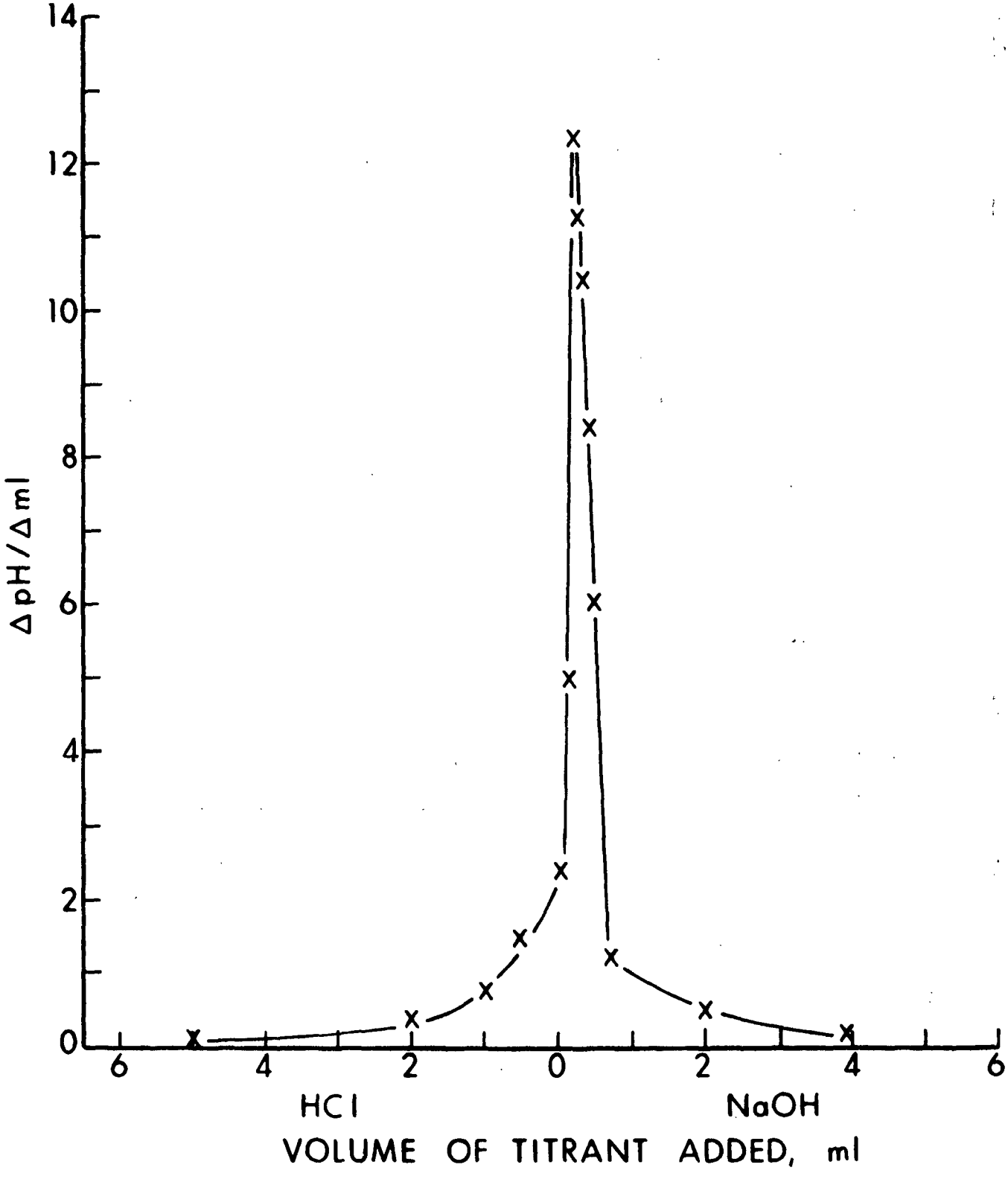

Figure 15. First Derivative of Potentiometric Titration of PSL

surface area. These values are concurrent with values determined by other workers using PSL particles (11,39,124,125).

Although quantitatively less precise than potentiometric titration, measurement of particle electrophoretic mobility provides a quick method of obtaining a measure of the net charge of a given particle. Electrophoretic mobilities were measured on a Zeta Meter microelectrophoresis apparatus. The electrophoretic mobility, ν, of a particle is defined as

$$\nu = U/\Pi, \tag{19}$$

where U = velocity of the particle in cm/sec

Π = voltage drop (in esu) per centimeter length of the suspending medium

The zeta potential, ζ, may then be calculated (153) according to

$$\zeta = \nu 4\pi \eta_o/\varepsilon, \tag{20}$$

where η_o = viscosity of the suspending medium (poise)

ε = dielectric constant (farads/cm)

The zeta potential of PSL at pH's 3, 6, 9, and 10 (no added salt) was determined to be -62.5 mv. This corresponds well with the zeta potential of Eggert's 0.794 μm PSL particles obtained from Dow in 1973 (39). The fact that the zeta potential is constant over the pH range of 3-10 is further support for the presence of only ionized sulfate groups as the stabilizing negative charges on the particle surfaces.

CHARACTERIZATION OF POLYVINYLAMINE

An infrared spectrum of the PVAm powder supplied by Bloys van Treslong was run in potassium bromate. Absorbance due to tertbutylcarbamate blocking groups, expected to appear at 1200 and 1750 cm^{-1}, are not present (Fig. 16-A).

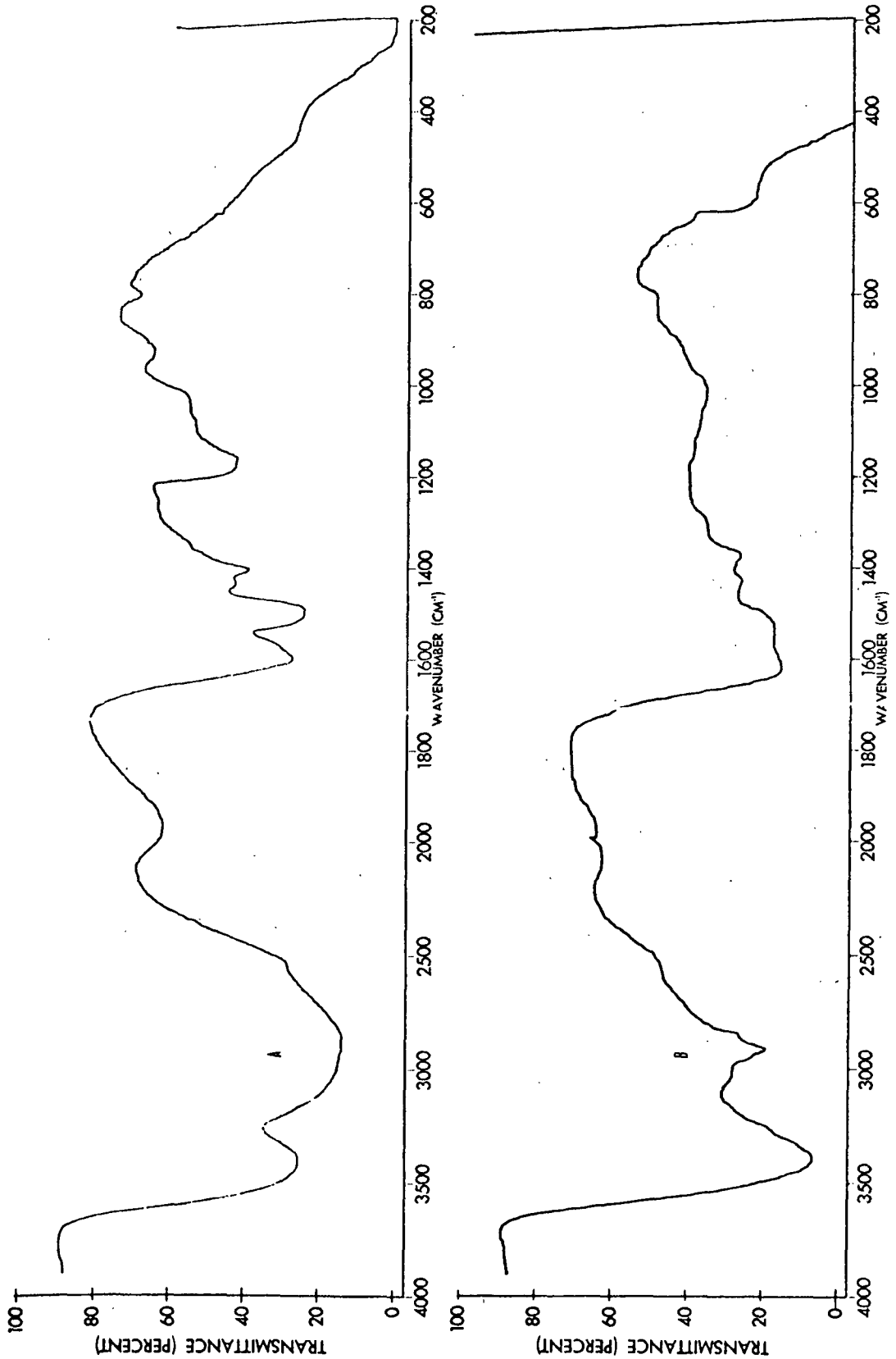

Figure 16. Infrared Spectrum of PVAm Samples in KBR. A: Supplied by Bloys van Treslong;
B: From Hydrolyzed PACE Supplied by Dynapol

This spectrum was used as a reference to check the purity of the PACE hydrolysis product (Fig. 16-B). Absorbance bands due to unhydrolyzed acetate groups around 1250 and 1750 cm^{-1} are absent. It was therefore assumed that the PACE sample was completely hydrolyzed to PVAm.

GEL PERMEATION CHROMATOGRAPHY

A total of five fractionation runs were performed to process the 0.66 g of PVAm(D) (from PACE supplied by Dynapol) available. A characteristic elution curve is shown in Fig. 17. No shift in appearance times between runs occurred, indicating that no column packing took place.

The most salient feature of this elution curve is the presence of two distinct peaks. A comparison to Fig. 18, the elution curve for the lower molecular weight PVAm(B) (supplied by Bloys van Treslong), suggests that there may have been some shear degradation of the PVAm(D) from the preparation procedure.

Because of the small quantity of polymer available, it was not possible to separate each peak into several fractions, assuming only one fraction would be used. The fractions containing the first peak were combined to form a single high molecular weight fraction, F1. The second peak was divided into ten separate fractions, with like fractions combined and designated as fractions F2 through F11 (see Fig. 17).

MOLECULAR WEIGHT

The weight average molecular weights of fractions 1 and 7 were determined by sedimentation equilibrium techniques. Experimental details and results are provided in Appendix I. The molecular weight of fraction 1 was 450,000 daltons. Fraction 7 was found to be 286,000 daltons.

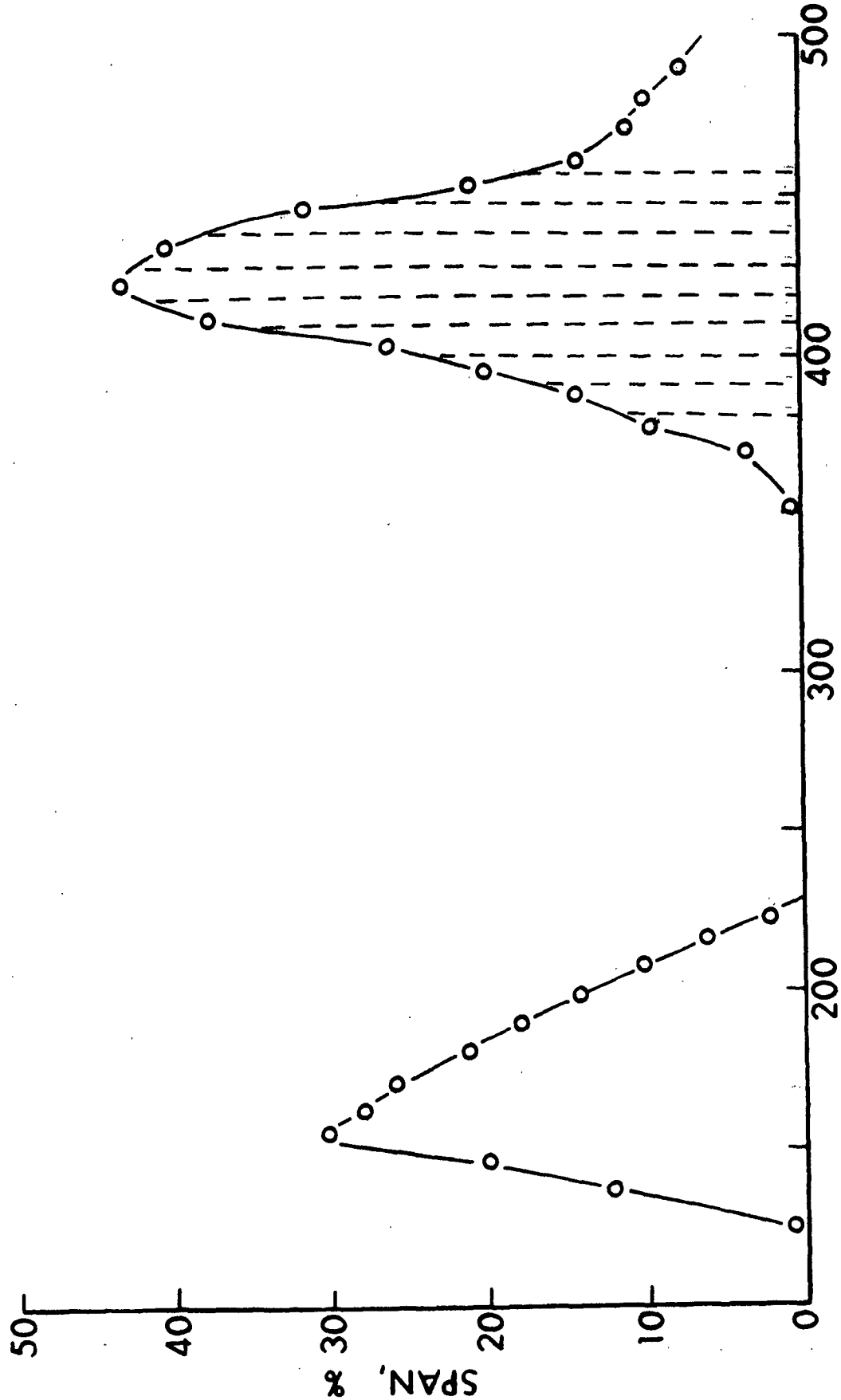

Figure 17. Elution Curve for PVAm(D)

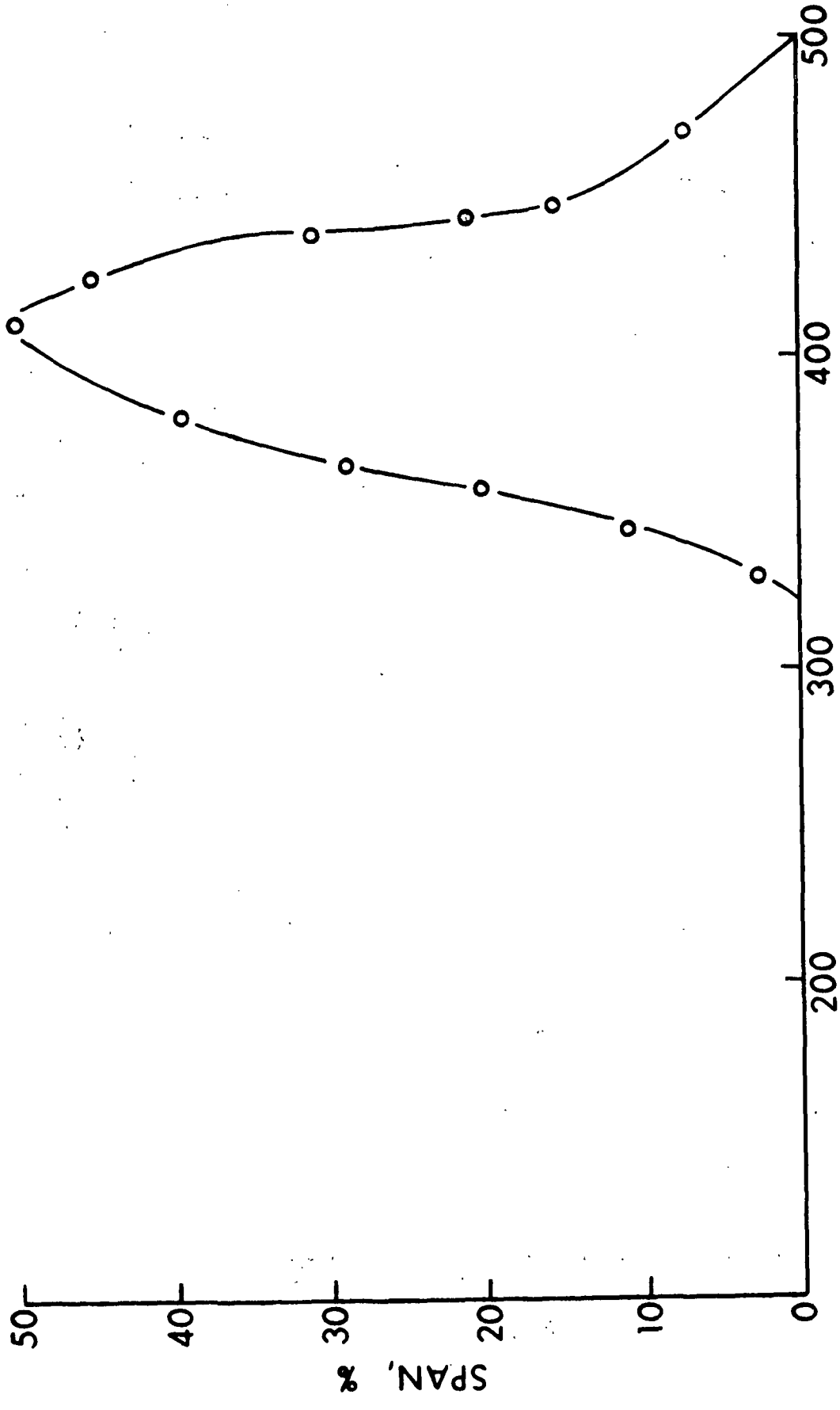

Figure 18. Elution Curve for Low Molecular Weight PVAm(B)

DIFFUSION COEFFICIENT

The diffusion coefficient of PVAm (fraction F1) was determined in 0.1N NaCl at pH 8 to be 2.5×10^{-7} cm^2/sec. The diffusion coefficient at infinite dilution, D_o, may be used to estimate the size of a hydrodynamically equivalent sphere with the same frictional coefficient, $q = 6 \pi \eta_o R_e$, through the Stokes equation (154):

$$R_e = kT/6\pi \eta_o D_o, \tag{21}$$

where R_e is the radius of the hydrodynamically equivalent sphere. This calculation is valid only under conditions in which macromolecular diffusion is not affected by electrophoretic effects, and can therefore be applied to PVAm in strong salt solutions. The calculated values of R_e for PVAm under these conditions is 87 A.

TITRATION OF POLYVINYLAMINE

The study of the potentiometric behavior of several polybases (155) has led to the conclusion that the dependence of degree of ionization on solution pH is essentially determined by the characteristics of individual ionic groups as modulated by the diffuse electrostatic field of all the charged groups on a given molecule.

To determine the degree of protonation of PVAm as a function of pH, a sample of Bloys van Treslong's PVAm was studied at a concentration of 0.001M in amine. Investigations of weak polybases have shown that titration behavior was independent of both molecular weight (156,157) and polymer concentration (156-158).

The degree of protonation, α, at any pH may be calculated from the electroneutrality condition,

$$\alpha = (C_H)_a - (C_H)_f + (C_{OH})_f/C_m, \qquad (22)$$

where $(C_H)_a$ = proton concentration resulting from addition of HCl

$(C_H)_f$ and $(C_{OH})_f$ = concentrations of free protons and hydroxyl ions as determined from titrations of strong acid and base

C_m = monomeric equivalent concentration of polyelectrolyte (128,129)

Figure 19 shows the curve pH versus α for PVAm with no added salt. Increasing the ionic strength of the solutions at constant polymer concentration would cause the normally encountered pH to shift to higher values: the "salt effect" has been demonstrated by others (158,159), and is attributed to a suppression of the polyion electrostatic potential by the added salt counterions. This phenomenon allows for a decrease of the repulsion of hydrogen ions in solution and a subsequent increased binding to the polyelectrolyte.

The shape of the curve in Fig. 19 is in general agreement with the curves obtained by Katchalsky, et al. (158), and Bloys van Treslong and Staverman (159). The steep change in pH with degree of ionization has been explained in terms of a strong nearest-neighbor interaction for the closely situated amino groups. A similar behavior has been reported for polyethylenimine by Kitchener and Shepherd (160) and Lindquist (12).

The thermodynamics of polybase titrations have been treated thoroughly by Katchalsky (161). Through his treatment he has shown that the titration curve should be symmetrical about the point of half neutralization. Such symmetry is apparent in Fig. 19. The steep change in pH from $\alpha = 0$ to $\alpha = 0.1$ can be attributed to Van der Waals attractions between various segments of the molecule (161). From $\alpha = 0$, protonation will take place quickly on the exterior amine groups of the hypercoiled molecule, since the maximum distance between like-charged groups occurs at the periphery of the molecular coil. This quick

protonation, in turn, results in large values for $d(pH)/d\alpha$ because the ionization repulsive field is insufficient to break the major portion of Van der Waals attractions. The molecule thus remains in a hypercoiled state (161,162). It is not until about 10% ionization that the electrostatic field energy is of sufficient magnitude to expand the coil. It is this same electrostatic field that produces a correspondingly steep change in $d(pH)/d\alpha$ as $\alpha \rightarrow 1$. Complete protonation becomes difficult as any potentially-adsorbed proton attempts to penetrate the electrostatic field of adjacent positively charged sites.

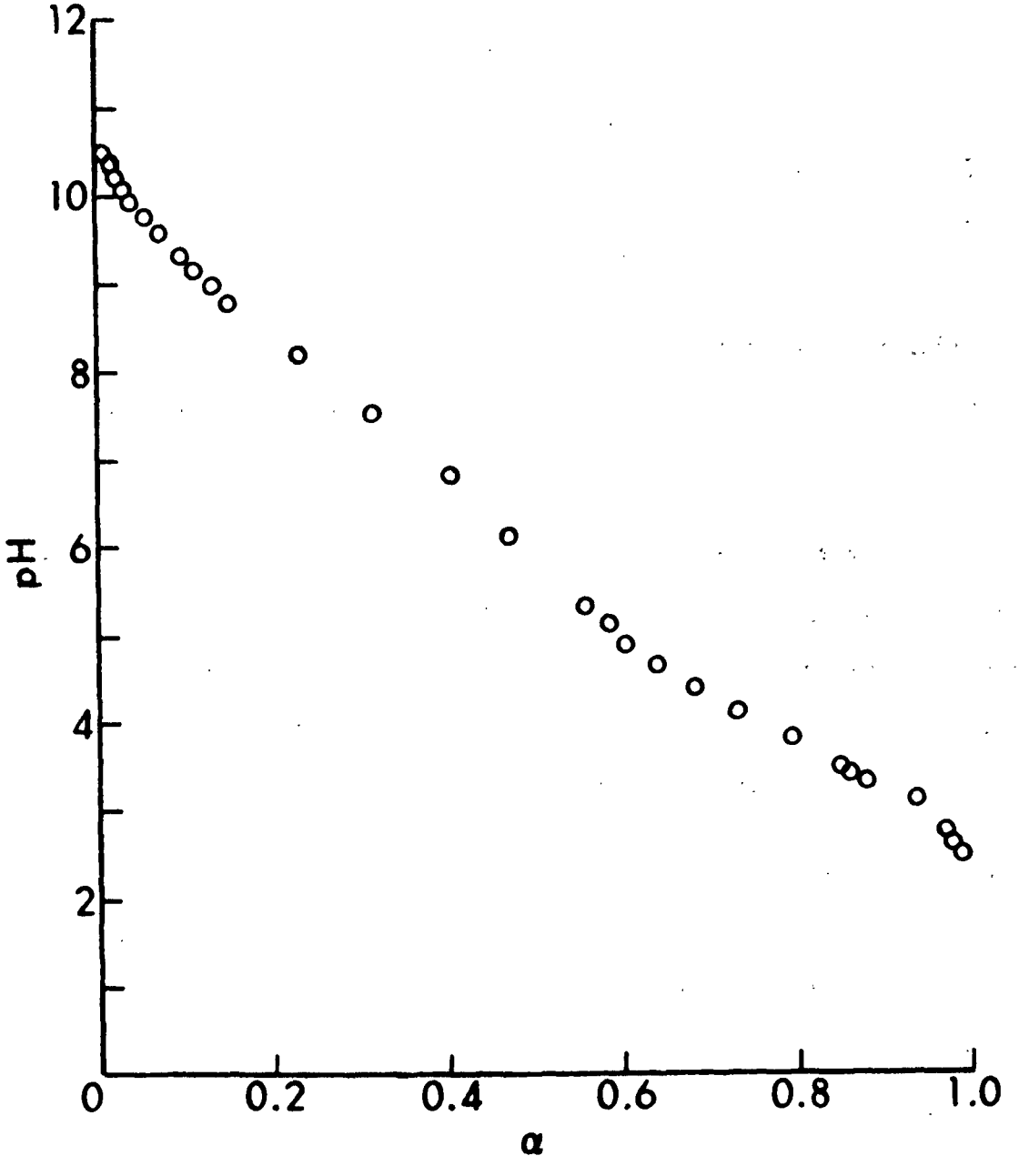

Figure 19. Degree of PVAm Protonation with pH

Katchalsky, et al. (158) used the Ising model of cooperative phenomena (163) to theoretically evaluate the fundamental potentiometric equation. They found a good agreement between experimental values and the theoretical curves. The titration equations obtained by Katchalsky are equivalent to those of Marcus (164) and Lifson (165). The apparent equilibrium constant, K_a, of the ionization reaction expressed in Equation (17) is related to the thermodynamic ionization constant, K_o, by (166,167),

$$pK_a = pK_o + (0.4343/kT)\ \Delta G_{el} \tag{23}$$

Attempts to derive theoretical expressions for ΔG_{el} based on model calculations (168) have been only qualitatively successful. As a result, the equation most applicable for discussions of titration data is

$$pH = pK_a - \log\ 1-\alpha/\alpha \tag{24}$$

Equation (24) is frequently referred to as the Henderson-Hasselbach equation. It predicts a monatonic decrease in pH with increasing α, and a constant ionization potential for all ionic species.

Figure 20 reveals that the apparent ionization constant of PVAm is not independent of charge density. Inflections of this type have been attributed to conformational changes in the macromolecular structure (162,169,170). A linear polyelectrolyte in solution would be expected to transform from a compact coil at $\alpha = 0$ to an extended and stiff chain as $\alpha \rightarrow 1$.

To test the theories concerning flocs formed with electrostatic patches, PVAm should be used in a solution where α approaches 1. According to Fig. 19 this occurs at about pH 3. Lowering the pH further results in very small increases in α, and challenges the stability of the PSL. For flocculation by polymeric bridging, a PVAm species with $\alpha \rightarrow 0$ is necessary. At pH 10, PVAm

is only 3% protonated. Because the possibility of a hypercoil exists to approximately 10% ionization, a third pH was chosen to test flocs formed by a low α polyion that was not in a hypercoiled state. From Fig. 19 it is evident that at pH 9 approximately 13% of the available nitrogens on PVAm will be protonated. At only 13% ionization it would be expected that the solution configuration of PVAm would still be approximated by a random coil. The relatively low electrostatic interaction potential with a PSL surface would suggest a flocculation mechanism best approximated by polymeric bridging.

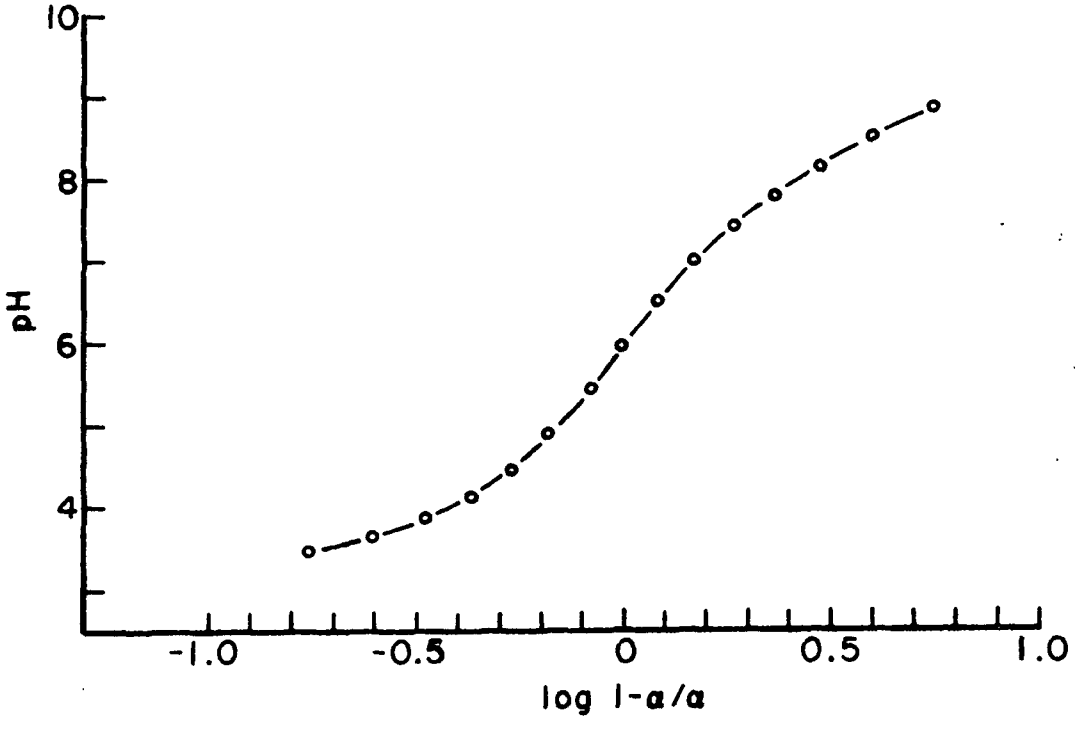

Figure 20. Titration Data for PVAm Solutions According to the Henderson-Hasselbach Equation (158)

VISCOSITY

The intrinsic viscosity, [η], of PVAm, fraction F1, was used to estimate the dimensions of the solvated polyion in 0.1N NaCl at pH 12, and at pH's 3, 9, and 10 without salt. The value of [η] was obtained from a linear least-squares extrapolation of η_{sp}/C to zero polymer concentration.

Figure 21 exhibits a traditional plot of specific viscosity against concentration for PVAm in 0.1N NaCl at pH 12. A value of [η] = 0.48 dl/g was obtained. The linearity of this plot suggests that under these conditions

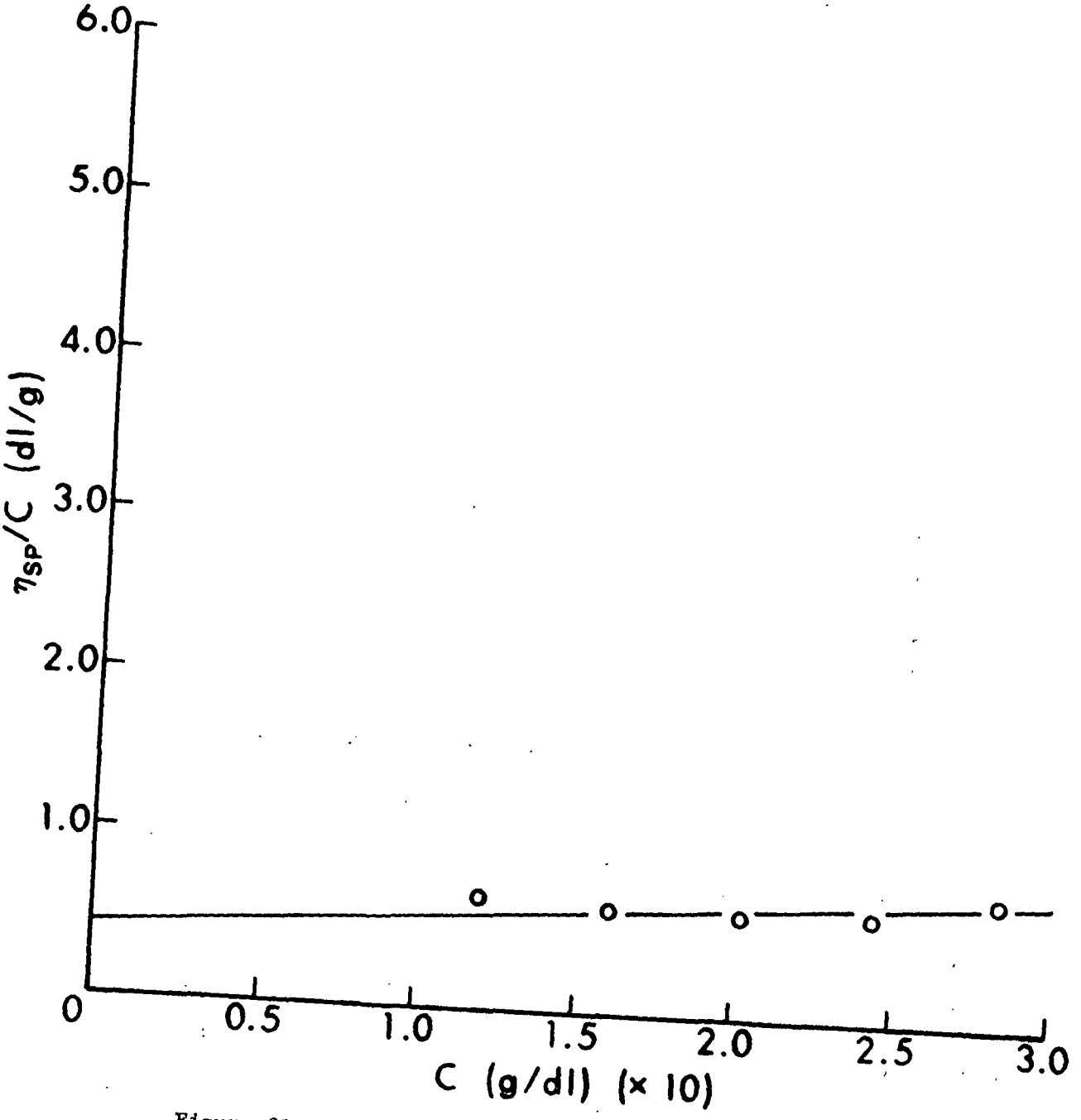

Figure 21. Viscosity of PVAm in 0.1N NaCl at pH 12

PVAm behaves as an uncharged molecule with randomly-oriented segments. Bloys van Treslong and Mora (120) reached an equivalent conclusion.

Using the emperical value for ϕ of 3.67×10^{22} the radius of gyration for an uncharged PVAm molecule at pH 12 in 0.1N NaCl may be calculated from Equation (6) as 180 A. The relationship between radius of gyration and radius of a hydrodynamically equivalent sphere has been proposed by Kirkwood and Riseman (171) to be

$$\xi = R_e/\langle s^2\rangle^{\frac{1}{2}} = 0.875 \qquad (25)$$

Their derivation of this relationship assumed the polymer chain to be a string of spherical beads, with bond lengths and bond angles treated as in the derivation of the equations of the radius of gyration. The result was averaged over all possible configurations of the polymer chain in a theta solvent. Flory (22) argues that in a good solvent, the segment density of the chain will be lower, providing greater freedom of motion for the solvent. This increased freedom of solvent motion was predicted to lower the value of ξ, and has been experimentally verified (23). When the viscosity of the solution, η, is related to that of the solvent, η_o, by

$$\eta = \eta_o(1 + 2.5\partial), \qquad (26)$$

where ∂ is the volume fraction of the solute in the total volume of the solution, Flory (22) predicts that $\xi = 0.665$. Both theories (22,171) predict that for polymer coils with the number of monomer segments exceeding 10^3, ξ will be constant. Using the value of $\xi = 0.665$, the radius of the hydrodynamically equivalent sphere for PVAm at pH 12 in 0.1N NaCl is 120 A.

If the viscosity of low ionic strength polyelectrolyte solutions is to be investigated, the effects of apparent chain expansion must be eliminated.

An empirical analytical expression proposed by Fuoss (172) to describe the concentration dependence of the viscosity of dilute polyelectrolyte solutions has been found to apply to several systems. Fuoss suggested that the data should follow the relation

$$\eta_{sp}/C = A/(1+B\sqrt{C}), \qquad (27)$$

where η_{sp} = specific viscosity of the solute

C = concentration of the solute

The Fuoss equation predicts a monotonic increase of the reduced viscosity with dilution and a finite intercept at zero concentration. Several workers (11, 12,173-175) have used such an expression to obtain extrapolated intrinsic viscosity values. However, Equation (27) has been shown to be inadequate if the polyion is very long (176).

Rosen, et al. (177) predicted that a maximum would occur in the reduced viscosity-concentration curve. This suggests that the Fuoss equation, while adequately describing viscosity behavior in a relatively concentrated solution, fails at high dilution. Careful studies of the viscosity of polyelectrolytes at high dilution and zero shear rate have substantiated this (178-187).

The increase in viscosity with dilution at constant pH can be explained in terms of an unfolding of the polyion coil due to decreased shielding of neighboring charges. The decrease is the result of a reduction of the counter-ion concentration about the fixed polymer charges. Hermans and Pals (188) have shown that this increase can be eliminated with isoionic dilution.

After the polyions have reached their maximum extension with dilution, the concentration dependence should be determined solely by intermolecular interactions. Darskus, et al. (189) suggested that further increases in

viscosity could be attributed to the energy dissipated when the molecules passing each other are displaced normally to the streamlines due to the long-range repulsive forces between their double layers. The magnitude of this effect is expected to be the highest for small molecules at low ionic strengths.

In terms of the Fuoss equation, $[\eta] = A$ at very low salt concentrations. In this case of extremely low salt concentrations but high degrees of ionization, the macromolecules are highly stretched, so that A is proportional to the square of the degree of polymerization (190). The value of B has been shown to depend on the dielectric constant of the medium, and is probably related to the magnitude of the electrostatic forces between segments of the polyion chain (172,175).

For the determination of values for A and B from experimental results, Equation (27) can be rearranged into the following form (191).

$$C/\eta_{sp} = 1/A + (B/A)\ C^{\frac{1}{2}} \qquad (28)$$

In plots of Equation (28) most weight is given to points in the range of higher concentrations where the precision of the measurement is better. However, if A is large, a precise determination of $1/A$ is not possible.

Figure 22 illustrates the viscosity data for PVAm with no added salt. Because polyelectrolyte effects are irrepressible under these conditions the data have been plotted in accordance with the Fuoss equation.

The steep slope of the pH 3 data suggests very strong electrostatic interactions between segments of a given chain. The fact that the extrapolated value of C/η_{sp} at zero concentration appears to be negative suggests both that the Fuoss theory is not valid at low concentrations (176-187), and that the

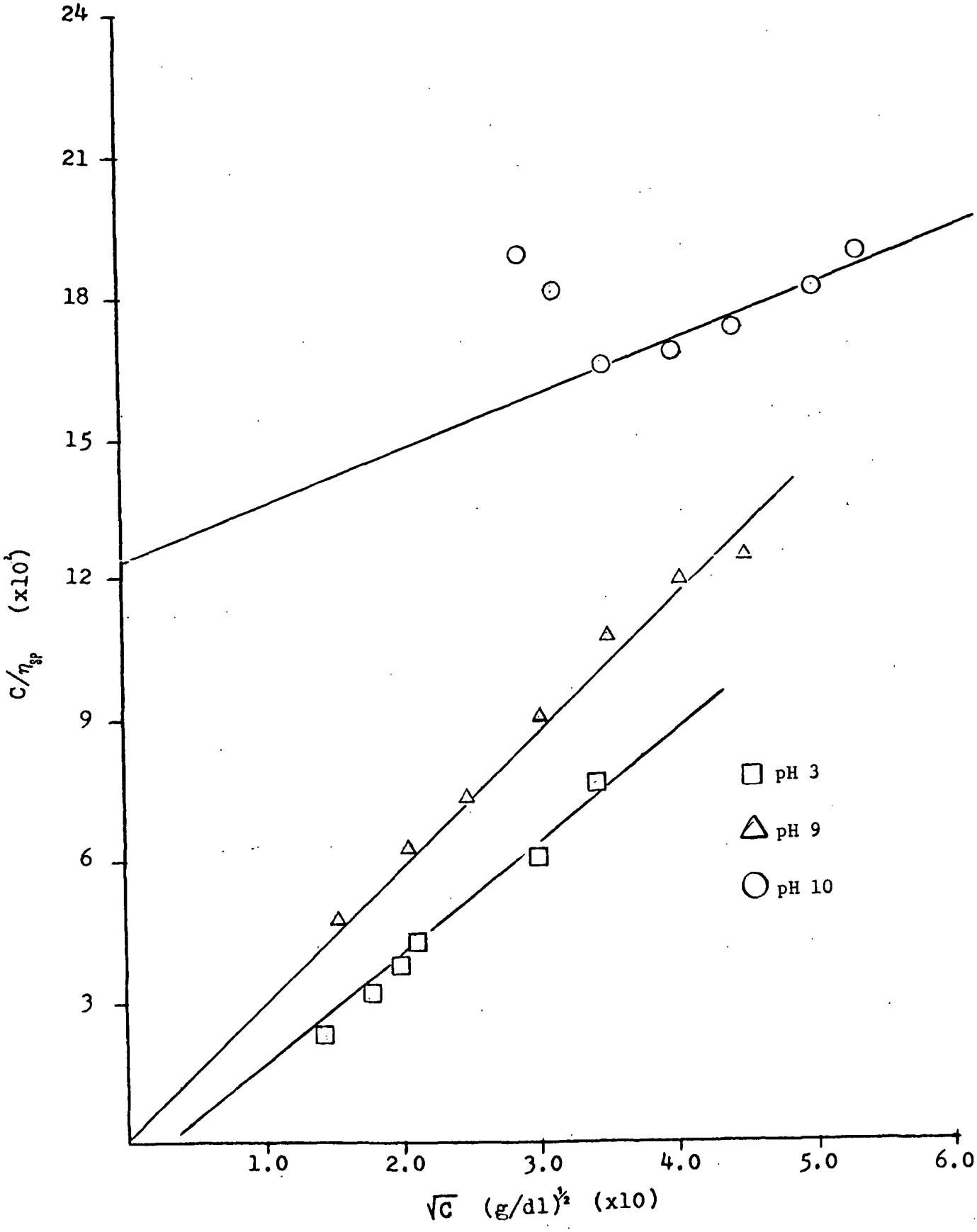

Figure 22. Viscosity of PVAm, No Added Salt

polyion is expanded to enormous dimensions in the extremely dilute concentrations. A point to be kept in mind is that the abscissa value for the PVAm optimum flocculation concentration would be 0.004 $(g/dl)^{\frac{1}{2}}$.

Salient aspects of the plot for pH 9 data are the much more gradual slope, indicative of a reduction in the magnitude of electrostatic interactions between neighboring monomer units. The value of C/η_{sp} at zero concentration is approximately 0.007, yielding an intrinsic viscosity of about 143 dl/g. The variation between this value and the value determined for the supposedly unperturbed molecule suggests that the configuration of PVAm at pH 9 is not approximated by a random coil. Assumption of an elliptical shape is more in order (177).

The slope of the plot for PVAm at pH 10 is even more gradual than that of the pH 9 data as would be expected from Katchalsky's theory (190). The break in the data at extremely low concentrations is consistent with previous results (176-187). The value of the intrinsic viscosity, as calculated by extrapolation to zero concentration is 7.98 dl/g. The remarkable change of this value from the value at either pH's 9 or 3 indicates the conformation and effective size change that the PVAm molecule undergoes as the pH of the medium is raised.

Although no precisely quantitative information can be gathered from the above treatment of the viscosity data collected, certain trends are prominent enough to prohibit their being ignored. In all instances, the free solution configuration of PVAm without salt has dimensions greater than the theoretical hypercoil found at pH 12 in 0 1N NaCl. As the pH is lowered and more monomer units acquire protons, the magnitude of the electrostatic repulsive interactions between neighboring segments increases markedly. As a result, the intrinsic viscosity rises as the molecules expand to very large dimensions.

Table I provides a summary of the intrinsic viscosity of PVAm under the various conditions mentioned above, and the radius of the hydrodynamic equivalent sphere as calculated from Equation (6) using Flory's value of $\xi = 0.665$. While the certainty with which values of the hydrodynamic radius can be experimentally determined decreases with increasing $[\eta]$, the extent of polyion expansion with increasing charge density is readily apparent. Values at pH 3 are merely estimates based on data trends and physically meaningful interpretations.

TABLE I

INTRINSIC VISCOSITY OF PVAm

Solvent	pH	$[\eta]$(dl/g)	R(A)
0.1N NaCl	12	0.48	120
Water	10	7.98	306
Water	9	143	800
Water	3	∿10,000	3,300

QUANTITATIVE ANALYSIS

The standard curve used for quantitative analysis of unknown PVAm solutions is shown in Fig. 23. Linear regression analysis of the data up to 0.1 mg/liter provided the following relationship:

$$\log [\text{concn. (mg/L)}] = 0.0843\ (\%\ \text{transmittance}) - 4.594 \qquad (29)$$

The break in the curve around 0.1 mg/liter is consistent with the results of several researchers. Shore, et al. (192) found that an acidified product of OPT and histamine yielded a Beer's Law relationship between luminescence and concentration from 0.005 to 0.5 mg/liter. Marton (193) found photofluorescent results with this fluorogenic reagent and primary amines that followed Beer's Law for concentrations up to 0.24 mg/liter. The slight variation in

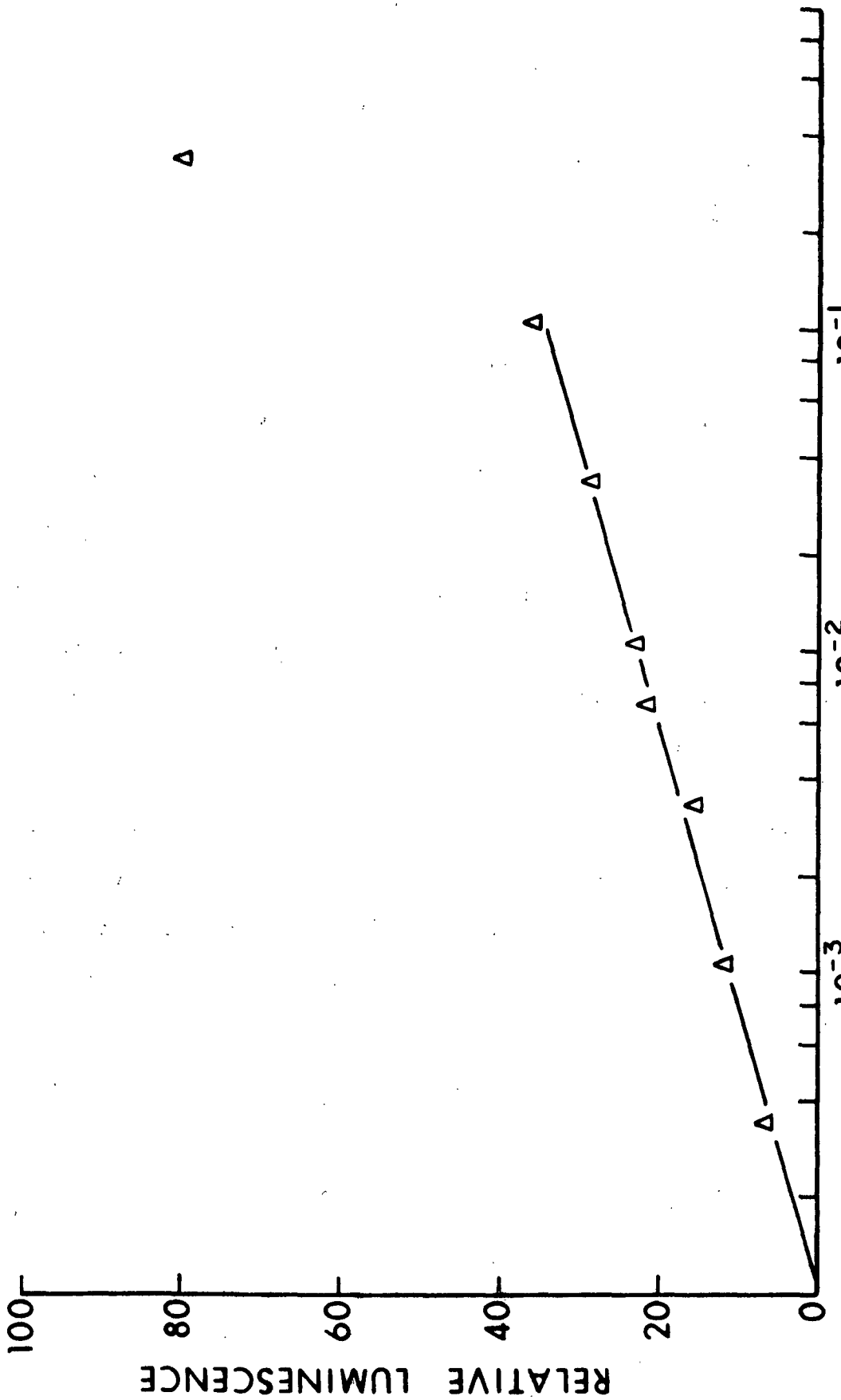

Figure 23, Standard Curve for PVAm Quantitative Analysis

break-off point can be attributed to variations in molecular weights. It is possible that the break from Beer's Law can be attributed to the induction of a solid phase resulting from low solubility of the fluorophor in water. This precipitation has also been noted by Seekles (194), as well as by Thiele and Winter (195).

FLOCCULATION OF POLYSTYRENE LATEX WITH POLYVINYLAMINE

The optimum flocculation concentrations (OFC) for the PVAm/PSL system were determined turbidimetrically at three pH's. The degree of protonation of PVAm at pH 3.0 is 95%; at pH 9.0 the degree of protonation is 13%; at pH 10.0 PVAm is about 3% protonated.

Figure 24 shows the flocculation behavior of the PVAm/PSL system at pH 3. The OFC has been arbitrarily characterized as the midpoint of the U-shaped zone of minimum relative turbidity. The concentration of PVAm at the pH 3 was determined as 0.178 mg/liter.

The 95% protonation of PVAm provided a model of a high interaction-energy system. The fact that the resultant charge of the PSL is still negative at the OFC indicates that a portion of PSL surface has not had its electrostatic charge neutralized or reversed. This phenomenon has been observed before (39) and is suggested to be characteristic of high interaction-energy systems in which patch-type adsorption of the polyion is thermodynamically preferred (11,39).

Figure 25 shows the flocculation behavior of the PVAm/PSL system at pH 10. The PVAm concentration at OFC was determined as 3.35 mg/liter.

Because the PVAm has only 3% of its amines in a protonated state, the major forces of attraction to an anionic PSL surface will be these few cations

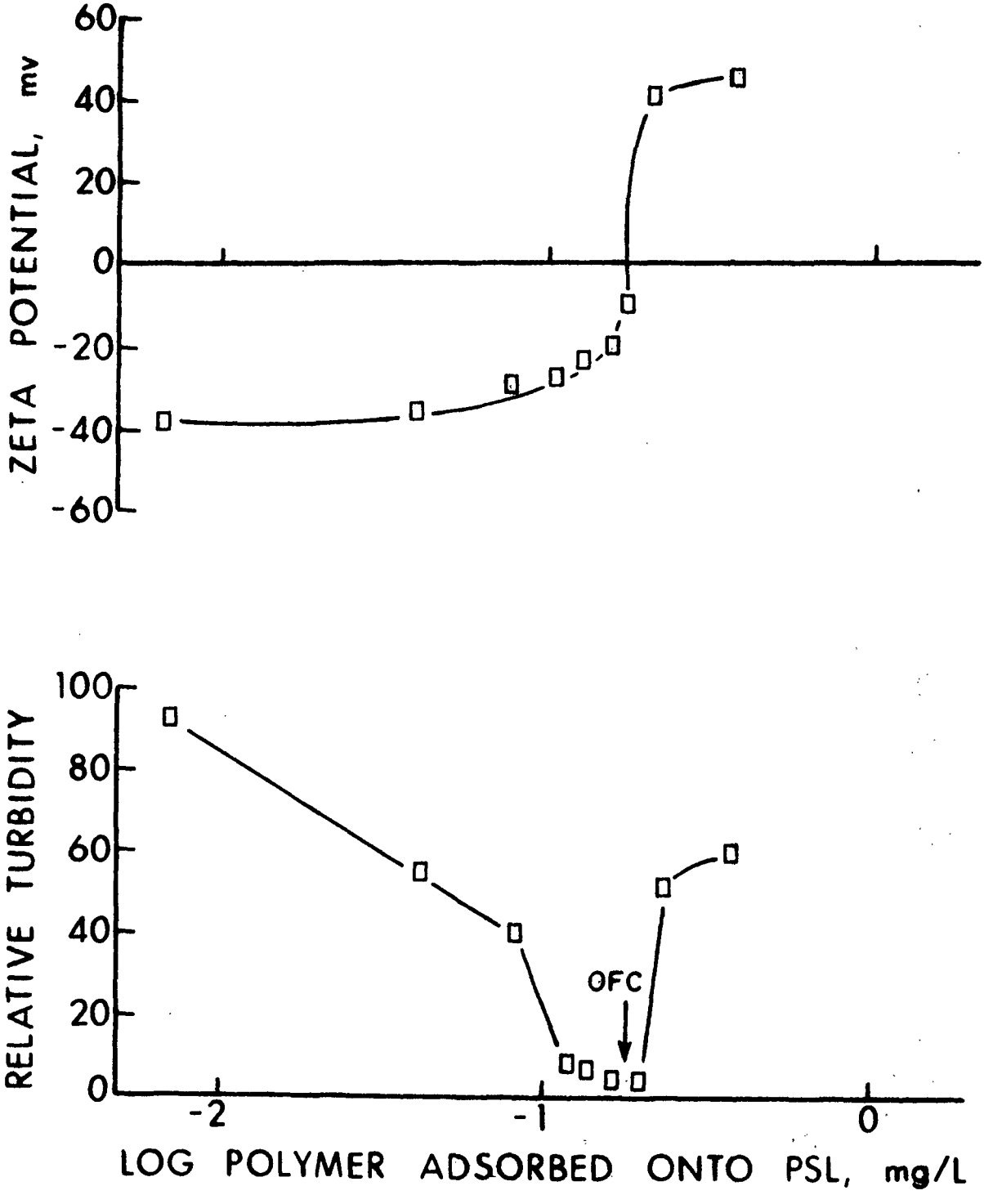

Figure 24. Flocculation Curve for PVAm at pH 3

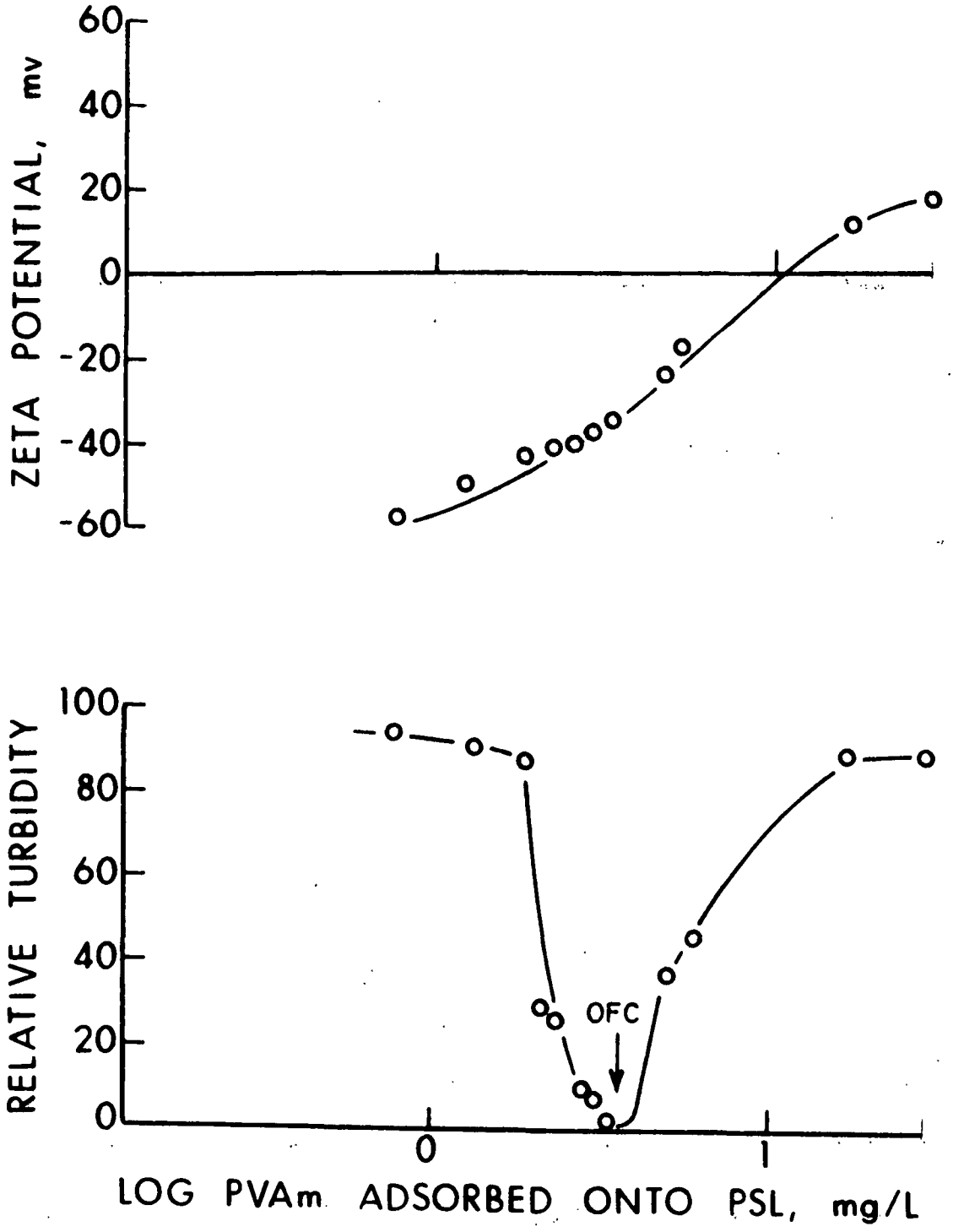

Figure 25, Flocculation Curve for PVAm at pH 10

and London-Van der Waals forces. These characteristics provided a suitable model as a system of low interaction energy.

Figure 26 shows the flocculation behavior of the PVAm/PSL system at pH 9. With only 13% of the available nitrogen groups of PVAm protonated, this system could be classified as a relatively low charge density system. However, it can be seen by comparison to Fig. 24 that the ability to flocculate optimally is already resembling that of a system containing a nearly fully-charged molecule. The concentration of PVAm at the OFC is 0.605 mg/liter. On the basis of this information it is possible to speculate that the adsorbed configuration of PVAm on PSL at pH 9 is patchlike.

Table II provides information concerning the total number of positive charges available at the OFC of each pH. The corresponding total number of PSL negative charges was 5.76×10^{16}. Inspection of the data in Table II reveals that the number of positive charges available in any of the systems is never enough to permit 1:1 association with all negative PSL charges. Arguments invoking simple charge neutralization are therefore not valid.

TABLE II

COMPARISON OF OFC'S

pH	OFC (mg/L)	ζ at OFC (mv)	No. of PVAm Molecules per PSL Particle	PVAm H^+ Available
10	3.35	-35	1233	1.38×10^{16}
9	0.605	-5	223	1.08×10^{16}
3	0.178	-10	66	2.31×10^{16}

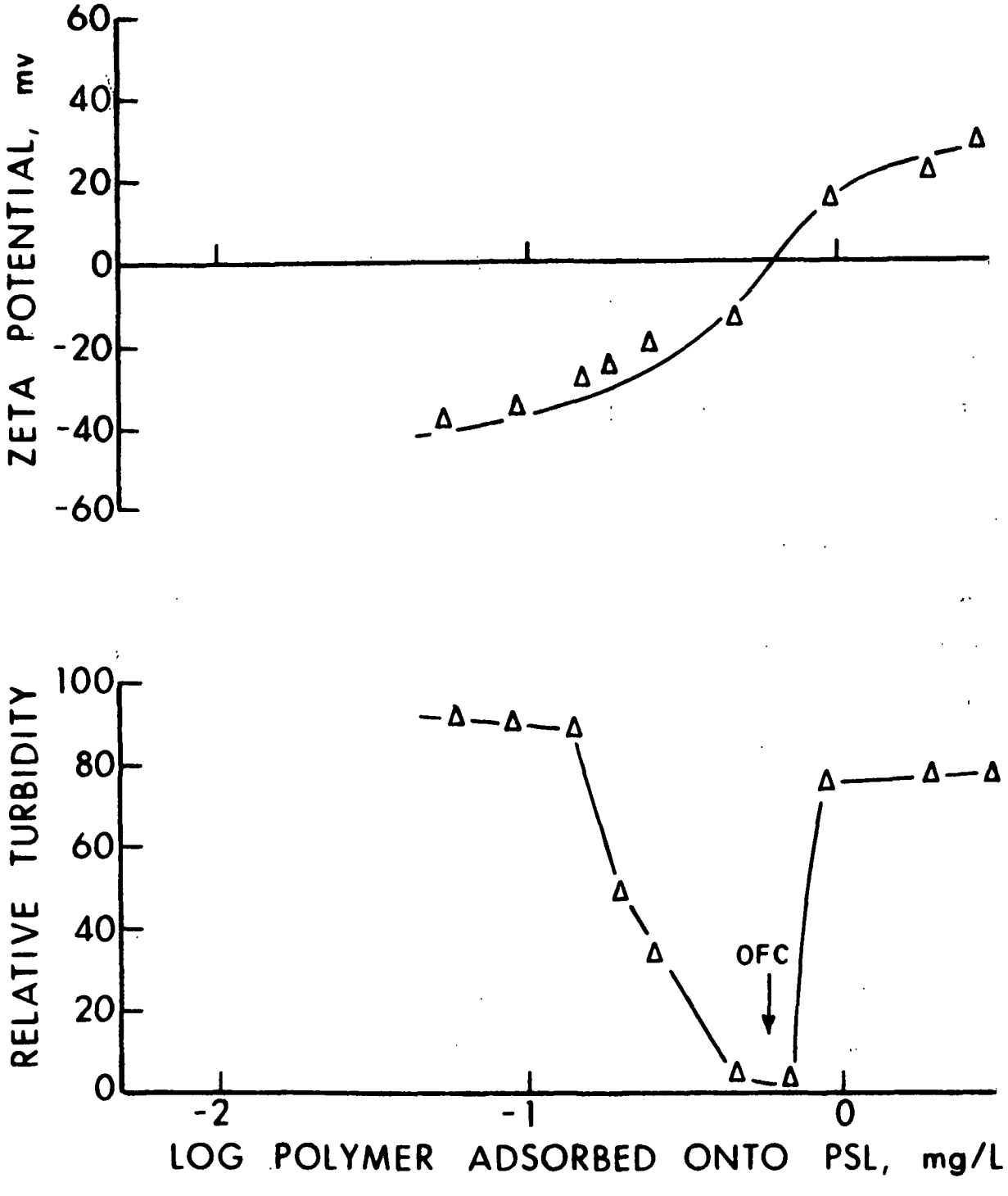

Figure 26. Flocculation Curve for PVAm at pH 9

RESPONSE OF AGGREGATES TO HYDRODYNAMIC SHEAR

CALIBRATION OF SHEAR APPARATUS

By assuming the apparatus to be approximated by a parallel plate system, the shear rate $\dot{\gamma}_r$ at radius r for a rotational velocity Ω (radians/sec) is given by

$$\dot{\gamma}_r = \frac{2\Omega(R_c/r)^2}{(R_c/R_b)^2 - 1}, \tag{30}$$

where R_c and R_b are the radii of cup and bob, respectively.

With the bob rotating inside a stationary cup, the material on the surface of the bob will rotate faster than any other material in the system. Centrifugal force eventually causes a radial migration and the onset of "Taylor turbulence." The limiting values of stability for Newtonian fluids are correlated using Reynolds numbers.

From the equation

$$(N_{Re})_{trans} = 41.3/(1-\lambda)^{3/2}, \tag{31}$$

where $\lambda = R_b/R_c$, one can calculate that the transition Reynolds number for this system was 8.93×10^4 (196). To remain in a laminar flow regime, then, the maximum bob speed for this apparatus was 2385 rpm. From Equation (30) it can be calculated that the shear rate generated at this upper speed limit was 41,634 sec^{-1}.

DETERMINATION OF SHEAR NECESSARY FOR COLLOID RESTABILIZATION

To obtain information concerning the behavior of flocculated systems in high shear fields it was necessary to first determine the amount of energy that

could be applied to a stable colloid system without inducing aggregation by mechanical impaction. PSL samples of appropriate dilution were subjected to a variety of shear stresses for several lengths of time. After shearing each sample, aliquots were taken immediately and again after 1 hour of settling time. Results of the subsequent turbidimetric analysis are given in Table III.

TABLE III

BEHAVIOR OF PSL IN SHEAR

Rpm	Number of Passes	Settling Time (hr)	Relative Turbidity (±0.02)
0	0	1	1.00
1170	1	0	0.68
1170	1	1	0.67
1170	2	0	0.68
1170	2	1	0.54
1750	1	0	0.69
1750	1	1	0.65
1750	2	0	0.67
1750	2	1	0.64
2200	1	0	0.70
2200	1	1	0.68
2200	2	0	0.68
2200	2	1	0.25
2200	5	0	0.15
2200	5	1	0.09
2385	1	0	0.56
2385	1	1	0.52

The conditions sought through this experiment were maximum shear rate and minimal particle settling. A comparison of turbidity values for one or more passes revealed that more than one pass through the system at any shear rate caused enough particle collisions to account for noticeable settling. At bob speeds that cause the transition Reynolds number to be exceeded, the particle collisions that result from mechanical force cause a certain amount of reaggregation. The fact that the turbidity of the suspension sheared at 2385 rpm is lower than that sheared at 2200 rpm supports this contention.

On the basis of these results it was decided that all shear experiments would be run at 2200 rpm for that length of time that would permit all volume elements of the test suspension to pass once through the shear annulus.

To insure that all volume elements would be allowed to pass through the shear annulus, a drop of food dye was inserted in the system at various positions. The apparatus was then run for the time calculated for the given test solution volume to pass once through the system. In all instances, the test solution of 20 mL was homogeneously colored in 7 min and 12 sec. These results indicated that all volume elements were most probably allowed to pass through the shear annulus in the theoretical time calculated for a sample volume of 20 mL.

RESPONSE OF FLOCS TO VARYING SHEAR

Figure 27 shows the response of flocs at each pH to various amounts of shear. Data plotted at 1 sec^{-1} are those of the flocs before any shearing in the concentric cylinder device. (Recall that the orthokinetic flocculation incorporated a mild agitation of ca. 1 sec^{-1}.) Data plotted at 10^2 sec^{-1} were obtained by passing the flocs through the concentric cylinder apparatus without bob rotation. All other data were obtained by shearing the flocs at appropriate bob speeds. The sheared flocs were then subjected to the mild agitation of the wheel in the water bath for 60 min before allowing undisturbed settling for 20 min. The most prominent trend worth discussion is that the pH 3 system does not appear to be changed by any shear rate used. While pH 9 flocs do not appear to be quite as efficient in reflocculating as pH 3 flocs, the difference in average final relative tubidity between pH's 3 and 9 is only about 7%. The experimental precision of the turbidity measurements is on the order of ±3%; therefore the difference, as plotted, may not be significant. It is

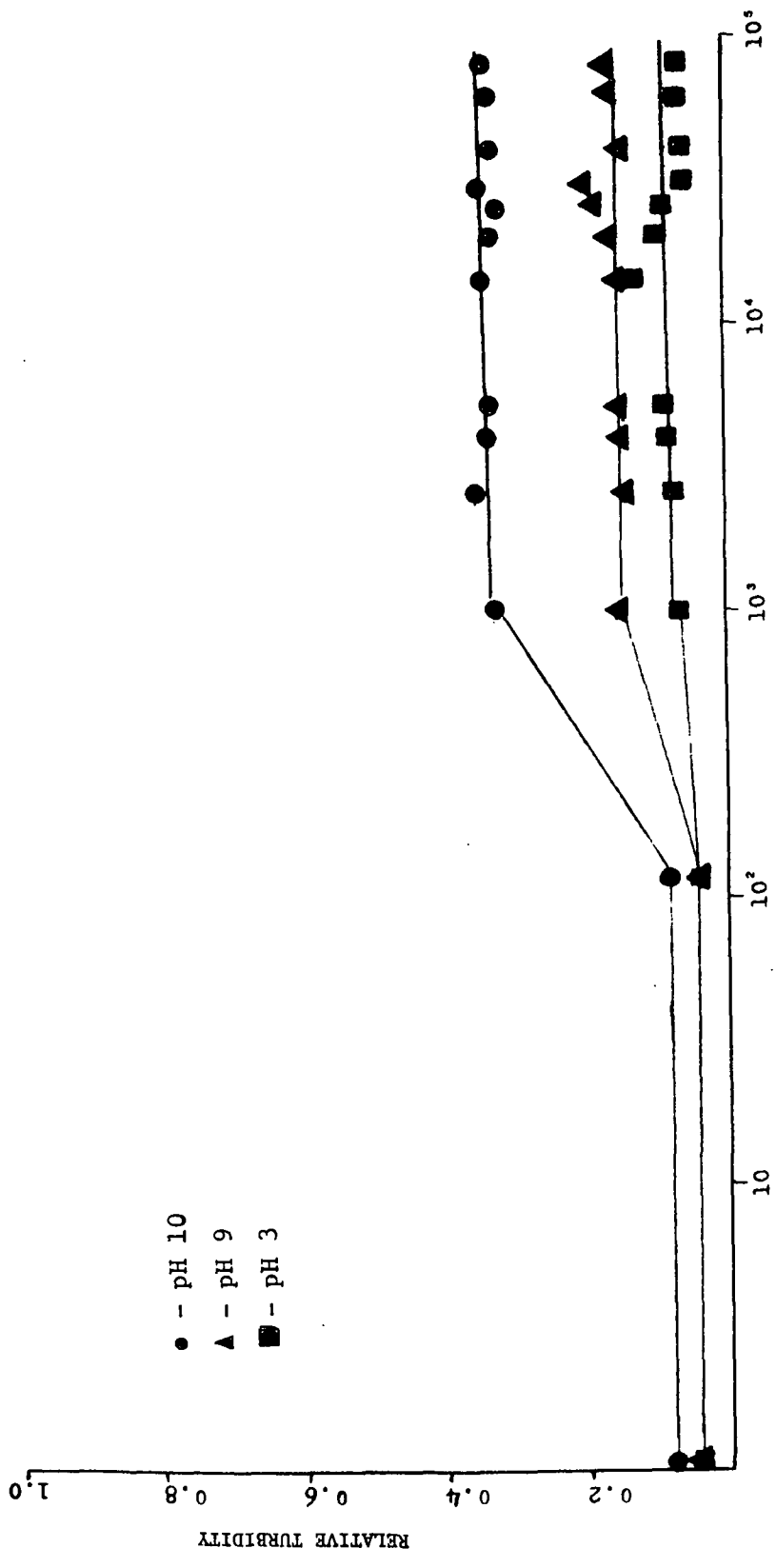

Figure 27. Response of Flocs to Various Rates of Shear

obvious, however, that pH 10 flocs have suffered a marked reduction in reflocculation efficiency as a result of the imposed shear. These trends might be expected if (1) at pH's 3 and 9 the adsorbed PVAm was not affected to any great extent by the hydrodynamic forces imposed during the shearing process, and (2) at pH 10 extensive charge diffusion or molecular degradation occurred.

KINETICS OF FLOCCULATION VS. REAGGREGATION AFTER RESTABILIZING SHEAR

The final extent of reflocculation at all pH's was used to gain insight into the relative configurational state of the adsorbed flocculating polymer after hydrodynamic shear. A comparison of the kinetics involved in reaching the final reflocculation value to the respective values for initial aggregation provided additional information.

KINETICS OF FLOCCULATION

The basic theory describing the Brownian motion of suspended particles is based on the premise that there exists a kinetic equilibrium between the molecules of the medium and any individual suspended particle,

$$(1/2)(M\overline{V^2})_{particle} = (1/2)(M\overline{V^2})_{medium} = 3/2\ kT \qquad (32)$$

where M = mass of the particle or medium molecule

$\overline{V^2}$ = mean square velocity

The mean kinetic energy of each freely moving element is thus completely determined by temperature.

Einstein (197) deduced that the relationship between the time and displacement of an element subjected to Brownian motion could be described by

$$\bar{x}^2 = 2ktT/6\pi\ \eta\ r, \qquad (33)$$

where $\bar{x}^2$ = mean square displacement projected in the x-direction in time, t

η = fluid viscosity

r = radius of the particle

It is obvious that the denominator in the right-hand side of Equation (33) is Stoke's expression for the force associated with the fluid movement about a sphere.

Fick's Law of diffusion (198) states that the product of the amount of material, a, which diffuses per unit time through a unit area and the reciprocal of the gradient of the concentration in the x-direction, dx/dc, should remain constant:

$$D = a\ (dx/dc) \tag{34}$$

Using this diffusion constant, Einstein (197) established that

$$D = \bar{x}^2/2t \tag{35}$$

For a spherical particle of radius r, the coefficient of diffusion may be expressed as

$$D = kT/6\pi\ \eta\ r \tag{36}$$

For PSL ($2r$ = 0.794 μm) this diffusion constant has a value of 5.5×10^{-9} cm^2/sec at 25°C.

If the electrostatic repulsion of the double layer surrounding each PSL particle were destroyed, a collision between two particles in Brownian diffusion would lead to the formation of a permanent aggregate. Von Smoluchowski (199) has developed an elegant analysis of the rate of such aggregation. The fundamentals of his work have been reviewed by Overbeek (198) and are also presented below.

Smoluchowski's initial assumptions were that n_o spherical particles of equal size are present in a unit volume at time $t = 0$, and that the repulsive forces have been removed entirely. As a first approximation, one of the particles was assumed to be stationary, while the others are in random Brownian motion. The number of collisions with the stationary particle was thus calculated to be

$$J = 4\pi DRn_o, \tag{37}$$

where R is the distance between the centers of two particles in permanent contact.

If the one stationary particle is also subject to Brownian motion the number of collisions with this particle is predicted by

$$J = 8\pi DRn_o \tag{38}$$

The rate of the disappearance of primary particles is then given by

$$-dn/dt = 8\pi DRn^2 \tag{39}$$

It is evident from Equation (39) that coagulation proceeds as a second-order process. As coagulation continues, the particle system is no longer a homogeneous one. At a given time there will exist a number of singlets, doublets, quartets, and higher-order clusters. Any of these species may collide with any other.

The number of collisions per unit time between primary particles is determined from Equation (39) as

$$P_{11} = 4\pi DRn^2 = 2\pi D_{11}R_{11}n_1^2 \tag{40}$$

The number of collisions between particles of types i and j can thus be expressed as

$$P_{ij} = 4\pi D_{ij} R_{ij} n_i n_j \tag{41}$$

At a given stage of the coagulation process the number of primary particles will be n_1, that of secondary clusters, n_2, the number of i-fold clusters, n_i. The number of k-fold clusters, n_k, thus increases by collisions of i-fold and j-fold clusters ($i + j = k$). In addition, the n_k clusters will decrease by collisions of k-fold and i-fold clusters.

As the diffusion constant D_{ij} of any cluster will be inversely proportional to the radius R_{ij} of the cluster,

$$D_{ij} R_{ij} = D_1 r_1 \left(\frac{1}{r_i} + \frac{1}{r_j} \right) (r_i + r_j) = 4 D_i r_i \text{ if } r_j = r_i \tag{42}$$

The rate of change of the total number of particles, irrespective of their size, is then given by

$$\frac{d}{dt} \left(\sum_{k=1}^{\infty} n_k \right) = - 4\pi DR \left(\sum_{k=1}^{\infty} n_k \right)^2, \tag{43}$$

where

$$\sum_{k=1}^{\infty} n_k = \frac{n_o}{1 + 4\pi DR n_o t} \tag{44}$$

Using Equation (44) Smoluchowski determined that the number of k-fold particles at time t can be found by

$$n_k = \frac{n_o (t/T_h)^{k-1}}{(1 + t/T_h)^{k+1}} \tag{45}$$

T_h is the time in which the number of particles is just halved, and for this discussion will be referred to as the half-life of a given suspension.

$$T_h = 1/4\pi DR n_o, \tag{46}$$

and if $D = kT/6\pi \eta r$ the half-life for an aqueous dispersion at 25°C is

$$T_h = 3.6 \times 10^{11}/n_o \tag{47}$$

Thus, T_h depends only on the number of particles in the suspension. For the PSL used here, T_h = 3.3 min.

Figure 28 illustrates the course of coagulation for a suspension of PSL, as predicted by Smoluchowski's theory. It is important to remember that there is assumed to be no repulsive interaction between particles. In addition, all motions are perikinetic.

An attempt was made to monitor the behavior of PSL under the above conditions. PSL and PVAm were mixed at optimum flocculation concentrations and allowed to sit, undisturbed, for the appropriate lengths of time. The extent of flocculation was followed by the intensity of scattered light produced by an aliquot removed 1 cm under the surface of the settled suspension.

For coagulating hydrophobic systems, light scattering is not suited to determine absolute values for the number of particles because the intensity of scattered light is related to both the size and the quantity of aggregates. However, Uriarte (200) has demonstrated the validity of turbidimetric techniques for the study of coagulation of PSL.

The first general theory of light scattering by homogeneous spheres of arbitrary size was presented by Mie (201). The Mie relationship for the turbidity, τ, of a system of spherical particles can be stated as

$$\tau = \Sigma N_i \pi r_i^2 K, \tag{48}$$

where r = radius of particle size i

K = dimensionless variable called the scattering coefficient

K is defined by

$$K = R_t/S_g, \tag{49}$$

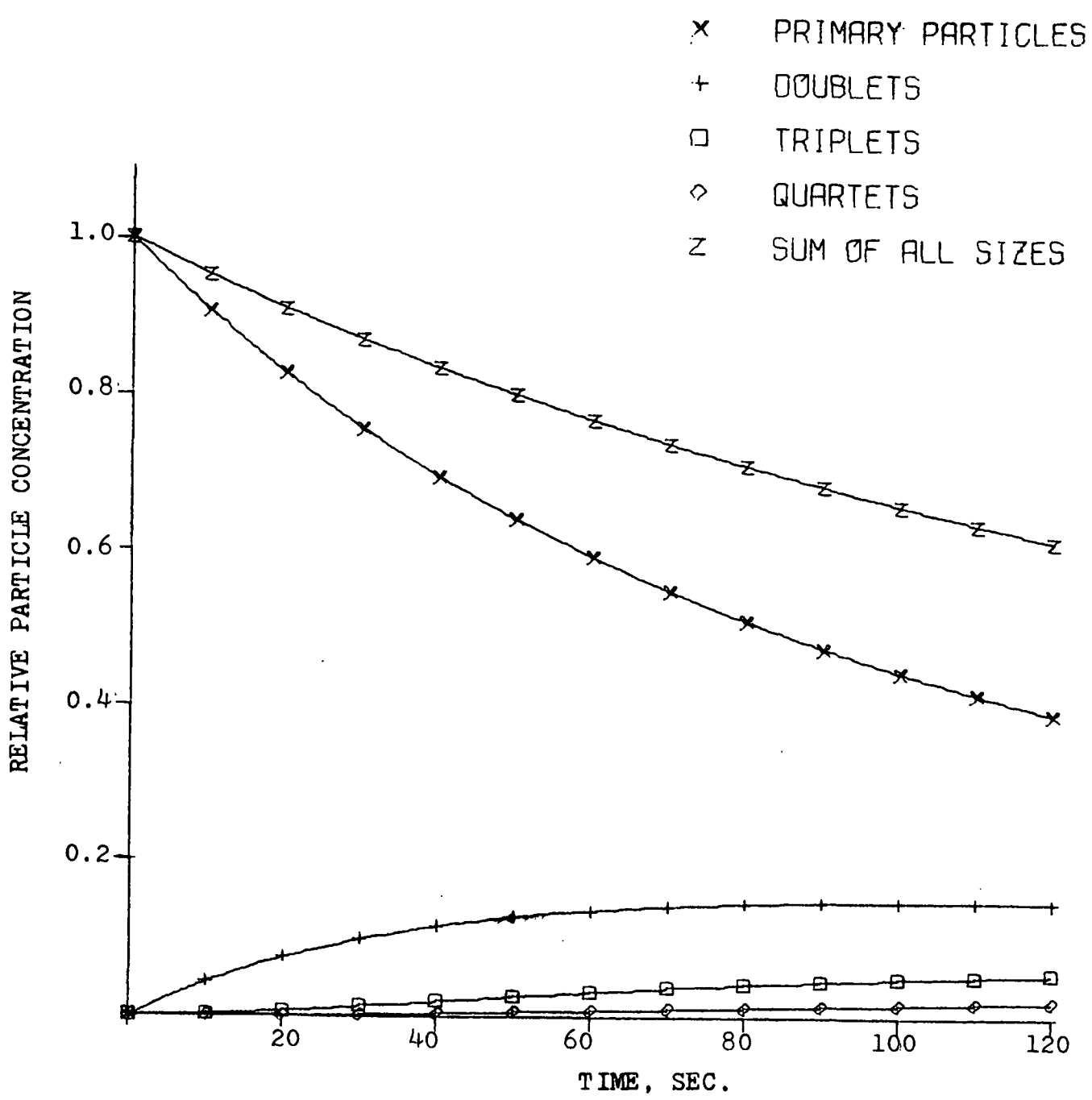

Figure 28. Smoluchowski Plot of Values Calculated for Collisions Due to Brownian Diffusion Only

where R_t = radiation scattered by a single particle per unit intensity of incident light

S_g = geometric cross-sectional area of the particle under consideration

For a spherical scatterer $S_g = \pi r_1^2$.

Equation (48) shows that for a system of coagulating particles, the turbidity will be affected by two variables:

(1) changes in the number concentration of kinetically independent particles, n_1, and

(2) changes in the size of the kinetically independent particles.

This charge will also affect the value of the scattering coefficient, K, since K is a strong function of particle size. In a discrete spectrum of particle sizes, the expression for turbidity becomes (200)

$$\tau = \pi \sum_j n_j \bar{r}_j^2 K_j, \tag{50}$$

where $\bar{r}_j$ is the mean radius of the j-tuple particle, and is defined as the radius of a single sphere which scatters the same amount of light as an aggregate of j spheres each of radius r_1. For large particles ($r > \lambda/20$) the scattering coefficients K_j must be evaluated from solutions of the Mie equations. Such solutions are available in tabulated form (202-204). Comparing the turbidity at time t to the initial turbidity of the system produces a dimensionless relative turbidity.

$$\tau_{rel} = \frac{\tau_t}{\tau_o} = \frac{\sum_j n_j r_j K_j}{n_o r_1^2 K} \tag{51}$$

From Equation (51) it can be seen that relative turbidity is a direct function of the integral size distribution of the particles in the coagulating system. Changes in the relative turbidity are thus a measure of the change in

the total number of particles in the system, irrespective of their size. Figure 29 illustrates the flocculation kinetics resulting from Brownian diffusion for PSL treated with optimum concentrations of PVAm.

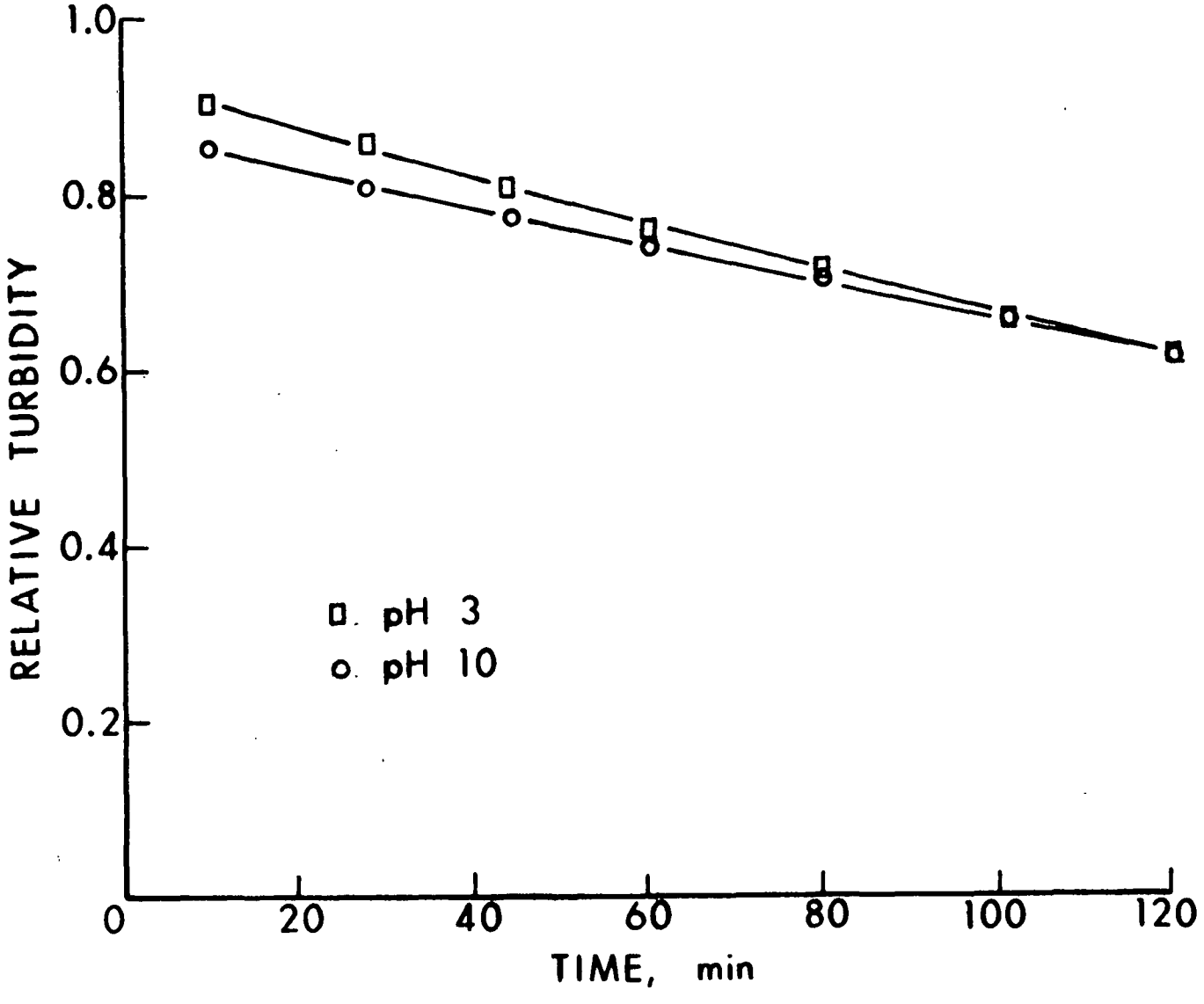

Figure 29. Flocculation Kinetics Resulting from Brownian Diffusion Only

Figure 30 shows the experimentally determined kinetics of flocculation under conditions of mild agitation. A comparison of the experimentally determined $T_{\frac{1}{2}}$ for perikinetic coagulation (>> 120 min) with that calculated from Smoluchowski's theory (3.3 min) provides an illustration of the importance of collision efficiency. Recall that to obtain the calculated $T_{\frac{1}{2}}$ = 3.3 min all

collisions were assumed to result in aggregation. It is obvious from a comparison to the experimental value that double layer repulsion must still exist in a system consisting of particles and an optimum flocculating concentration of polyelectrolyte. Also apparent is the fact that only a portion of the particle surface has been covered by polyion. A comparison of the relative turbidity at 120 min in Fig. 29 (0.65) with τ_{rel} at 60 min in Fig. 30 (0.10) demonstrates that efficient flocculation is very dependent on orthokinetic collisions. Others (7-9,198) have also noted that the process of colloidal aggregation is promoted by agitation of the sol.

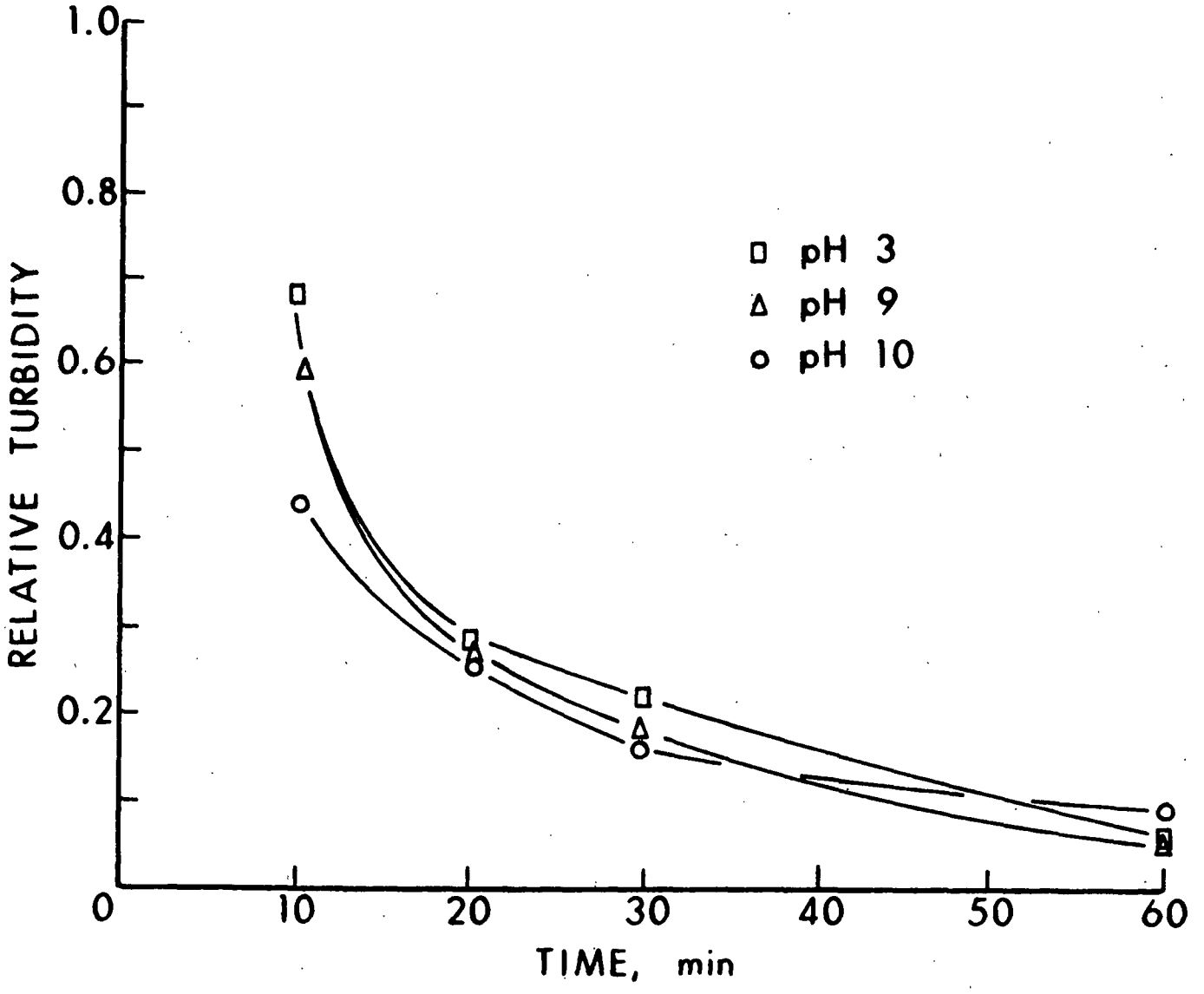

Figure 30. Kinetics of Aggregation with Orthokinetic Motions Induced by Mild Agitation

Smoluchowski (199) predicted that the frequency of two-body orthokinetic collisions would be

$$O_{ij} = (4/3)\ (R_{ij})^3\ n_i n_j\ \dot{\gamma}, \tag{52}$$

where $\dot{\gamma}$ is the effective shear rate. $\dot{\gamma}$ may be estimated for turbulent or laminar flow (205) from

$$\dot{\gamma} = \sqrt{E/\eta}, \tag{53}$$

where E = power input per unit volume of fluid

η = viscosity of the suspension

Comparing Equation (52) to Equation (41) yields a ratio of the two collision probabilities

$$\frac{O_{ij}}{P_{ij}} = \frac{(R_{ij})^2 \dot{\gamma}}{3\pi\ D_{ij}}, \tag{54}$$

which is strongly dependent upon the collision diameter of the particles. For particles with a diameter of 0.8 μm and a shear rate of 1 sec^{-1}, O/P has a value of about 0.06. Orthokinetic collisions thus have a negligible effect on the rate of aggregation of such a sol. As the particle size approaches even 10 μm, orthokinetic collisions ($\dot{\gamma}$ = 1 sec^{-1}) are 120 times as important as perikinetic collisions.

Expressing Equation (52) as a time rate of change of the concentration of n_k uniformly-sized particles yields

$$-\frac{dn_k}{dt} = (4/3)\ \dot{\gamma}\ R^3 n_i^2 \tag{55}$$

The solution to Equation (55) is thus

$$1/n_k - 1/n = (4/3)\ \dot{\gamma}\ R^3 t \tag{56}$$

According to the Smoluchowski theory, then, the concentration of k-tuple particles may be calculated from

$$n_k = \frac{n_o[(4/3)\,\dot{\gamma}\,n_o\,R^3t]^{k-1}}{[1 + (4/3)\,\dot{\gamma}\,n_o\,R^3t]^{k+1}} \qquad (57)$$

There is an interesting trend displayed in Fig. 30 that deserves further discussion. At early contact times the separation of turbidity values for pH's 3 and 10 is consistent with the concept of flocculation mechanisms changing from primarily bridging to primarily electrostatic patch formation as the charge densities of the components are increased. Similar results have been noted by Gregory (37).

At pH 10, the molecules of PVAm have a very low charge density. In this condition, the electrostatic attraction to the anionic PSL surface will be minimal. The adsorption configuration of a PVAm molecule at this pH will therefore most likely approximate the solution configuration of a random coil. As the apparent volume of a PSL particle with adsorbed PVAm should be substantially greater than that of an uncovered particle, the rate of aggregation under these conditions should be very quick when compared to the aggregation rate for a system with smaller particle volumes.

INITIAL FLOCCULATION VS. REAGGREGATION

Figure 31 shows the difference in behavior of initial formation of flocs and that of the reaggregation process at pH 10. It is quite apparent that reaggregation does not occur to the original extent after the pH 10 flocs have been disturbed by hydrodynamic forces. Currently accepted theories predict that, because of the low charge density of PVAm at pH 10, polymeric bridge-type structures would be the most prevalent aggregation geometry for a dispersion of PVAm/PSL. Van Vliet and Lyklema (206) studied the rheological behavior of paraffin oil-in-

water emulsions stabilized by polyelectrolytes. Their studies showed that the viscosity of the emulsion decreased with increases in the charge density of the stabilizing polyelectrolyte. This provides additional support to the concepts of electrostatic "patch" formation in high interaction-energy systems, and polymeric bridging in low interaction-energy systems.

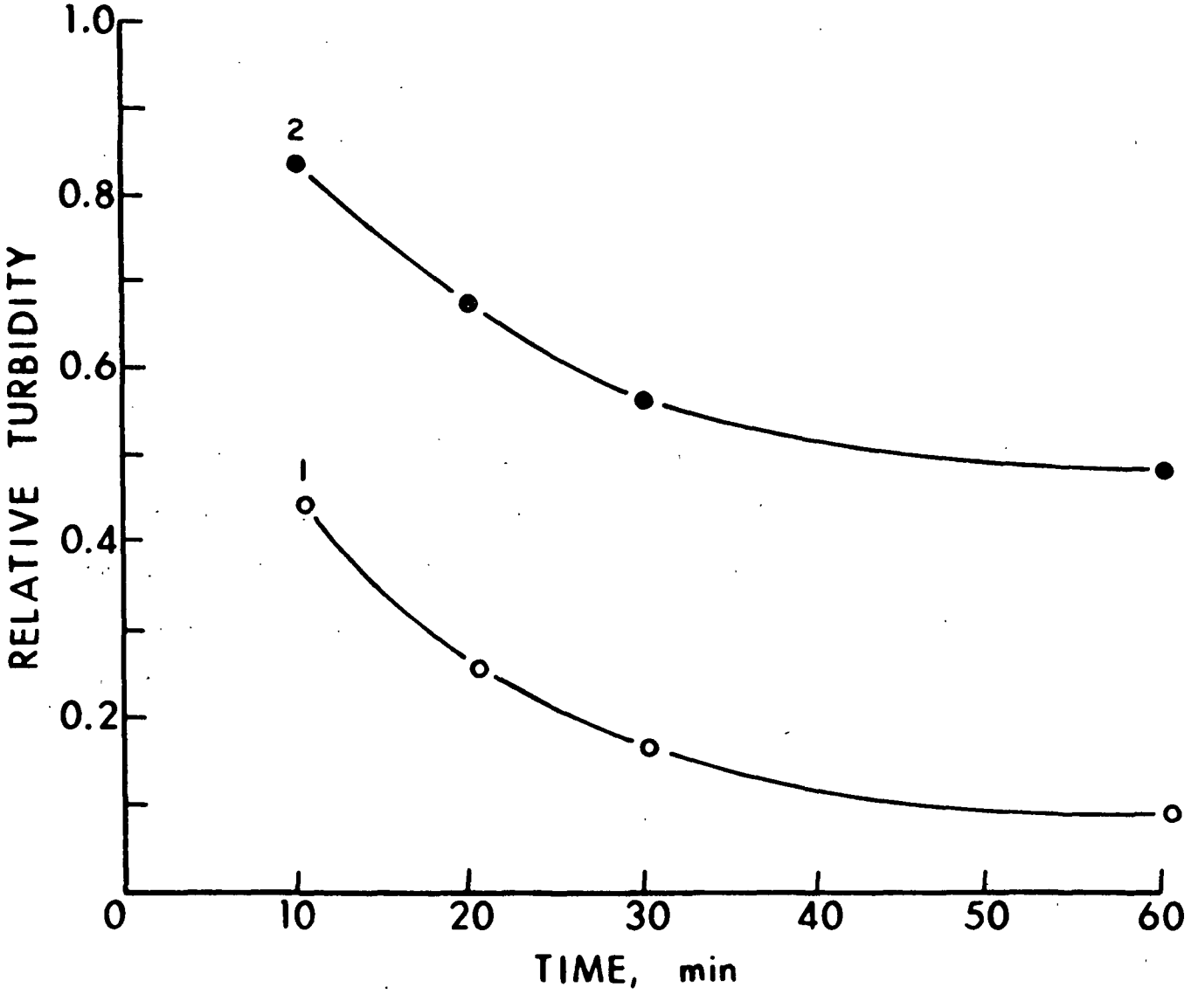

Figure 31. Kinetics of Aggregation vs. Reaggregation at pH 10. Curve 1 is Initial Flocculation. Curve 2 is Reaggregation After Shear

Figure 32 shows the aggregation/reaggregation behavior of the PVAm/PSL system at pH 3. Reaggregation appears to occur as completely, but more quickly than initial flocculation. Support for the above ideas concerning the available pathways for the pH 3 system before and after shear should be apparent from a

superposition of the data from the two cases. Such a superposition has been attempted in Fig. 33. A time shift of 20 min puts data from both processes on the same curve. This implies that after an initial "induction" period of about 20 min, the mechanisms of flocculation may be the same.

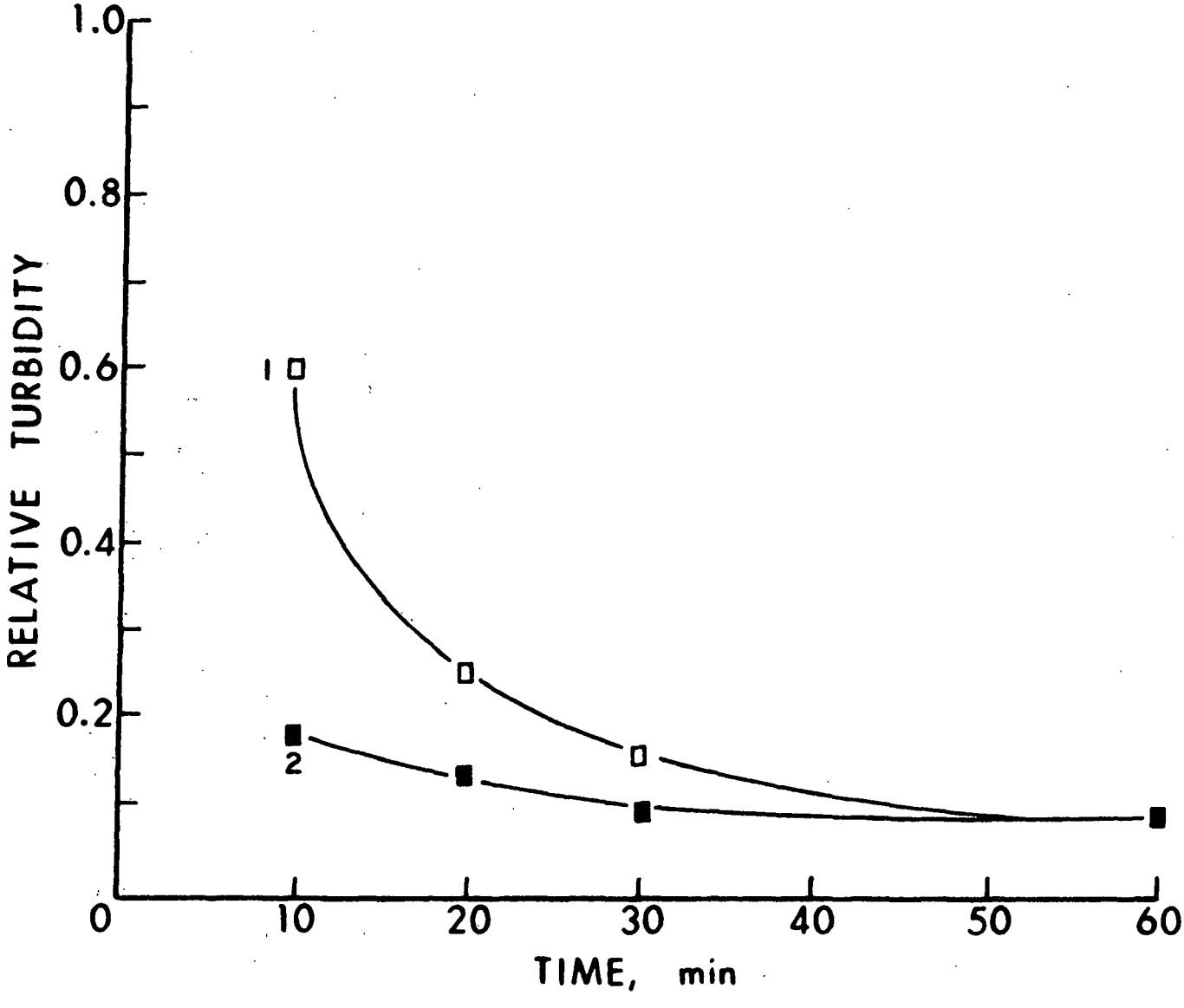

Figure 32. Kinetics of Aggregation and Reaggregation at pH 3. Curve 1 is Initial Flocculation. Curve 2 is Reaggregation After Shear

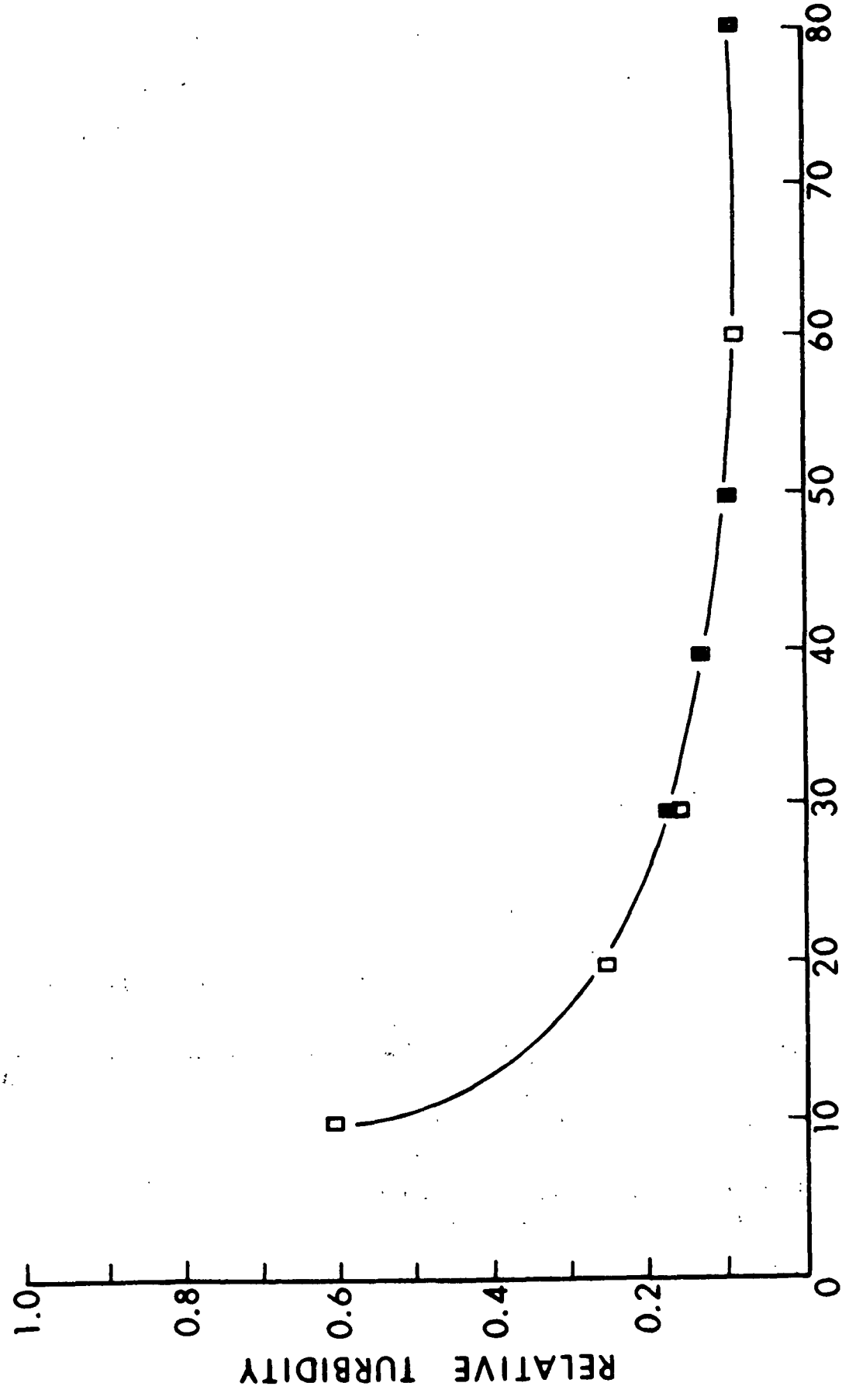

Figure 33. Superposition of Data from Reflocculation (■) Onto Data for Initial Flocculation (□), pH 3. Data (■) has Been Shifted 20 Minutes to the Right

There are two possible explanations for the apparent time shift. The first is that while reaggregation is dependent only on the rate of "favorable" particle collisions, the initial flocculation depends also on the diffusion of the polymer molecules to particles and the subsequent adsorption. Gregory and Sheiham (148) reported that polyelectrolyte adsorption on PSL occurs within 0.12 sec at optimum concentrations. Franco and Stratton (207) have found that adsorption under turbulent conditions can occur within 0.06 sec.

Calculations of the diffusional collision frequency of two PSL particles yields an average time between collisions of approximately 61 sec. Polymer diffusion to and adsorption onto a PSL particle is thus predicted to occur at least 100 times faster than interparticle collisions. Therefore, the mass transfer of polymer to particle surface cannot account for the 20 min time shift in Fig. 33. The second possible explanation for the time shift is that the flocs are not completely degraded to primary particles by the imposed hydrodynamic forces. Reflocculation would thus have a "head start" over the initial flocculation process.

Inspection of Fig. 34 reveals that up to a time of 20 min, the dominant factor affecting the total particle concentration of a flocculating system is the disappearance of individual particles. Parker, et al. (208) have demonstrated in any shear gradient there exists a maximum stable floc size. The actual dimensions of this stable floc size is in part dependent on the floc geometry (114).

A major difference between compact flocs and flocs formed with polymeric chains is that the greatest tension in a loose floc is located at the center links of polymer molecules in the middle of the floc, whereas the maximum tension found in the compact flocs is found at the periphery (112,209). It

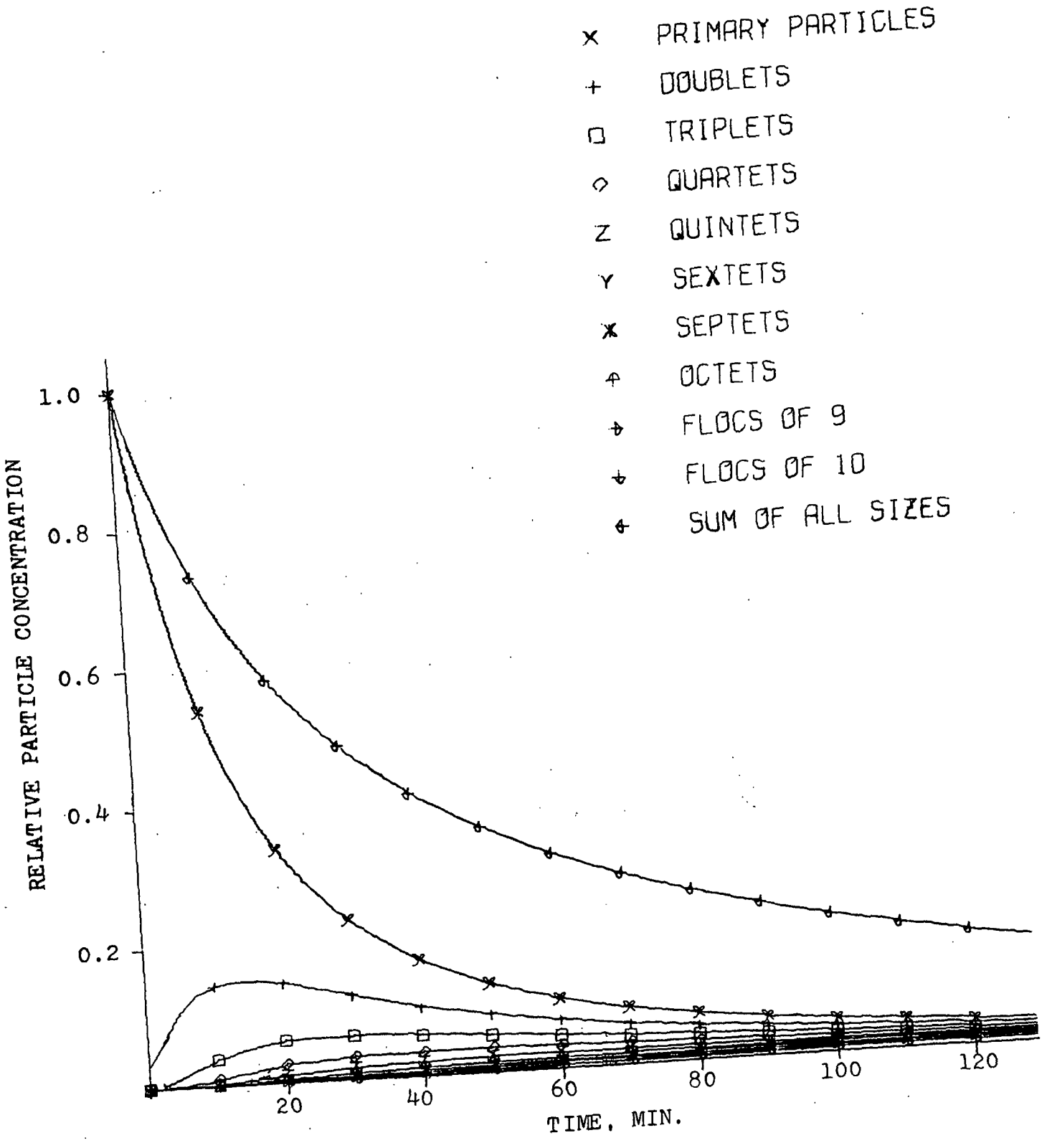

Figure 34. Predicted Values of Relative Particle Concentrations During Flocculation Under Mild Agitation

would be expected therefore, that floc break-up would be less extensive at pH 3 than at pH 10. The data at time zero in Fig. 35 illustrate this concept well.

A significant portion of the 20-min shift in the superposition of data in Fig. 33 can thus be contributed to a necessary reduction in the number of PSL singlets.

Simply stated, to induce gravitational settling of colloidal matter, the particle cluster must reach a critical size. At time zero, the process of reaggregation (pH 3 and 9) has a cluster size distribution similar to that of an initial flocculation process that has proceeded for approximately 20 min.

The data of reflocculation at pH 10 are not superimposable on the data of initial flocculation. This indicates that the "grappling ability" of the polymer has been reduced by the shear field. Such a reduction could be the result of molecular degradation or reconformation of the polymer on the particle surface (9,117).

Figure 36 shows the superposition of reaggregation data on initial flocculation data at pH 9. The time shift for this curve was only 16 min, indicating that the pH 9 flocs have been broken down a little more than the pH 3 flocs.

POLYVINYLAMINE MOLECULAR WEIGHT DISTRIBUTIONS AFTER SHEAR

CALIBRATION OF THE SMALL GEL PERMEATION CHROMATOGRAPHY SYSTEM

To estimate the extent of molecular weight degradation of PVAm that resulted from the hydrodynamic shear of dilute solutions, calibration of the small gel permeation chromatography (GPC) column was necessary. The method of calibration involved determination of the relationship between retention

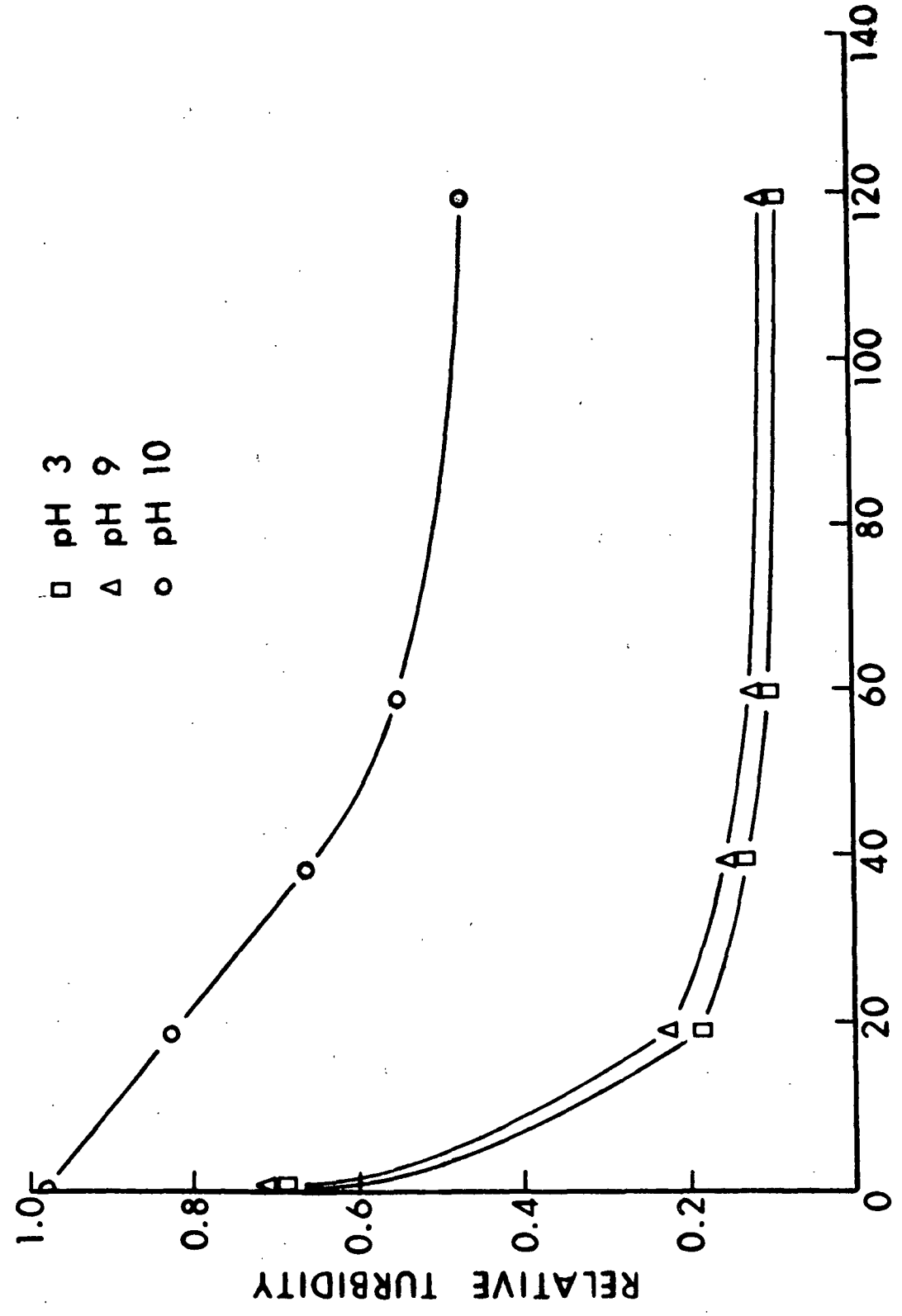

Figure 35. Kinetics of Reaggregation

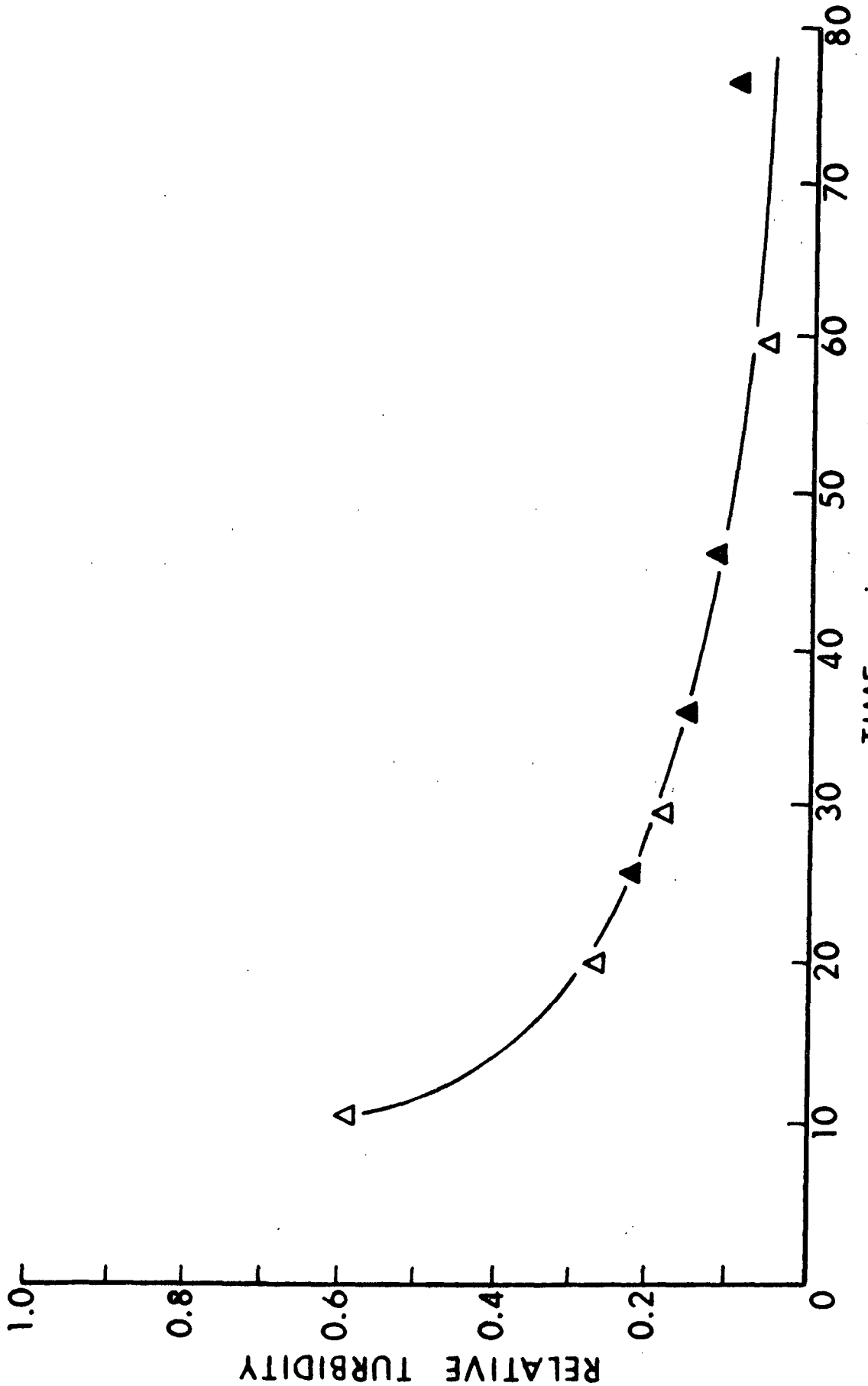

Figure 36. Superposition of Data from Reflocculation (▲) onto Data for Initial Flocculation (Δ), pH 9. Data (▲) has Been Shifted 16 Minutes to the Right

volume and molecular weight. McCrackin (210) has described two methods of calibrating GPC columns from samples of known molecular weights. These methods are more mathematically involved than most calibration methods, and require considerable calculation. Computer programs for these calculations greatly facilitate application. Such programs have been obtained from McCrackin and modified for an IBM 360/40 by G. Ring at The Institute of Paper Chemistry (211).

Four samples of fractionated poly-N-vinylacetamide were obtained through the courtesy of Dr. P. L. Dubin at Dynapol. These samples had molecular weights ranging from 28,000 to 300,000 daltons. Hydrolysis to PVAm was performed according to methods that have been described previously. The values in Table IV were obtained by ultracentrifuge analysis at The Institute of Paper Chemistry.

TABLE IV

MOLECULAR WEIGHTS OF PVAm
USED FOR GPC CALIBRATION

Sample	M_w
F1	450,000
Bloys van Treslong	280,000
Dynapol A	151,500
Dynapol B	42,850
Dynapol C	23,800
Dynapol D	8,200

An aliquot of each PVAm sample was run through the GPC column under conditions described earlier.

The total amount of eluted polymer as calculated from the quantitative analysis showed that 1.74×10^{-3} mg of PVAm was collected from the initial

fractionation on this column. This value is well within experimental error of the 1.78×10^{-3} mg of PVAm that was initially added to the column, suggesting that little or no PVAm was adsorbed onto column materials.

The relationship between elution volume and polymer molecular weight for the small GPC column is illustrated in Fig. 37.

POLYVINYLAMINE BEHAVIOR IN FLOCCULATED SUSPENSIONS UNDER SHEAR

The elution curve on the small GPC column for virgin PVAm is shown in Fig. 38. A check was made using flocs at each pH to determine the percent of initially added PVAm that could be recovered. In all cases, the amount recovered, as determined by spectrophotofluorometric analysis, was within the 5% experimental error of the analysis techniques. It would be expected that any polymer fraction not recovered would consist of the highest molecular weights in the system. The reasons for this expectation are 2-fold. In the first case, the higher molecular weight molecules would be the most thermodynamically stable adsorbed species on the PSL surface. As a second consideration, it must be remembered that the separation technique involved rather severe centrifugation conditions of 75,000 g for 2 hours. It is possible that some high molecular weight material could be sedimented close to the PSL pack at the bottom of the centrifuge tubes. It was most important to be able to detect the presence of any lower molecular weight species that might be generated from the high molecular weight species. Therefore, a slight loss of high molecular weight material was not regarded as being detrimental to any logical argument that might result from the analysis of the data collected.

The results of experiments conducted with flocs formed at pH 3 are shown in Fig. 39. The most noticeable feature of this data is that no PVAm degradation is apparent. When considering the high charge densities involved in

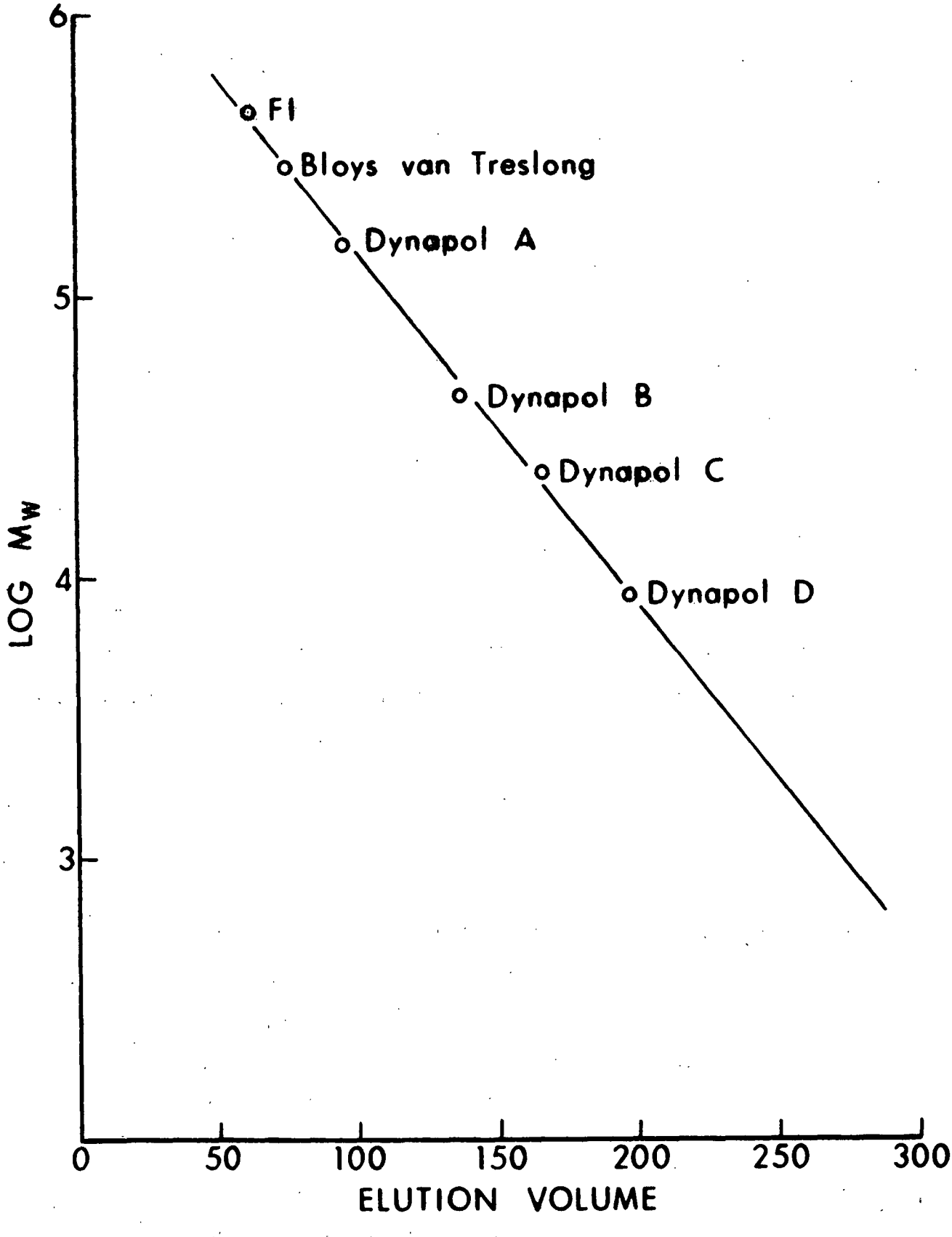

Figure 37. Calibration Curve for Small GPC Column

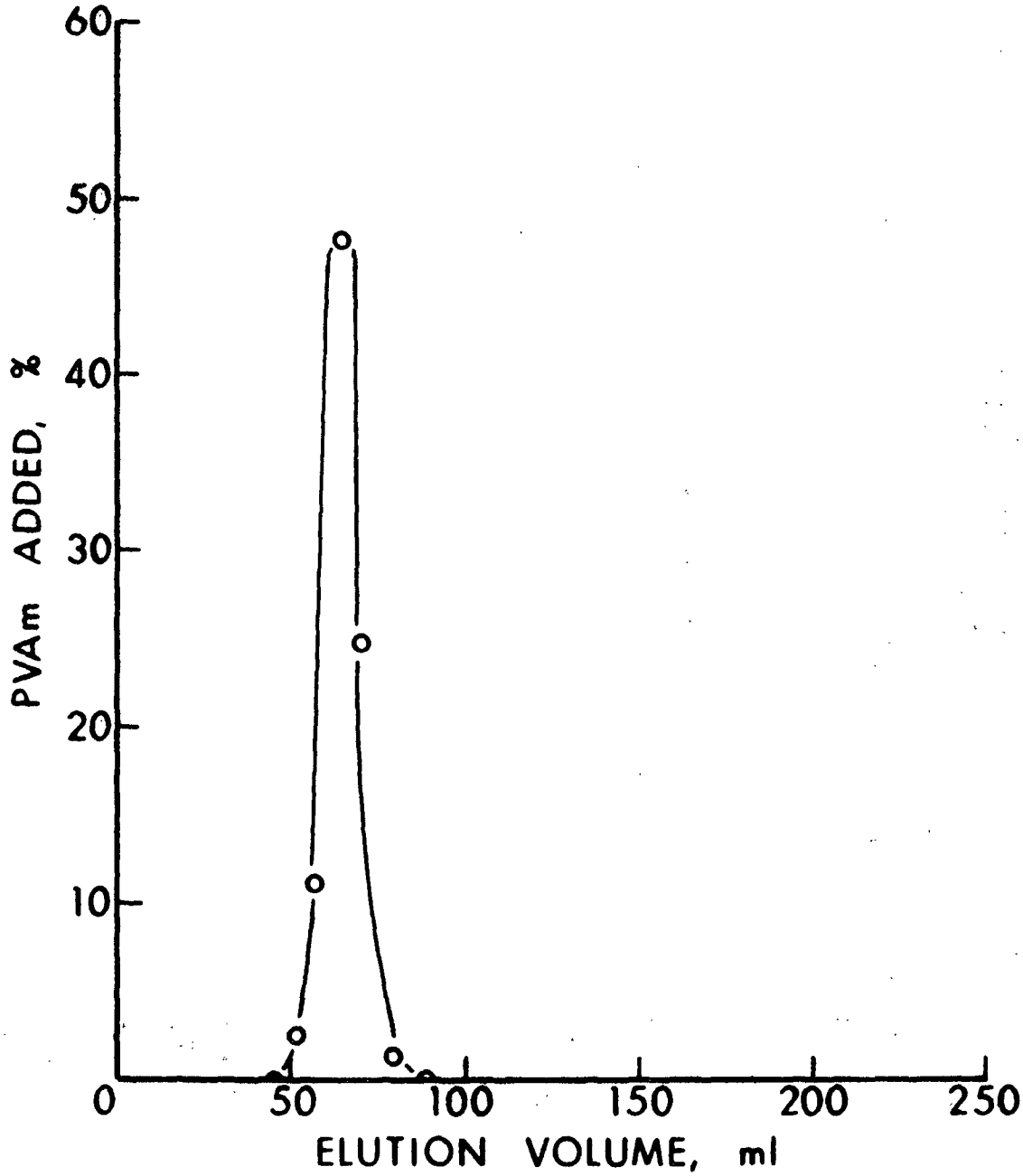

Figure 38. Elution Curve for Unsheared PVAm

this system, it is easy to conclude that the great number of electrostatic points of attraction between PSL and PVAm should result in a very strong floc. Lack of PVAm degradation under these conditions supports the theory that PVAm has most likely assumed a patchlike configuration on the PSL surface.

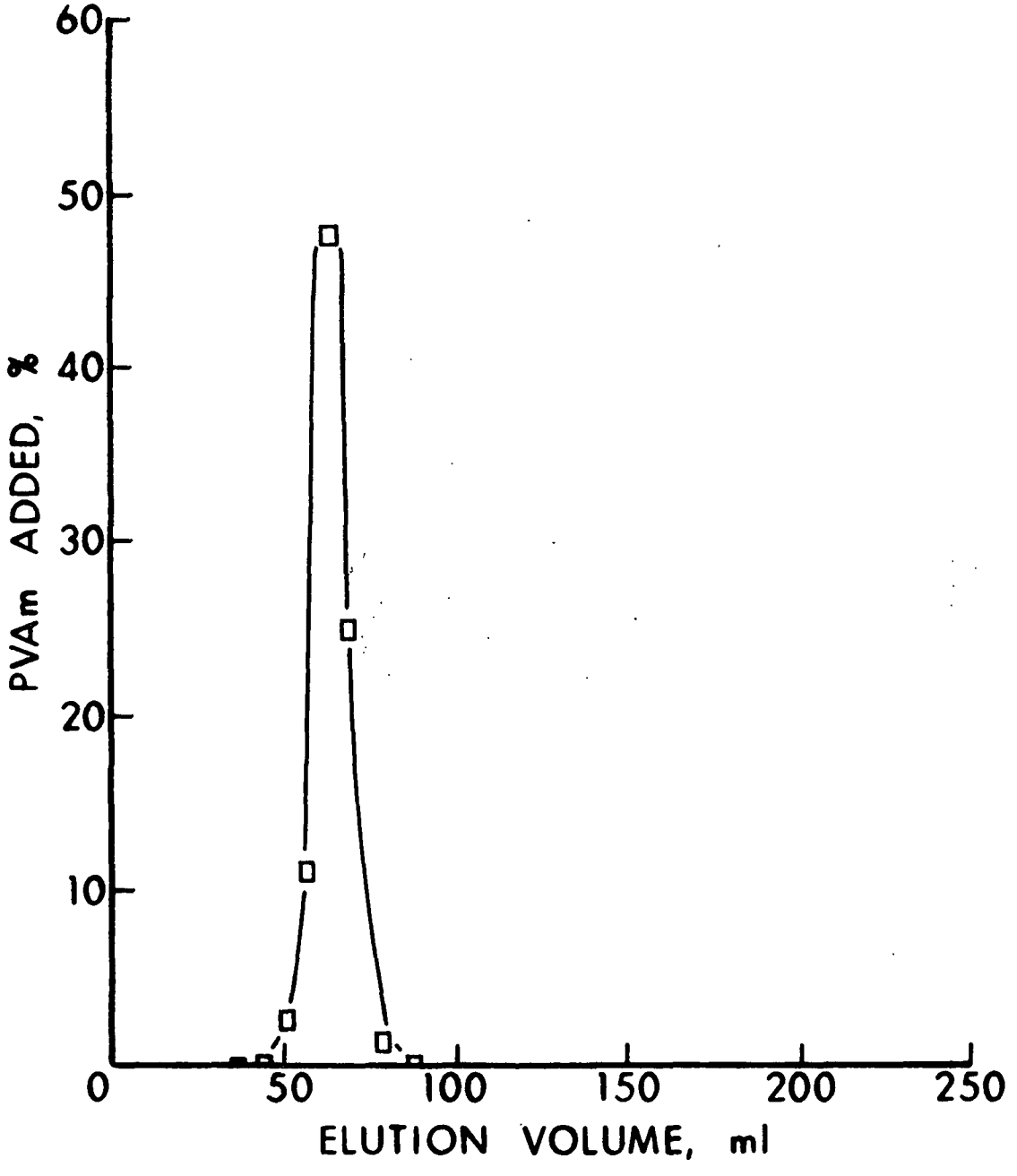

Figure 39. Elution Curve for PVAm Sheared with Flocs at pH 3

Because a patch should have reduced hydrodynamic dimensions in a direction normal to the particle surface, there would be less polymer molecule for the shear stresses to act on. Nakano and Minoura (92) have produced evidence to support a definite relation between the mechanical scission of the polymer chains and their hydrodynamic volume. Forces exerted on a given PVAm/PSL aggregate will thus be experienced preferentially by the PSL particles rather than by the PVAm molecules sandwiched between them. Reasons for aggregate degradation occurring at the polymer/particle interface in this system reduce simply to more energy being exerted at the interface than on the polymer molecule itself.

The results of the experiments conducted with flocs formed at pH 9 are shown in Fig. 40. Again, no PVAm degradation is apparent, suggesting that even at a PVAm charge density of only 13% the polyelectrolyte has assumed a patchlike configuration on the particle surface.

The results of the experiments conducted with flocs formed at pH 10 are shown in Fig. 41. It is interesting to note that two peaks now appear for the system that was sheared under conditions permitting only 3% of the polyelectrolyte units to carry a positive charge. The molecular weight of the shear-degraded PVAm was calculated to be about 40,000 daltons. This corresponds to approximately a 10-fold reduction in the molecular weight of the original PVAm. A possible explanation for the bimodal distributions centers around a shear-induced reorientation on the particle surface before molecular degradation can occur. Those PVAm molecules not immediately smeared onto the particle surface might be pulled off before and/or during the shear, permitting rapid degradation.

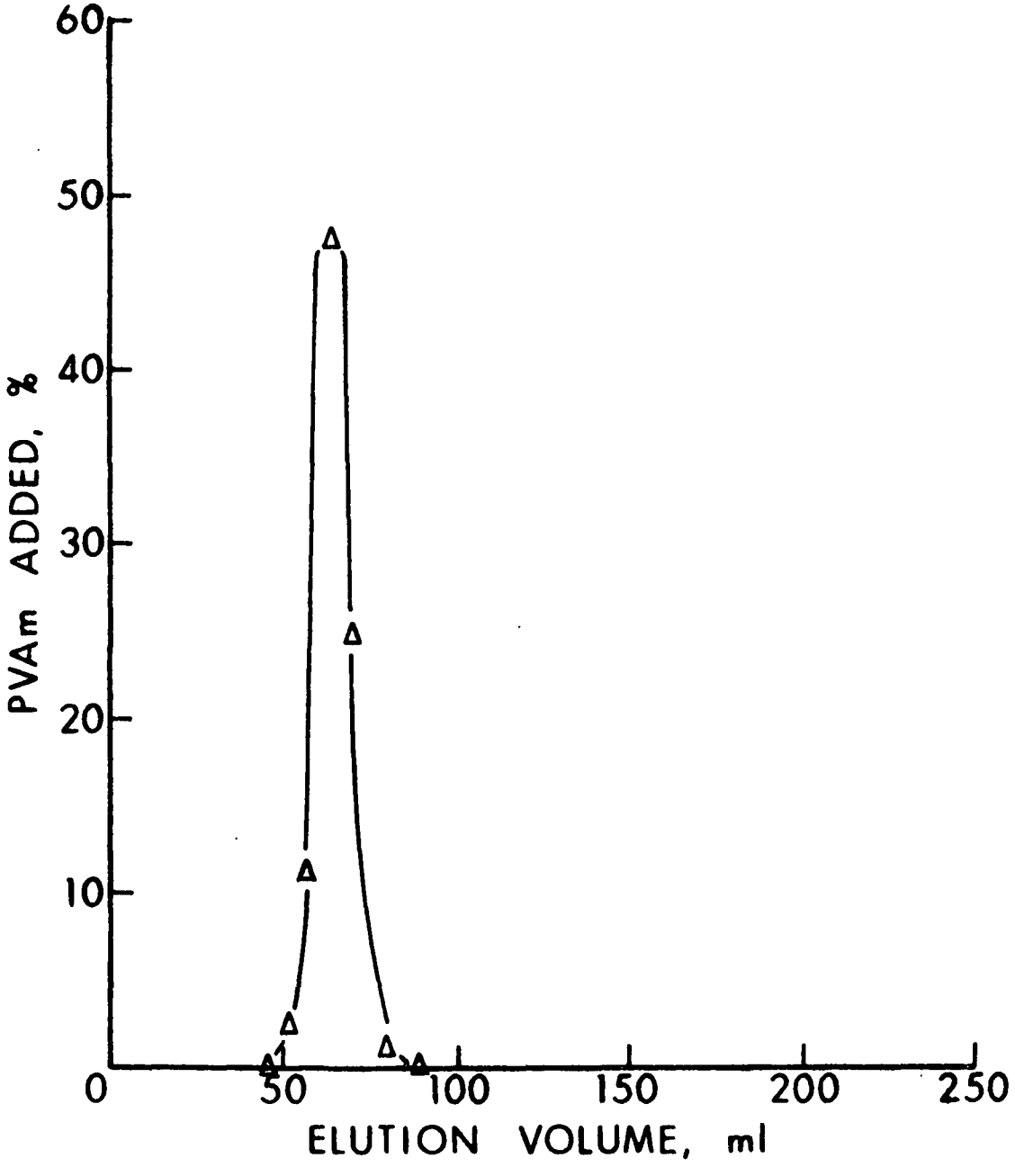

Figure 40. Elution Curve for PVAm Sheared with Flocs at pH 9

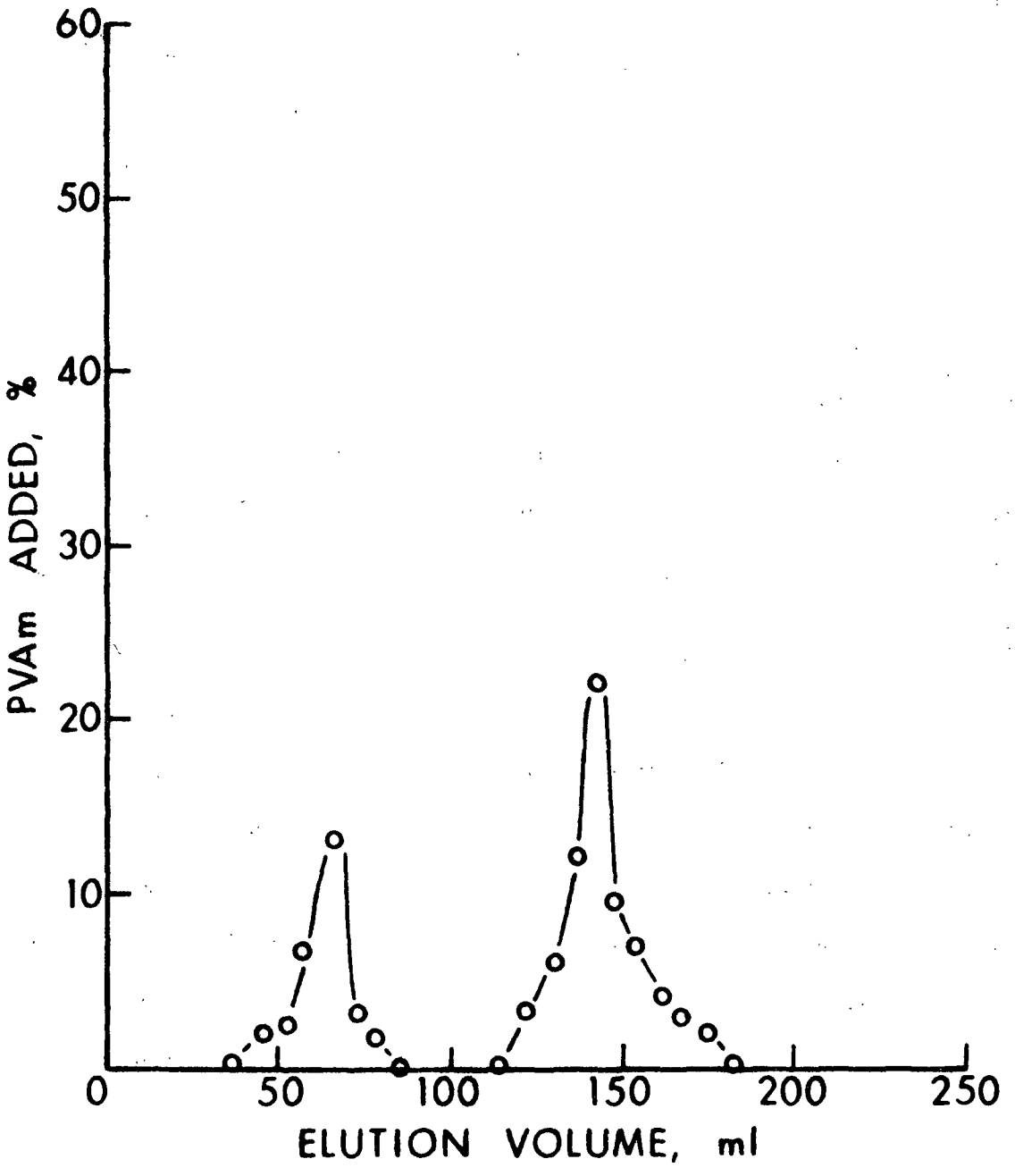

Figure 41. Elution Curve for PVAm Sheared with Flocs at pH 10

Morris and Schnurmann (71) reported degrading polymers with molecular weights of 100,000 with shear rates on the order of 10^5 sec^{-1}. Using polyisobutylenes ($M \approx 10^6$) and a shear rate of 65,000 sec^{-1}, Bestul and Belcher (72) noticed that viscosity was reduced to 50% of its original value. Abdil-Alim and Hamielic (212) found that degradation of a 0.7% solution of polyacrylamide required less than 1 min to attain equilibrium at a shear rate of 5×10^3 sec^{-1}. Calculations have demonstrated that the minimum shear rate generating conditions for degradation of a molecule of 10^4 repeating units is on the order of 10^3 sec^{-1}. PVAm with a molecular weight of 450,000 daltons would have about 10^4 repeating units. Based on this information, it is possible to conclude that restabilization via molecular weight reduction of the PVAm/PSL flocs could indeed occur at the shear rate used.

To summarize, the results of the analysis of the data presented thus far, at pH's 3 and 9, corresponding to PVAm charge densities of 95 and 13%, the polyelectrolyte adsorbs on the PSL surface in configurations that have hydrodynamic volumes small enough to withstand the shear generated in the system. At pH 10, however, where the charge density of PVAm is only 3%, the polyelectrolyte adsorbs on the PSL surface in a configuration that has an effective hydrodynamic volume of sufficient magnitude to induce chain scission when subjected to a shear rate of 10^4 sec^{-1}.

DILUTE SOLUTION BEHAVIOR OF POLYVINYLAMINE UNDER SHEAR

When placed in laminar shear flow, a rodlike polymer molecule in solution has two alternative courses of action, depending on the original alignment of the molecule relative to the field of flow (82).

In the first, the most obvious case, the molecule would be aligned with its major axis perpendicular to the field of flow, as shown in Fig. 42. Forces acting on the ends of the molecule will cause a rotation of the molecule (52).

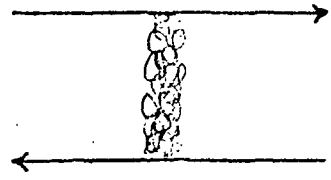

Figure 42. Alignment of Molecule Perpendicular to Field of Flow

The rotation will continue at least until the molecule aligns itself with the flow field. Each internal bond at this point would be experiencing an equal "tug" from both directions.

At points between these extremes there will be finite incremental forces pulling from each end of the molecule (Fig. 6). As these forces work from each end, they will be acting in summation of the vectoral components in the direction of the molecular chain. Under these circumstances they will meet in opposition and at maximum magnitude in the center of the molecule. Thus, the longer the molecule, the greater magnitude the vectoral force components will sum to, and the smaller the magnitude of the initial shear rate that must be imposed for molecular scission to occur.

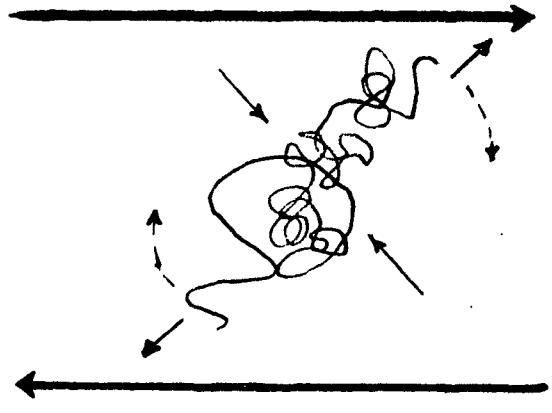

Figure 6. Tensile and Compressive Forces on a Threadlike Particle in Shear Flow. Heavy Lines Indicate Flow Lines, Light Solid Lines the Stresses on the Particle, the Dashed Lines the Direction of Rotation of the Particle

In this case, the stretching force at an angle relative to the field of flow may be described as

$$F = \int_0^{L/2} f \dot{\gamma} L \sin \theta \cos \theta \, dL \qquad (58)$$

where f = frictional drag per unit length, L

$\dot{\gamma}$ = velocity gradient (52)

Because the forces being summed are only components of the total shear stress, maximum degradation will occur when the molecule is aligned at a position of 45° with respect to the field of flow. Equation (58) may then be reduced to

$$F = f \dot{\gamma} L^2/16 \qquad (59)$$

From Equation (59) it can be seen that the force required to break a molecule is directly proportional to the square of its effective length. As the PVAm molecules at OFC's for pH's 3 and 9 were tightly held to the PSL surface in an essentially two-dimensional patch, the effective length subjected to frictional drag was greatly reduced. Molecules at the OFC for pH 10, however, were most likely adsorbed in a configuration resembling that of the free-solution molecule: a configuration upon which the derivation of Equation (58) is based.

To test the validity of the above theories, and to lend credence to the arguments presented to explain the results of the shear experiments conducted with flocs, a series of tests was run to examine the behavior of PVAm in hydrodynamic shear ($\dot{\gamma}$ = 38,400 sec^{-1}) at equivalent OFC's for pH's 3, 9, and 10. The results of experiments at all three pH's are shown in Fig. 43.

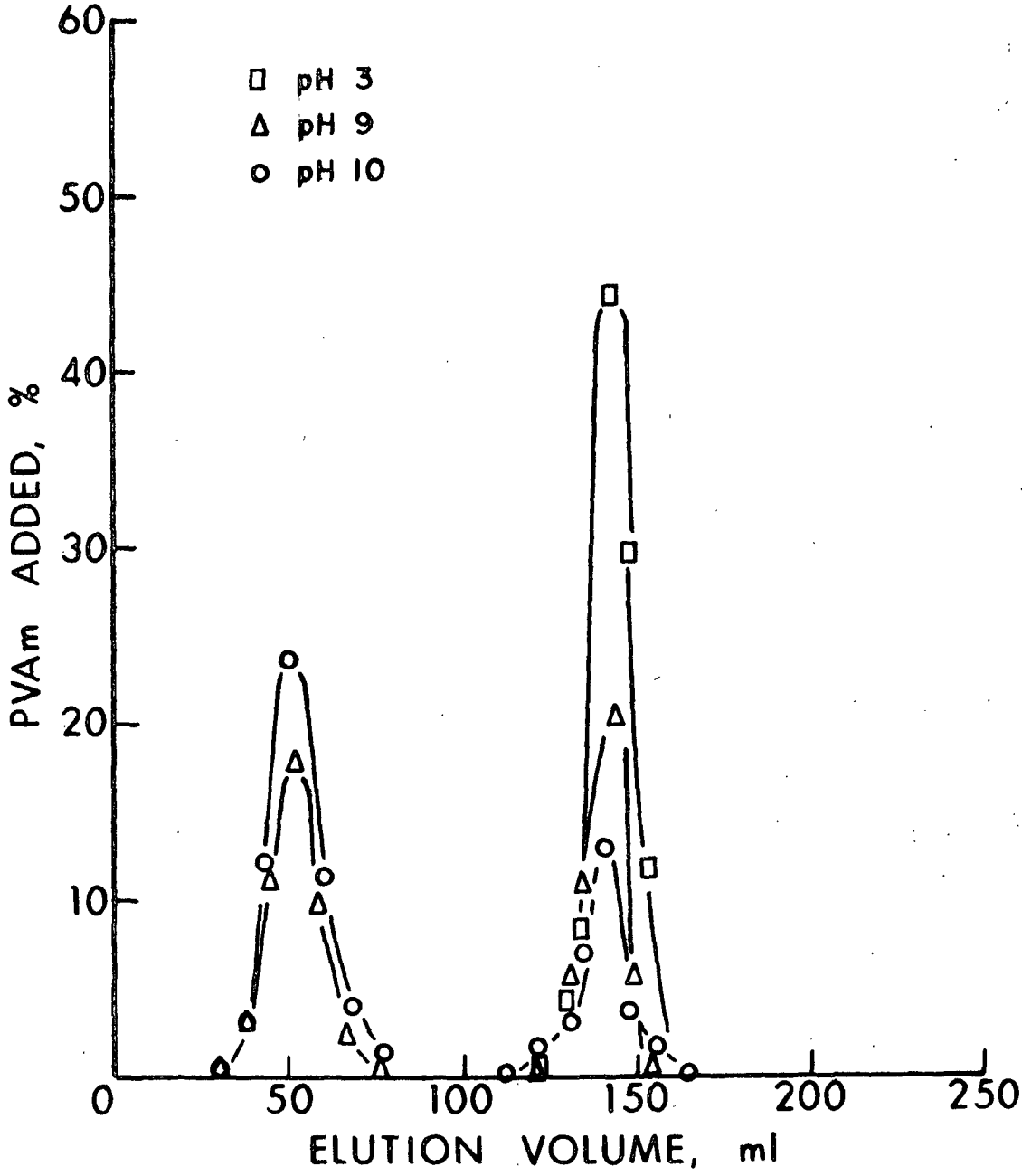

Figure 43. Elution Curves for PVAm Sheared Without PSL

It is significant that at pH's 9 and 10 the PVAm sample has been only partially degraded, while at pH 3 the degradation is complete. The extended solution dimensions due to the proximity of electrostatic charges on a PVAm molecule at pH 3 would seem to most readily lend itself to mechanical degradation if the above theories hold. Certainly the near-random coil configuration of a PVAm molecule at pH 10 could resist a certain amount of shear that would prove to be damaging at pH 3.

Several workers have reported more extensive degradation occurring with increased time of exposure to a constant shear rate. It is possible, then, that an increase in time of exposure to the shear field would more completely degrade the PVAm samples at pH's 9 and 10. The fact that PVAm degraded at pH 10 in the presence of PSL suggests that the added mass at the effective ends of the molecule was enough to compensate for the lack of critical molecular dimensions and/or shear rate. An alternative explanation is that the PVAm molecules were separated completely from all PSL surfaces so suddenly that molecular degradation could proceed via the same pathway followed by the solitary PVAm sample.

It is very interesting that at pH 9 PVAm exhibited a shear behavior similar to a high charge density molecule when in the presence of adsorbent PSL particles, but in their absence responded as a relatively random coil. This behavior accentuates the important role of electrostatic attraction in the determination of the adsorbed configuration of a polyelectrolyte on a surface of opposite electrical potential.

A peculiar trend of the data in Fig. 43 is that the degradation of PVAm at pH's 9 and 10 produced a distinctly bimodal molecular weight distribution. It appears that molecules were either completely degraded to lengths one-

eighth as long as the original chain, or they went completely undegraded. Abdel-Alim and Hamielic (212) found similar results, as shown in Fig. 44. No satisfactory explanation for the lack of intermediate degradation products is available.

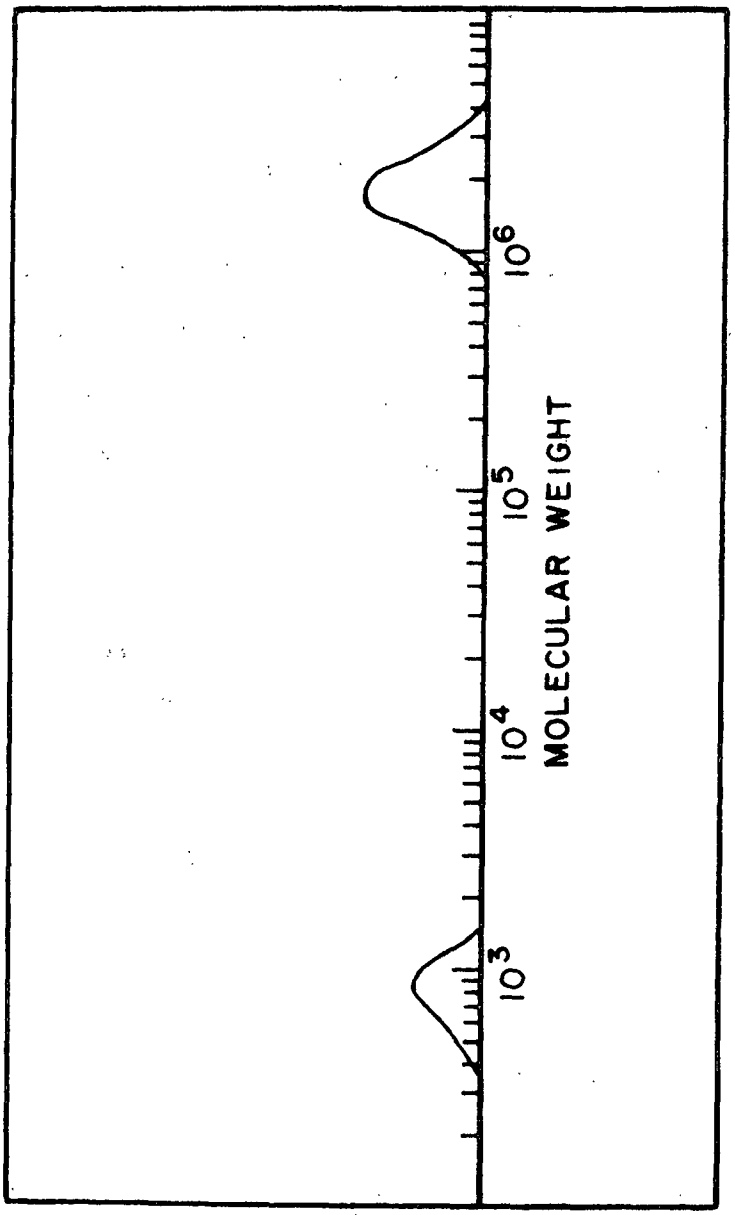

Figure 44. Bimodal Degradation of Polyacrylamide (212)

As Forgacs and Mason (107) have pointed out, if a filament is long enough to permit independent movements of either end, the filament will uncoil completely only when closely aligned with the fluid flow field. It is possible that in the time span during which the PVAm molecules are exposed to the shear field, only a select population of orientations about the axial direction of flow result in favorable alignments. Molecular degradation may then proceed through uncoiling and stress propagation. After the initial break in the molecule, however, it will take a longer time for the fragments to recoil (107,209); this, in turn, will permit further rapid degradation.

SURFACE CHARGE MEASUREMENTS

Particle electrophoretic mobility was used to determine the appropriate concentration of TDA for 1:1 adsorption on negative PSL sites at a concentration of 1.82×10^9 particles per mL of solution. A plot of zeta potential versus initial solution concentration of TDA is shown in Fig. 45.

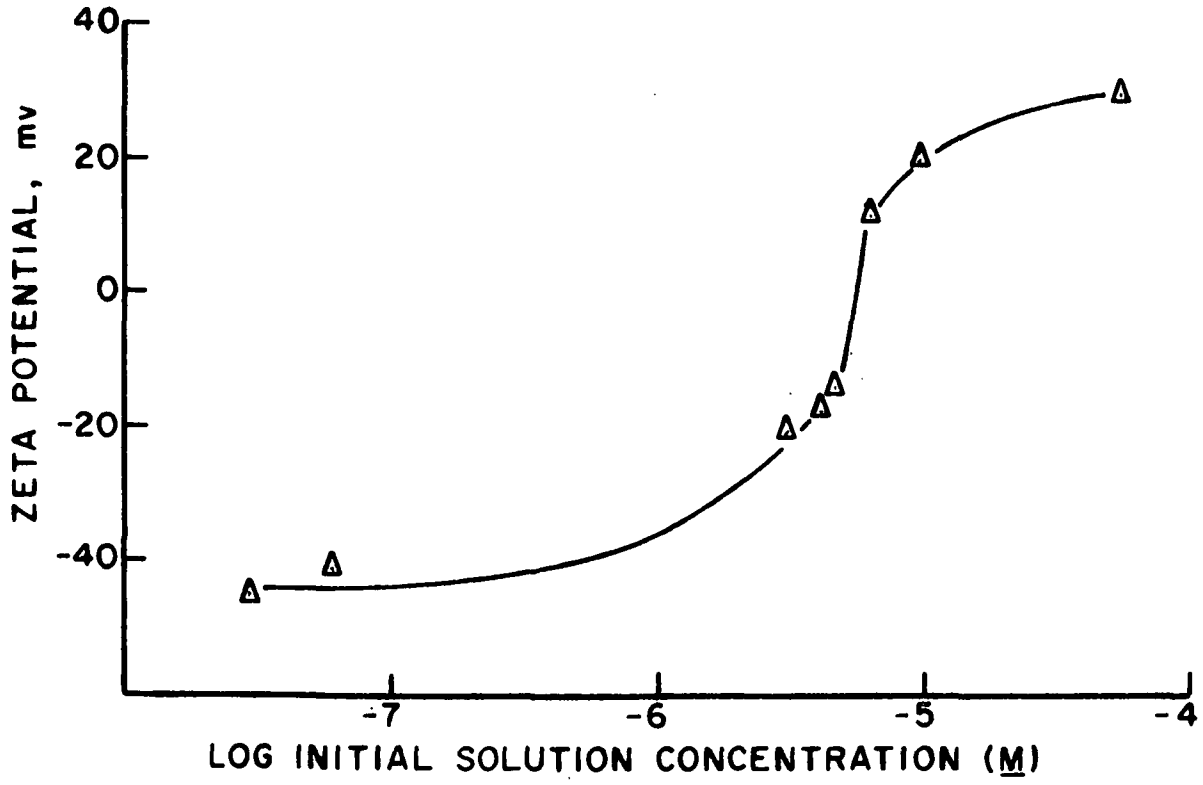

Figure 45. Zeta Potential of PSL in TDA Solutions

A conclusion deduced by Connor and Ottewill (153) was that a stoichiometric association of TDA occurred with PSL surface charges at the point of zero electrophoretic mobility. The initial TDA concentration producing zero mobility in Fig. 45 was 5.0×10^{-6}M. This concentration was used for all other TDA adsorption experiments.

TDA molecules at concentrations lower than the "knee" were found to be very firmly bound to the PSL surface. They could not be desorbed by water up to 100°C; nor could they be displaced by quaternary ammonium ions of shorter or longer chain lengths (151). The tenacity of this adsorption can be attributed to the hydrophobic association of the alkyl chain with the latex surface.

Experiments were conducted at each pH to check the possibility of displacement of either TDA or PVAm by the other adsorbate. A saturation ("knee") concentration of TDA was allowed to equilibrate with PSL, and then an overdose (48 mg/liter) of PVAm was introduced and allowed 4 hours to displace the TDA. This time of contact was an hour longer than any actual contact times during the "surface area change" experiments. No TDA was detected in the supernatant after PVAm contact. PSL was then "overdosed" with 48 mg/liter PVAm before TDA addition. An additional 4 hours of contact resulted in no detectable TDA adsorption. These results concur with the findings of Connor and Ottewill concerning the tenacity of TDA adsorption.

FREE SURFACE CHARGES AT OPTIMUM FLOCCULATION CONDITIONS

A comparison of TDA adsorption on virgin PSL to adsorption on PSL treated with OFC's at pH's 3, 9, and 10 provided a means of calculating the PSL surface charges consumed by PVAm in the flocculating systems. Results of this comparison are presented in Table V. The TDA solution alone produced 12,000

counts per minute (cpm). Adsorption of TDA on virgin PSL produced a count of 800 cpm. Counting was performed with a 2σ statistical error of ±0.2% (213). Variations from duplicate runs are noted in parentheses.

TABLE V

TDA ADSORPTION ON PSL AT OFC'S

	TDA in Supernatant (cpm)	Molecules of TDA Adsorbed ($\times 10^{-16}$)
Virgin PSL	800 (±7)	5.62 (±0.05)
OFC 3	1548 (±13)	5.25 (±0.04)
OFC 9	2476 (±18)	4.78 (±0.03)
OFC 10	3053 (±22)	4.49 (±0.03)

The total number of TDA molecules adsorbed on the virgin PSL is within 2% of the number of anionic surface charges available, as calculated from potentiometric titration data (5.76×10^{16}). This provides significant evidence that TDA adsorption at the adsorption isotherm "knee" occurs stoichiometrically on PSL surface charges.

FREE SURFACE CHARGES OF FLOCCULATED POLYSTYRENE LATICES UNDER SHEAR

The objectives of this part of the investigation were 2-fold. Initially, it was intended to determine the extent of particle/polymer separation during shear. In addition, examination of the concept of polymer "smearing" on the particle surface during shear was desired.

It was assumed that if anionic surface sites were generated by the "plucking off" of PVAm cations, TDA would have a much greater chance of reaching the anions than would the PVAm. Such a phenomenon would be more certain to occur in instances where the number of sequential PVAm segments desorbed inhibited a

diffusional return to the surface before TDA diffusion/adsorption could occur. Because of the hydrophobic association of TDA tails with aliphatic PSL surface sites, it was not expected that any adsorbed TDA would be pulled off by hydrodynamic forces.

To test the feasibility of floc degradation due to separation at the particle/polymer interface, flocs at each pH were sheared in the presence of TDA. Results of this experiment are presented in Table VI.

TABLE VI

TDA ADSORPTION ON FLOCCULATED PSL DURING SHEAR

	TDA in Supernatant (cpm)	Molecules of TDA Adsorbed ($\times 10^{-16}$)
OFC 3	1418 (±12)	5.31 (±0.04)
OFC 9	1790 (±15)	5.12 (±0.04)
OFC 10	987 (±8)	5.53 (±0.04)

Because all "excess" PSL surface charges were in quantitative association with TDA molecules in the last experiment, it was not possible for PVAm to be redistributed on the particle surface during shear. To test the feasibility of this phenomenon during the shear of flocs, it was necessary to add the surfactant to the suspension after shear. This was accomplished by slowly introducing the TDA throughout the shearing procedure at a point just above the shear zone of the apparatus. Results of this experiment are given in Table VII.

TABLE VII

TDA ADSORPTION ON FLOCCULATED PSL AFTER SHEAR

	TDA in Supernatant (cpm)	Molecules of TDA Adsorbed ($\times 10^{-16}$)
OFC 3	1446 (±12)	5.30 (±0.04)
OFC 9	1790 (±15)	5.12 (±0.04)
OFC 10	1274 (±8)	5.38 (±0.03)

SUMMARY OF RESULTS

Table VIII provides a summary of the experimental results obtained in this investigation.

TABLE VIII

EXPERIMENTAL RESULTS

pH	3	9	10
Charge on PVAm	95%	13%	3%
OFC of PVAm	0.178 mg/L	0.605 mg/L	3.35 mg/L
Radius of PVAm	3,300 A	800 A	306 A
PVAm degraded with floc	No	No	Yes
PVAm degraded without floc	Extensively	Partially	Partially
Total PSL charges covered by PVAm at OFC (±1%)	6.6%	14.9%	20.1%
Total PSL charges covered by PVAm during shear	5.5%	8.9%	1.6%

FLOCCULATION MODELS

The experimental evidence presented in this work indicates that at various pH's in the PVAm/PSL system different flocculation mechanisms are significant contributors to the particle aggregation process. In the following sections flocculation models are constructed for the PVAm/PSL system at each pH studied.

pH 3 FLOCS

At pH 3 approximately 95% of the available PVAm nitrogens carry a positive charge. In this case, neighboring segments of the molecule try to repel one another, thus preventing any resemblance to a molecular random coil. Viscosity data support the contention of the existence of a very extended and rigid configuration of the PVAm molecule under these conditions.

Additionally, it has been demonstrated that an extremely small quantity (0.178 mg/liter) of PVAm is required to optimize the flocculation of a PSL suspension of 1.82×10^9 particles/mL. At these concentrations there exists only one positive charge for every 2.4 negative charges in the system. An argument of simple charge neutralization is therefore obviously invalid. Together, this evidence suggests that in its highly charged and extended solution configuration a PVAm molecule is very efficient in aggregating colloidal particles of opposite charge.

The investigation of molecular weight distributions of PVAm after hydrodynamic shear while in a flocculated configuration revealed no degradation. When a solution of PVAm at the same concentration but without PSL particles present was subjected to the same shear, extensive molecular degradation was produced. Implicit in these results is a PVAm adsorbed configuration that has significantly reduced molecular extension into the solution in comparison to the unadsorbed dimensions.

The high interaction energy resulting from the abundance of opposite charges distributed between PVAm and PSL also supports a somewhat flattened configuration of PVAm adsorbed on the PSL surface. To minimize the electrostatic free energy, the components should tend to maximize the 1:1 association of positive and negative charges. On the average, there are about 11.2 A between the negative charges on a PSL surface. PSL has been probed with krypton atoms and found to be relatively smooth (123). Assuming a PVAm monomer length of 2.54 A, five monomer units are necessary to linearly bridge the average space between PSL negative sites. A schematic representation of this relationship is shown in Fig. 46. Extending bonds to maximize the size of the PVAm loops between PSL negative sites produces a loop size of about 4 A. When compared to the calculated 68 A of the double layer thickness, no provisions

are evident for the existence of polymer bridges. The polyelectrolyte must exist as a "patch" on the particle surface.

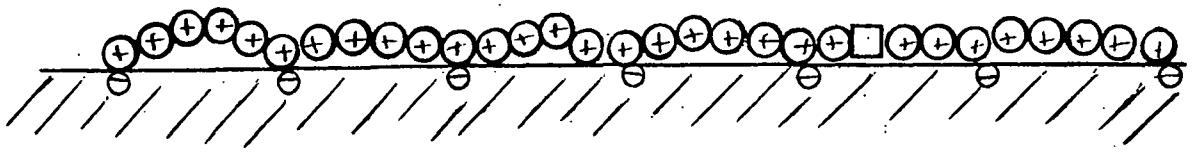

Figure 46. Scale Drawing (2 mm = 1 A) of the Proposed Cross Section of Maximum Association of PVAm Protonated Sites with Ionized PSL Surface Group. ⊕ Represents a Protonated Monomer Unit. □ Represents an Unprotonated Monomer Unit

As shown in Table II, the total number of positive PVAm charges present in this experimental system was 2.31×10^{16}. Because only one out of five protonated monomer units can be geometrically associated with a negative surface site on one particle, only 8.0% of a given particle's ionized groups may be paired with an oppositely-charged polyion group at OFC.

Because of the flat adsorption configuration of PVAm, only a small portion of any one molecule would be available for association with the surface of a second particle. From Table VIII, the number of PSL negative sites covered at OFC is about 6.6% (±1%) of the total in the system. After shearing 5.5% (±1%) of the PSL sites remained covered by PVAm. The overlap of experimental uncertainty of these measurements suggests that under optimum flocculation conditions, PVAm adsorbs in a configuration that tends to maximize the quantitative association of protonated amines and ionized PSL surface groups.

The fact that the experimentally-determined PVAm coverage of PSL surface sites is somewhat lower than the absolute maximum that is geometrically possible is consistent with the statistical mechanical interpretation of the configuration of a polyelectrolyte coil.

Particles have a mean diameter of 7940 A and a double layer thickness of 68 A. When flocculated with PVAm at pH 3, interparticle separation is probably not much greater than 4 A. The floc geometry is thus very dense. Collision of any two particles must occur through electrostatic attraction, because the stabilizing double layer around each particle is 17 times as thick as the maximum extension of adsorbed polyion segments into solution. A cross section of such a floc is schematically illustrated in Fig. 47.

pH 9 FLOCS

As shown in Table VIII, 13% of the available PVAm nitrogens carry a positive charge at pH 9. Having a moderately low charge density, the molecular coil would most likely possess an elliptical solution configuration (20,177). This hypothesis is borne out by the viscosity data.

While carrying one-seventh the number of cations of the pH 3 molecule, just over 3 times the amount of PVAm used at pH 3 is required to produce optimum flocculation at pH 9. This concentration of 0.605 mg/liter provides one positive PVAm charge for every 5.3 negative PSL charges in the system. Simple charge neutralization is again not possible.

The investigation of molecular weight distributions of PVAm after hydrodynamic shear while in an aggregated state showed no molecular degradation. Shear of the unadsorbed polymer at the same concentration resulted in appreciable degradation. The adsorbed polyion configuration deduced from this evidence is one whose dimension perpendicular to the PSL surface is much smaller than the radius of gyration of the unadsorbed molecule.

Assuming a monomer length of 2.54 A and 13% protonation, there would be an average of 19.5 A between charges on a PVAm molecule. This spacing would permit a 1:1 association with negative charges located an average of 11.2 A

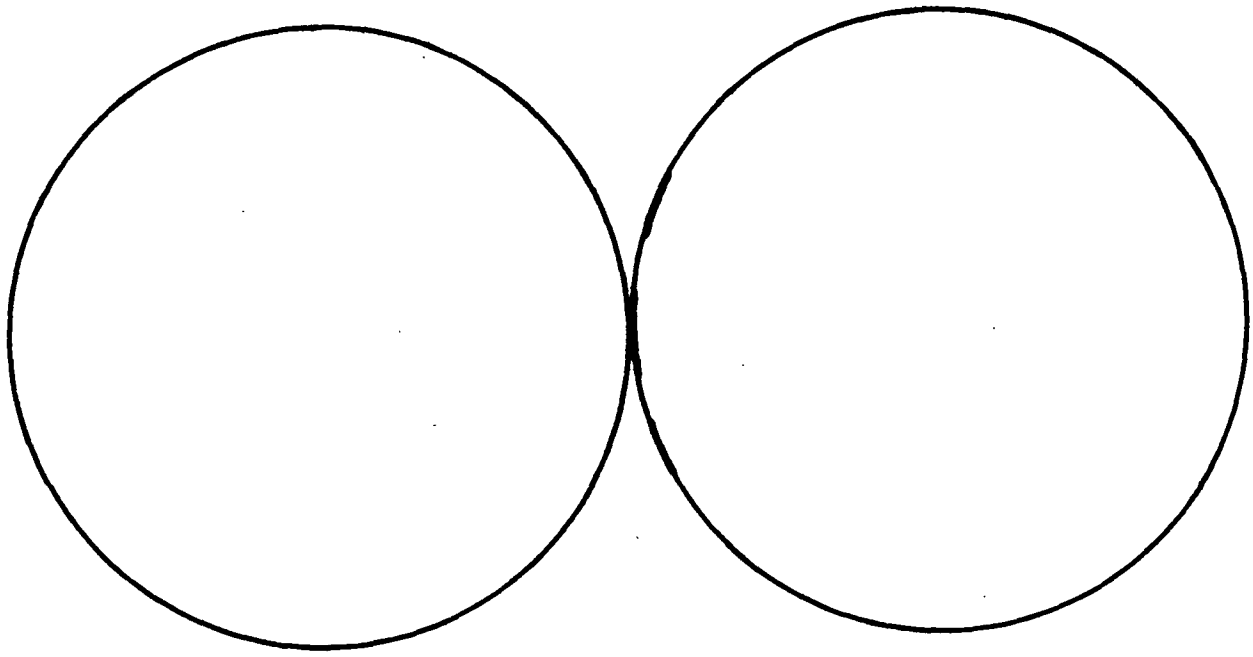

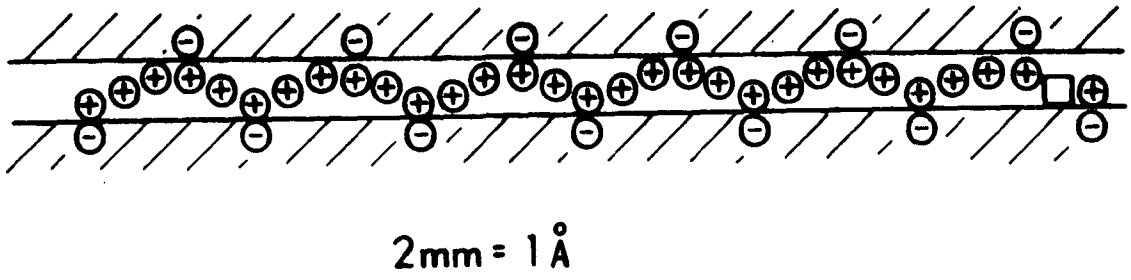

Figure 47. Scale Drawings of Proposed Cross Section of Patch-Type Floc at pH 3. Polyion is 95% Protonated. ⊕ Represents a Protonated Monomer Segment; □Represents an Unprotonated Monomer Segment

apart. If this were in fact what happened 18.7% of the PSL charges would be neutralized by PVAm cations. A schematic representation of this relationship is shown in Fig. 48. It is evident from this representation that complete association of PVAm protonated groups with only one particle is theoretically possible.

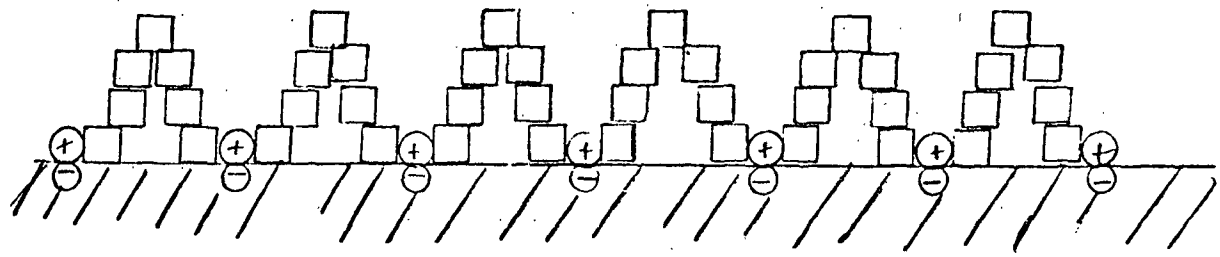

Figure 48. Scale Drawing (2 mm = 1 A) of Cross Section of Maximum Association of PVAm Protonated Sites with Ionized PSL Surface Groups. ⊕ Represents a Protonated Monomer Segment. □ Represents an Unprotonated Monomer Segment

Because this model provides no means for electrostatic interactions of the adsorbed polyion and a second particle surface, it is not considered physically valid. A more realistic model would include loops of at least twice the size of those shown in Fig. 48. Attachment to a second particle, as shown in Fig. 49, could also thus produce an 18.7% neutralization of PSL charges by PVAm cations. The maximum PVAm loop extension between two PSL surfaces as shown in Fig. 49 is about 19 A. Such a polyion conformation is not physically unreasonable, as a significant number of polyion segments must order themselves to permit the maximum association suggested in Fig. 48. In addition, the unadsorbed PVAm configuration is significantly more coiled than is the molecule at pH 3, where maximum association has been found to occur. As presented in Table VIII, approximately 14.9% (±1%) of the total PSL surface charges are in association with PVAm protonated groups at OFC. Comparison of the theoretical maximum (18.7%) PSL surface site coverage at pH 9 with the experimentally determined coverage suggests that the configuration of the adsorbed polyion is not far removed from equilibrium at the time of flocculation.

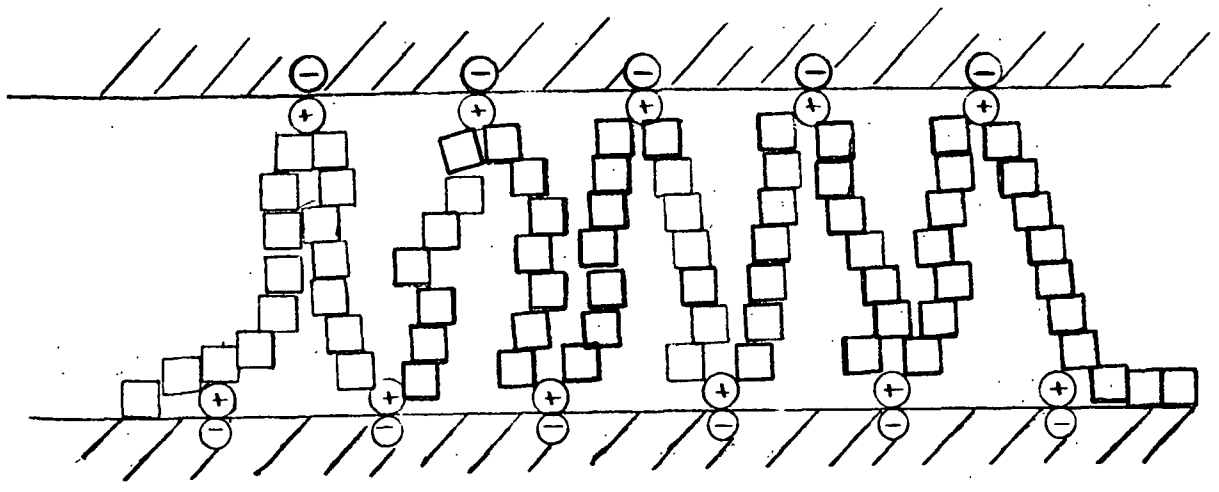

Figure 49. Scale Drawing (2 mm = 1 A) of Cross Section of Maximum Association of PVAm Protonated Sites with PSL Surface Groups During Flocculation. ⊕ Represents a Protonated Monomer Segment. □ Represents an Unprotonated Monomer Segment

Continuing on the assumption that loop size is approximated by that shown in Fig. 49, viz., 19 A, comparison to the double layer thickness of 68 A still leaves no possibility for the existence of polymer bridges. The polyelectrolyte must exist as a "patch" on the surface of the particle, and the floc is thus dense. Collisions between any two particles must occur through electrostatic attractions, because the stabilizing double layer of either particle is still 3.6 times as thick as the maximum extension of adsorbed polymer segments into solution.

In addition to the positive charges on PVAm producing a strong interaction with PSL surface, it is probable that uncharged segments of the PVAm would associate at least to some extent with the hydrophobic portion of the PSL surface. Such interaction would reduce the extension of any loops, leaving the value of 19.0 A between flocculated particles as a maximum value. It is speculated that the interparticle distance would be much less than this value.

A schematic representation of the proposed model is shown in Fig. 50.

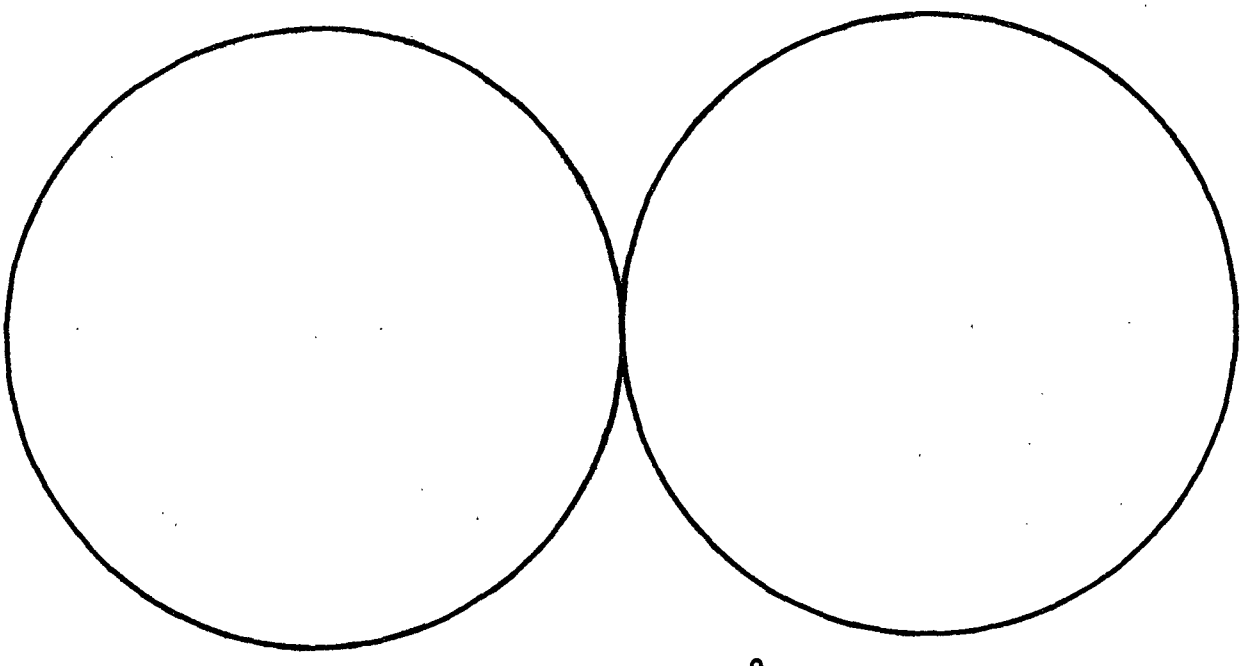

1mm = 100 Å

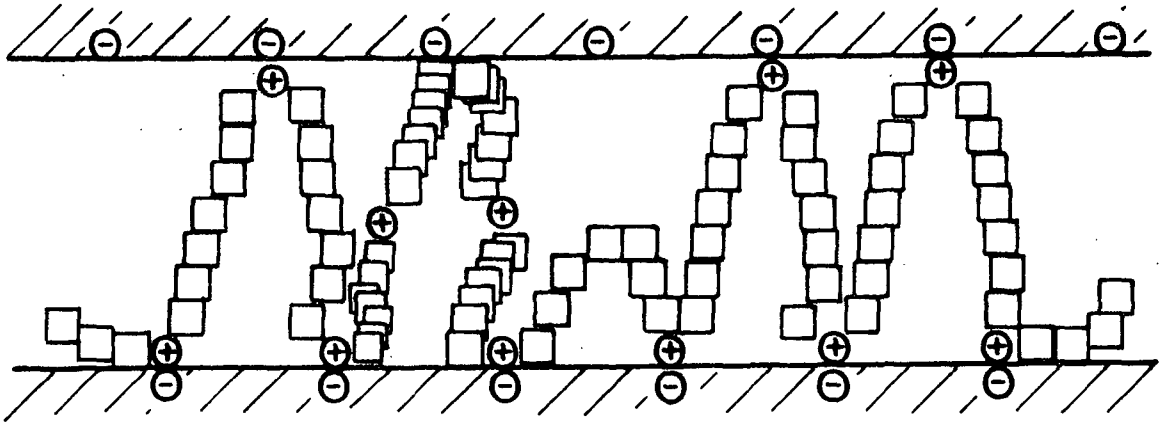

2mm = 1 Å

Figure 50. Scale Drawings of Cross Section of Patch-Type Floc at pH 9. Polyion is 13% Protonated. ⊕ Represents a Protonated Monomer Segment. ☐ Represents an Unprotonated Monomer Segment

pH 10 FLOCS

As shown in Table VIII, only 3% of the available nitrogens on a given PVAm molecule are protonated at pH 10. As such, the unadsorbed configuration of the molecule is best approximated by a random coil.

An optimum flocculation concentration of 3.35 mg/liter is almost 20 times the amount necessary for optimum flocculation at pH 3. The number of cations per PVAm molecule provides one positive charge for every 4 negative charges. Once more the occurrence of coagulation by simple charge neutralization is not possible.

The results of the investigation of molecular weight distributions of PVAm after hydrodynamic shear of the flocs proved to be very interesting. There appeared to be more degradation of PVAm in a flocculated state than there was in free solution. This can be explained by the increased tension exerted on a molecule due to the attachment of the bulky polystyrene spheres.

The fact that extensive molecular degradation occurs strongly suggests that the adsorbed configuration of PVAm at pH 10 is no more compact than the free solution configuration. Without the presence of strong electrostatic interactions there is no reason (other than random diffusion) for molecular segments at any appreciable distance to be transported to the PSL surface. Eirich (214) has used adsorption isotherms and studies of adsorbate layer thickness to conclude that uncharged macromolecules are held by relatively few attachments as essentially "solvent pervaded" coils with dimensions similar to those of coils that are free in solution.

The 3% charge density of PVAm at pH 10 would allow an average of 85 A between charges on the molecular backbone if they were spaced evenly. However,

hydrophobic interactions and Van der Waals forces will cause a molecule of less than 10% ionization to remain in a coiled configuration (20), and the charges will be spaced at the periphery of the coil (161).

The radius of gyration of the molecular coil at pH 10 has been estimated from viscosity data to be about 338 A, producing a diameter of 920 A. This extension and the presence of positive charges at the periphery of the coil provide an excellent specimen for polymer "bridging," as the combined thickness of the double layers of colliding particles is only about 460 A. A schematic diagram of this model of polymer bridging is shown in Fig. 51.

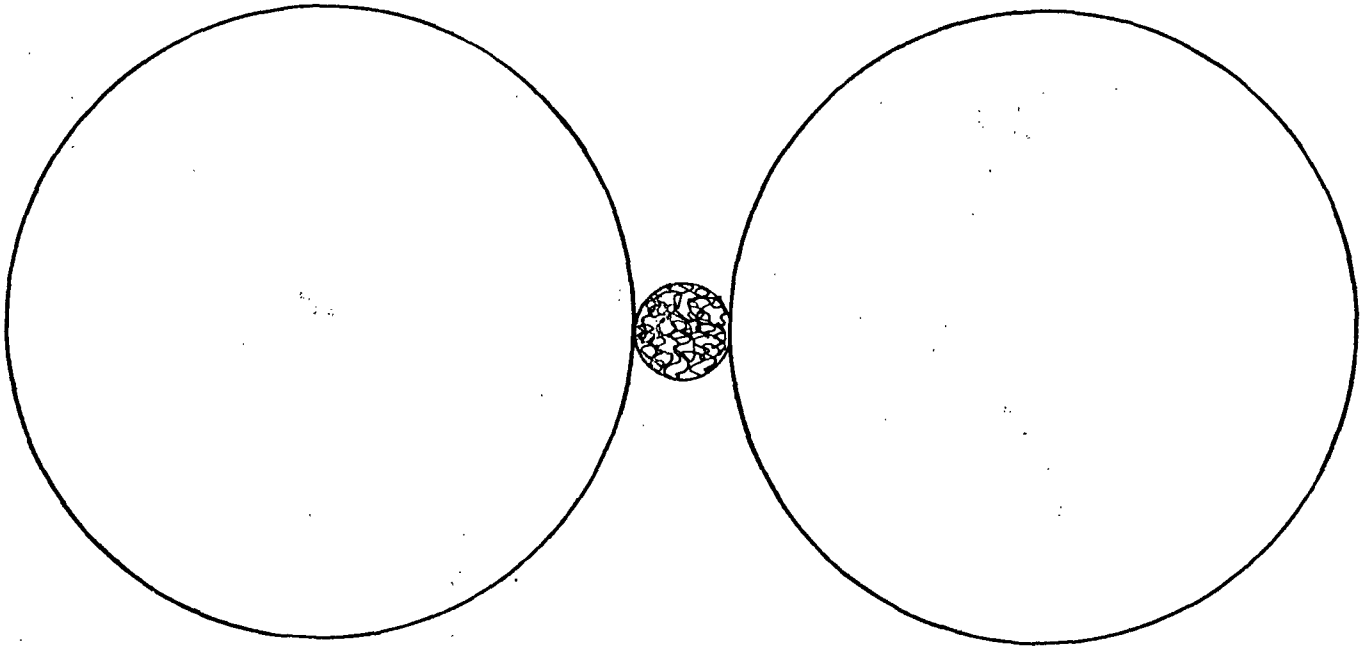

Figure 51. Scale Drawing (1 mm = 100 A) of Cross-sectional View of Possible Bridge-type Floc. Polyion is 3% Protonated

Chan, et al. (215) have concluded from statistical mechanical investigations that in situations where polymer-adsorbent interaction energies approximate the magnitude of polymer segment-polymer segment interaction energies, the center of mass of the polymer is a significant distance from the surface. Such a configuration was proposed to be the result of competition between the energy gained through adsorption and the consequent loss of configurational

entropy. Because hydrophobic interactions of PVAm are of sufficient magnitude to withstand the coil-expanding tendencies of the electrostatic field energy of the molecule at pH 10, adsorption of the polyion on PSL surfaces should be governed by Chan's theory.

Calculations based on the number of PVAm molecules adsorbed on PSL (Table II, p. 86) show that simultaneous adsorption of all molecules will not permit a surface configuration as large as that approximated from the unadsorbed radius of gyration. Neighboring molecules will push a given molecule away from the surface. An illustration of this adsorption model and the comparable solution dimensions of the molecule is shown in Fig. 52.

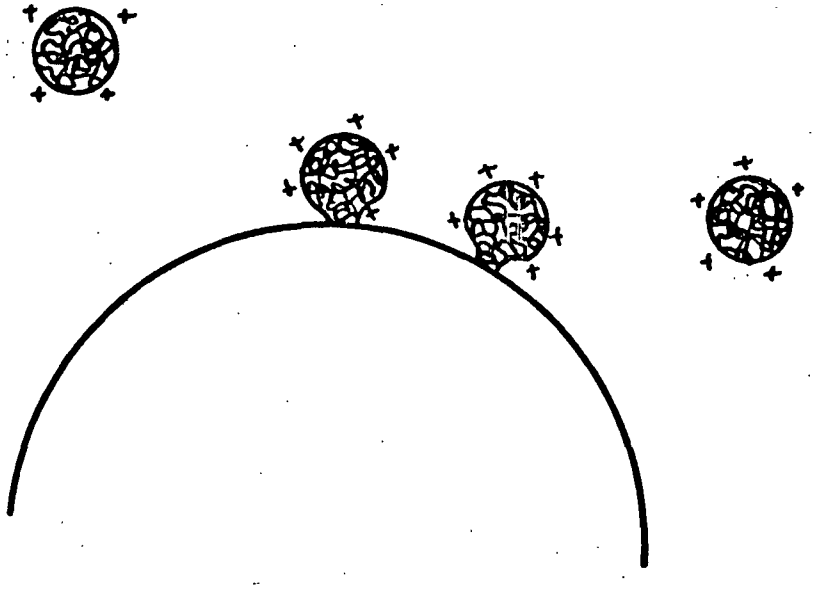

Figure 52. Scale Drawing (1 mm = 100 A) of Cross Section of Proposed Polymer Adsorption Model and Comparable Unadsorbed Solution Dimensions

As presented in Table VIII, TDA adsorption results suggest that approximately 20% (±1%) of the total available PSL negative sites have associated with PVAm cations at OFC 10. If all the available PVAm cations were stoichometrically associated with PSL anions, 23.9% of the surface sites would be covered by PVAm.

The variation between theoretical maximum and experimentally observed values can be explained by the location of the cations at the periphery of the PVAm coil. Because of the close packing it is not possible for all of the PVAm to be in contact with particle surfaces. However, redistribution of PVAm protonated sites to maximize electrostatic associations would be possible.

A schematic diagram of the proposed model of an equilibrium bridge-type floc is shown in Fig. 53.

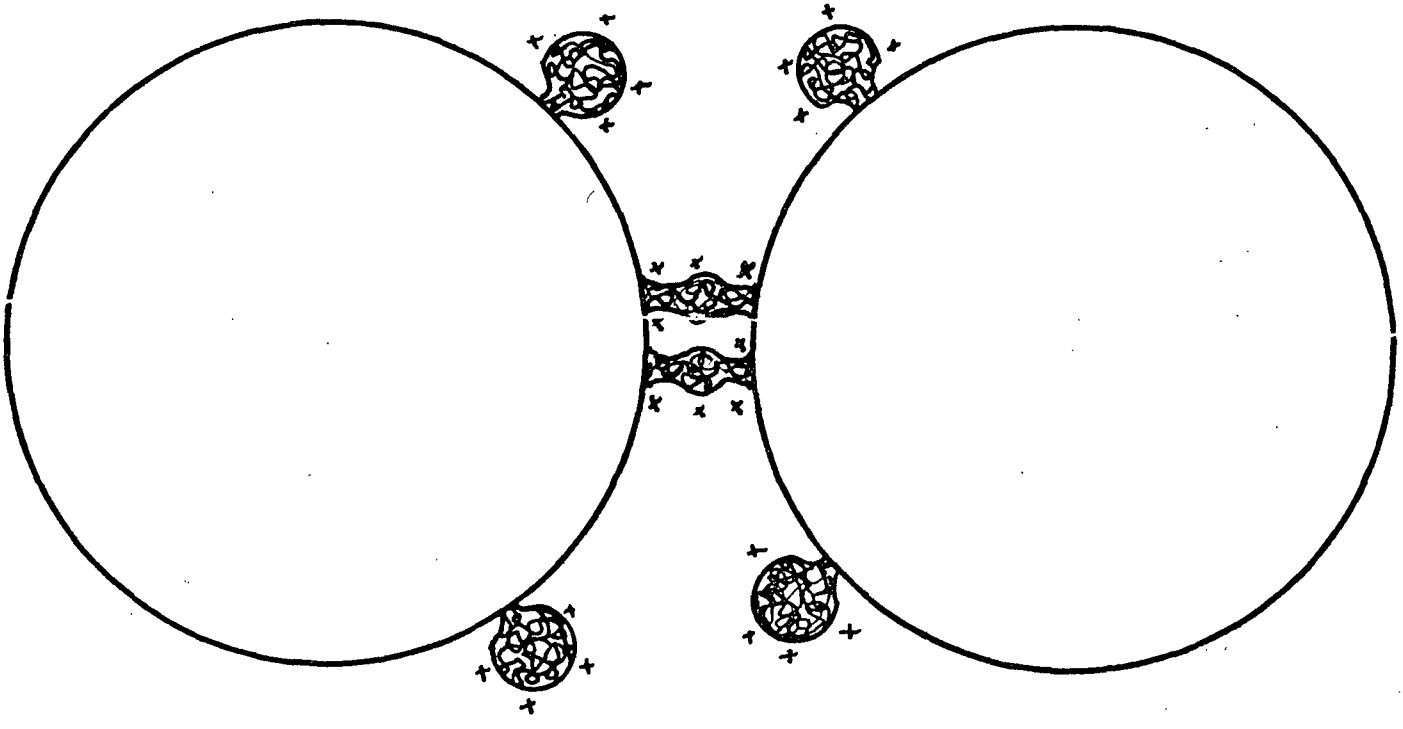

Figure 53. Scale Drawing (1 mm = 100 A) of Cross Section of Proposed Equilibrium Bridge-type Floc. Polyion is 3% Ionized

MECHANISMS OF FLOC DEGRADATION

In their discussion of theoretical and practical contributions to the elucidation of retention problems in papermaking systems, Beck, et al. (118) have speculated that shearing colloidal material flocculated with bridge-forming polyelectrolytes results in a degradation of both flocs and the polymer chains. In cases of flocs formed by simple charge neutralization or electrostatic patches the flocs were disrupted by shear; however, reflocculation was

reported to take place immediately after a reduction in the shear forces. Shear forces were also reported to break up flocs formed by bridges and patches. Patch-type flocs reformed after a reduction in shear forces, while bridge-type flocs did not.

It was the hypothesis of this research that the actual mechanism of aggregation should have a direct consequence on the mechanism of aggregate degradation in a shear field. It was proposed that a study of aggregate degradation in a shear field would yield additional insight to the preferred mechanisms of flocculation of a colloidal dispersion by a high molecular weight polyelectrolyte. In the previous section evidence was presented for aggregate models formed by bridging and electrostatic patches. The following sections will describe the most likely pathways of aggregate degradation followed by these different floc geometries.

pH 3

The flocs at pH 3 are formed by the so-called electrostatic patch mechanism. The configuration of these flocs is one of closely packed particles connected by a relatively flat patch of polyion which, in turn, exhibits a strong electrostatic attraction for the particle surface.

According to the model developed in the previous section, PVAm adsorbs strongly to the PSL surface. The configuration on the surface is one of small loops: only five or six monomer segments in length. It is proposed that the polyion must "zipper" down on the surface in a geometric shape resembling the rigid-rod solution form. In this extended form on the surface only a small segment of the molecule will be able to adsorb on a second particle. Because individual electrostatic associations are weaker than carbon-carbon covalent

bonds, separation at the interface between the polyion and the second particle will require much less energy than intramolecular polyion rupture.

The data in Table VIII for OFC 3 suggest that a small amount of surface area was generated by shearing the flocs at pH 3. This indicates that separation at particle-polyion interfaces has occurred. A comparison of the data for OFC in Tables VI and VIII (p. 128 and 129) indicates that no polyion rearrangement takes place on the particle surface during shear. These trends would be expected if the polyion reached an adsorption equilibrium configuration before interparticle collisions occurred during the initial flocculation process.

Because the PVAm adsorption configuration is extremely flat, the viscous drag experienced by adsorbed molecular segments is very small in comparison to those imposed on segments greatly extended into the solution. No molecular degradation occurred as a result of hydrodynamic shear. Additionally, the lack of PVAm rearrangement on the particle surface left restabilized particles in a condition to reflocculate via the same mechanism followed during initial aggregation.

The compactness of these aggregates enables them to withstand hydrodynamic shear. Disruption of aggregates does not proceed all the way to individual particles, but stops when a critical size has been reached. Because the extent of flocculation is a function of the number of discrete particles present, reflocculation of a suspension consisting largely of multiple particles will initially be more efficient than original flocculation of the virgin suspension.

To summarize, then, aggregate rupture at pH 3 proceeds by polyion-particle separation with no ensuing reconformation of the adsorbed polyelectrolyte on the particle surface. Also, no molecular degradation of the polyion occurs.

Subsequent reaggregation takes place via the same mechanism as initial flocculation. A schematic representation of this process is shown in Fig. 54.

pH 9

The flocs at pH 9 are also formed with electrostatic patches, although the patches are not quite as compact or highly charged as those at pH 3. These flocs consist of closely packed particles connected by a relatively flat patch of polyion exhibiting a strong attraction for the particle surface. This attraction is manifested by the opposite charges of polyelectrolyte protonated amines and particle sulfate groups, and also by the hydrophobic interaction of unprotonated monomer segments and polystyrene aliphatic chains.

The data in Table VIII show that PVAm associated with about 15% of the available PSL anions of the virgin flocs, and only 9% of the available surface groups during shear. It may thus be deduced that about 40% of the PVAm segments originally paired with a particle surface group became desorbed during shear.

A comparison of appropriate data in Tables VI and VII shows that no polymer reconformation on the particle surface has taken place. Loops are therefore not much larger than the theoretical minimum possible, and little viscous drag is experienced by the molecular segments. As a result, no molecular degradation occurred. Restabilized particles were therefore in a condition to reflocculate via the same mechanism followed during initial aggregation.

Because the number of protonated sites available to a given PVAm molecule is much smaller at pH 9 than at pH 3, it stands to reason that the pH 9 flocs should submit more readily to shear disruption than would the pH 3 flocs. According to the data in Fig. 27 (p. 91) this is actually the case. Because these

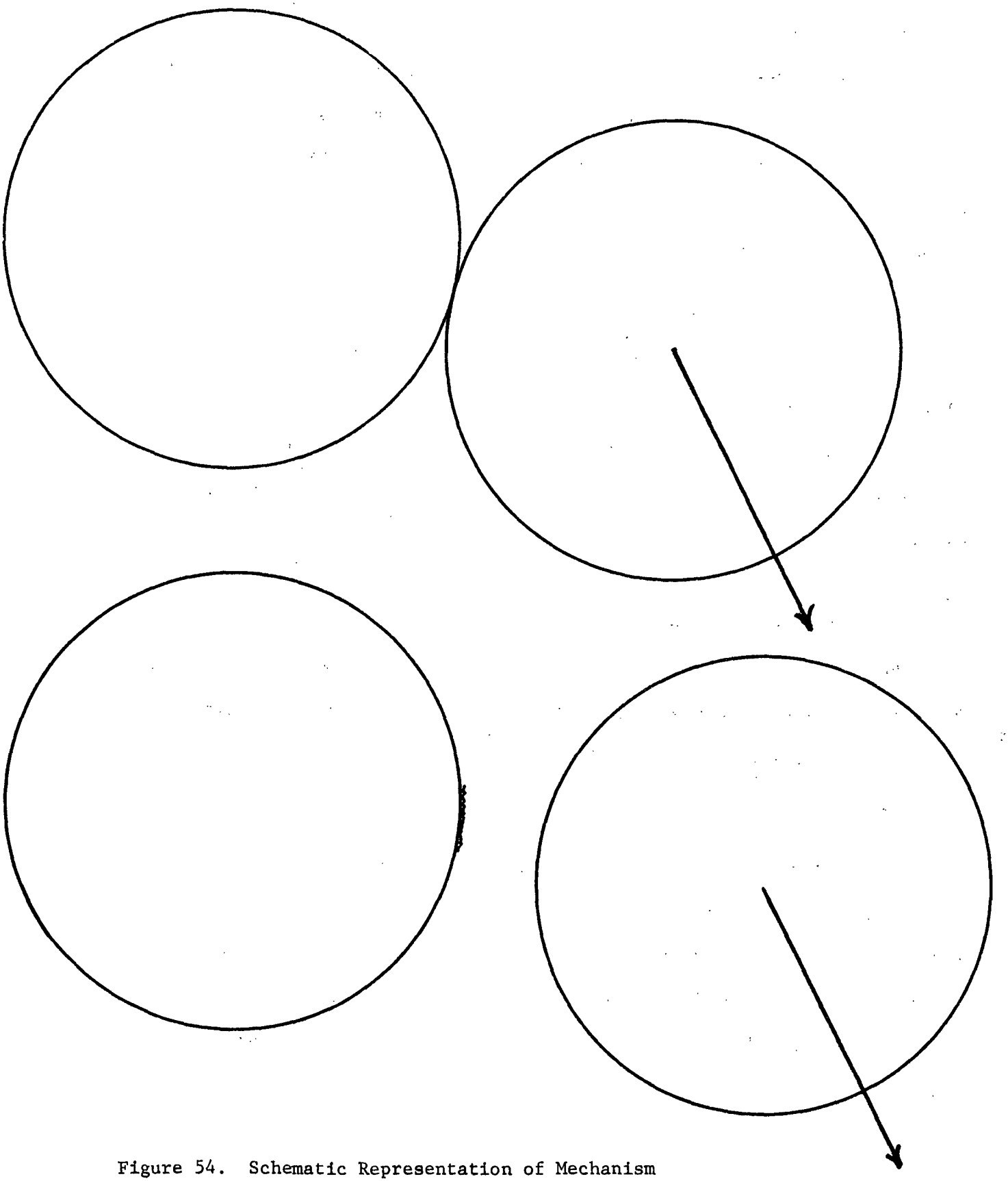

Figure 54. Schematic Representation of Mechanism of Aggregate Rupture at pH's 3 and 9

flocs are more easily degraded and are slightly less dense than flocs at pH 3, aggregate rupture should proceed to smaller particle sizes. This, in turn, would provide an explanation for a slight decrease in noticed extent of flocculation at a given period of time when compared to the pH 3 situation (Fig. 27). However, reflocculation of the disrupted pH 9 flocs was still quicker than initial flocculation, as complete degradation to singlets did not occur (Fig. 36, p. 110).

In summary, aggregate rupture at pH 9 proceeds by polyion-particle separation with no ensuing redistribution of the adsorbed polyelectrolyte on the particle surface. The compact adsorption configuration prevents molecular degradation of the polyion. Subsequent reaggregation takes place via the same mechanism as initial flocculation. A schematic representation of this process is shown in Fig. 54.

pH 10

The flocs at pH 10 are formed through a bridging of two particles by a PVAm coil adsorbed almost equally to both particle surfaces. The particles in these flocs are not closely packed, but exist in a weak and deformable networklike array.

Because the number of contacts of polyelectrolyte with particle surface is equally distributed between particles, separation is not preferred at either polyion-particle interface. The low charge density of the polyion permits only a small number of electrostatic contacts between a given molecule and particle. Healy (216) found that the number of segments of adsorbed polymer decreased with increasing time of agitation.

The data in Table VIII reveals that when all "extra" PSL sites are covered with TDA before shear, over 90% of the initially adsorbed PVAm is removed from the particle surfaces by shear. On the other hand, using the data in Table VII (p. 128), if additional surface sites are available for polymer reconformation about 30% of the initially adsorbed PVAm remains on the surface. In light of the imposed tension and compressive forces, shown in Fig. 6 (p. 22), and the proposed PVAm adsorbed configuration, shown in Fig. 53 (p. 140), it seems likely that a large portion of the adsorbed polyion is removed by the tensile hydrodynamic forces, while a portion of the PVAm molecules are compressed onto the surface made available by such removals.

Removal of polyions from the particle surface is facilitated by the few points of attachment and large polyion segment density forced into solution by the crowding effect of neighboring molecules. The increase in molecular extension resulting from neighboring molecules and the hydrodynamic tensile forces should facilitate degradation of the molecule. Investigations of the molecular weight distributions after shearing pH 10 flocs showed that approximately 70% of the original PVAm had degraded.

With 70% of the flocculating polyelectrolyte degraded to one-eighth of its original size, and the remaining 30% flattened out against the particle surface, reaggregation of the disrupted bridge-type flocs was only about 50% as effective as initial flocculation.

To summarize, aggregate rupture at pH 10 proceeds primarily by polyion-particle separation. About 70% of the polyion is removed from all particle surfaces, due to the paucity of electrostatic attractions. In being removed, the polymer coil becomes elongated in the hydrodynamic flow field and is degraded severely. Those polyion coils which are not separated from the

particle surface are redistributed in a configuration with reduced dimensions normal to the particle surface, and are not degraded. Because the grappling ability of the low charge density polyion is impaired by molecular degradation and reconformation, the process of reaggregation is severely inhibited. Collisions resulting in an increased particle size occur only when the kinetic energy of the individual constituents is great enough to overcome the electrical double layers, which have been reduced to some extent by adsorption of polyion segments. A schematic diagram of the proposed process is shown in Fig. 55.

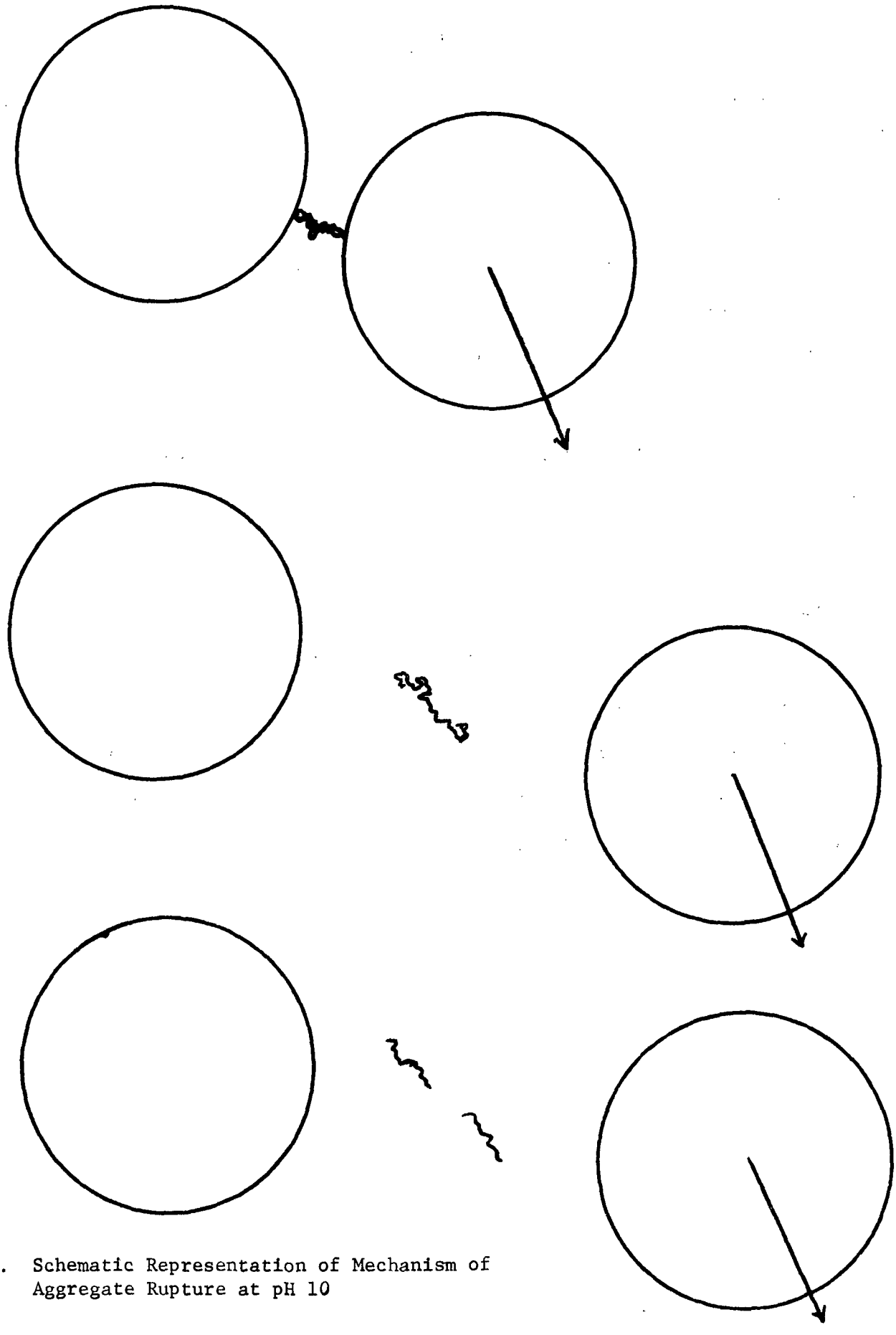

Figure 55. Schematic Representation of Mechanism of Aggregate Rupture at pH 10

CONCLUSIONS

Over a range of polymer degrees of protonation from 3-95% hydrodynamic shear-induced disruption of flocs occurs through separation at the polyion-particle interface.

In systems providing a polyelectrolyte degree of protonation greater than 10%, colloidal destabilization occurs through the formation of cationic polyion patches. The small dimension of these patches in a direction normal to the particle surface prevents molecular reorientation and/or degradation. Reaggregation of the hydrodynamically disrupted floc proceeds via the same mechanism as initial destabilization.

When the polymer is 3% protonated, polymer bridging is the dominant mechanism of initial destabilization. Hydrodynamic shear induces separation of most of the polyion from all particle surfaces. In doing so, the molecule is stretched and then ruptured by the shear. Those molecules which are in a favorable position on the particles become compressed and rearranged on the surface without molecular degradation. Reaggregation of the hydrodynamically stabilized floc is incomplete.

SUGGESTIONS FOR FUTURE RESEARCH

The present study has shown that high molecular weight polyelectrolytes form patch-type flocs when the polyion charge density is as low as 13%. A thorough investigation of the adsorption-flocculation characteristics of a polyion series with charge densities between 0 and 15% would enhance present understandings of flocculation trends and shear resistance characteristics. This would be of special significance to papermakers attempting to maximize retention on high-speed machines.

Eggert (39) has shown that for patch-forming polyelectrolytes, efficiency of initiating flocculation is dependent on patch size. A study of the relative importance of charge density and molecular weight of the flocculating polyelectrolyte in developing shear resistance and reflocculation ability would also be an important step in maximizing retention on a paper machine.

ACKNOWLEDGMENTS

The Board of Trustees and member companies are thanked for their unfailing support to The Institute of Paper Chemistry. The staff and faculty members are commended for their enthusiasm and unselfishness which has produced an enriched atmosphere for a graduate studies doctoral program.

Special recognition is due the Thesis Advisory Committee for contributing valuable time and knowledge throughout the course of this study. Robert A. Stratton served as Chairman of the Advisory Committee. I thank him sincerely for being my mentor and good friend. The exceptional contributions of Gary A. Baum and John W. Swanson as members of the Advisory Committee are appreciated. Their willingness to provide expertise during many discussions has proved invaluable.

There is a myriad of others to whom I am obliged for assistance. I am indebted to C. J. Bloys van Treslong, D. J. Dawson, and P. L. Dubin for supplying samples of polyvinylamine and knowledge of its characteristics. Special thanks are extended to John A. Carlson for operating the instruments necessary for determination of molecular weights and diffusion coefficient. The careful work of Marvin C. Filz and Paul F. Van Rossum in constructing and repairing countless mechanical devices is gratefully acknowledged.

The encouragement, patience, and enthusiasm displayed by my bride, Jan, deserves distinctive accolade. Her transcendant support through countless marathon stints in lab and at the typewriter yielded this manuscript as a token of her love.

NOMENCLATURE

C = solution ion concentration, moles/liter

D_o = diffusion coefficient at infinite time and dilution

e = elementary charge

f_n = normal stress

f_t = tangential stress

f_i = force on ith group

F = Faraday's constant

F_x = component of force in x-direction

$F(x)$ = force at point x

G = gravitational constant

G_{el} = electrostatic free energy

ID = inside diameter

k = Boltzmann constant

K = scattering coefficient

K_a = apparent equilibrium constant

L = length of a link

M = molecular weight

$M(w)$ = weight average molecular weight

MERC = 2-mercaptoethanol

n = solution ion concentration, ions/mL

n_j = number of j-tuple particles

n_k = number of k-tuple particles

n_o = number of primary particles

N = Avagadro's number

OFC = optimum flocculation concentration

OPT = *ortho*-phthalaldehyde

PACE = polyvinylacetamide

PSL = polystyrene latex

psi = pounds per square inch

PVAm = polyvinylamine

$\underline{q}$ = Stoke's friction coefficient

$\underline{Q}$ = total charge on polyion

$\underline{r}$ = radius of spherical particle

$\langle \underline{r}^2 \rangle^{\frac{1}{2}}$ = root-mean-square end-to-end displacement of macromolecule

$\underline{r}_{\underline{e}}$ = ellipsoidal axis ratio

$\underline{R}$ = radius of polyion coil

$\underline{R}_{\underline{e}}$ = radius of hydrodynamically equivalent sphere

rpm = revolutions per minute

$\underline{s}$ = number of links

$\langle \underline{s}^2 \rangle^{\frac{1}{2}}$ = root-mean-square radius of gyration

$\underline{S}$ = surface area, m^2/g

$\underline{t}$ = time, sec

$\underline{T}$ = absolute temperature

$\underline{T}_{\underline{h}}$ = half-life of colloidal suspension

$\underline{T}_{\underline{r}}$ = period of rotation

TDA = N,N,N-trimethyldodecylammonium halide

$\underline{U}$ = velocity, cm/sec

$\underline{V}$ = molar volume

$\underline{\bar{x}}$ = displacement

α = degree of ionization

ξ = $\underline{R}_{\underline{e}} / \langle \underline{s}^2 \rangle^{\frac{1}{2}}$

∂ = volume fraction of solute

Π = voltage drop, esu/cm

ε = dielectric constant of bulk solution

θ = angle of orientation to direction of flow

γ = shear strain

$\dot{\gamma}$ = shear rate, sec^{-1}

Γ = specific adsorption, mg/m^2

κ = Debye-Huckel parameter, cm^{-1}; reciprocal of double layer thickness

η = viscosity coefficient, poise

η_o = solvent viscosity, poise

$[\eta]$ = intrinsic viscosity, dl/g

η_{sp} = specific viscosity, dl/g

λ_{em} = emission wavelength

λ_{ex} = excitation wavelength

ν = electrophoretic mobility

Ω = rotational velocity, radians/sec

π = 3.1416

ℓ = solution density

ϕ = Flory's universal constant

ψ_o = surface potential

σ = surface charge density, $\mu coulombs/cm^2$

τ = turbidity

τ_{rel} = relative turbidity

ω = angular velocity, sec^{-1}

LITERATURE CITED

1. Mason, S. G., Pulp Paper Mag. Can. 51(5):93(1950).

2. Hubley, C. E., Robertson, A. A., and Mason, S. G., Can. J. Res. B28:770 (1950).

3. Mason, S. G., Tappi 37:494(1954).

4. Robertson, A. A. and Mason, S. G., Pulp Paper Mag. Can. 55(3):263(1954).

5. McKenzie, A. W., Appita 21(4):104(1968).

6. Strazdins, E., Tappi 53(1):80(1970).

7. Strazdins, E., Tappi 55(12):1691(1972).

8. Chiu, K. F. Force of fiber flocculation and fines retention provided by polymer as influenced by hydrodynamic shear. Special Studies Report, Appleton, Wis., The Institute of Paper Chemistry, 1973. 40 p.

9. Birkner, F. B. and Morgan, J., J. Am. Water Works Assoc. 60:175(1968).

10. LaMer, V. K. and Healy, T. W., Rev. Pure Appl. Chem. 13:112(1963).

11. Kasper, D. R. Theoretical and experimental investigations of the flocculation of charged particles in aqueous solutions by polyelectrolytes of opposite charge. Doctor's Dissertation. Pasadena, California, California Institute of Technology, 1971. 201 p.

12. Lindquist, G. M. The role of polyelectrolyte charge density and molecular weight on the adsorption and flocculation of colloidal silica with polyethylenimine. Doctor's Dissertation. Appleton, Wis., The Institute of Paper Chemistry, 1975. 239 p. Lindquist, G. M. and Stratton, R. A., J. Colloid Interface Sci. 55:45(1976).

13. Black, A. P., Birkner, F. B., and Morgan, J., J. Colloid Interface Sci. 21:626(1966).

14. Delahay, P. Double layer and electrode kinetics. New York, Interscience, 1965. 321 p.

15. Matijevic, E. Surface and colloid science. Vol. 7. New York, Wiley, 1974. 356 p.

16. Verwey, E. J. W. and Overbeek, J. Th. G. Theory of the stability of lyophobic colloids. New York, Elsevier, 1948. 205 p.

17. Derjaguin, B. and Landau, L., J. Expt. Theor. Phys. 11:802(1941); ibid. 15:662(1945). (Russian)

18. Adamson, A. W. Physical chemistry of surfaces. Second ed. New York, Interscience, 1967. 747 p.

19. Lifson, S. and Katchalsky, A., J. Polymer Sci. 13:43(1954).

20. Katchalsky, A., J. Polymer Sci. 7:393(1951).

21. Flory, P. J. Principles of polymer chemistry. Ithaca, New York, Cornell University Press, 1953.

22. Flory, P. J. and Fox, T. G., Jr., J. Am. Chem. Soc. 73:1904(1951).

23. Krigbaum, W. R. and Carpenter, D. K., J. Phys. Chem. 59:1166(1955).

24. Schulze, H., J. Prakt. Chem. 25(2):431(1882); ibid. 27:320(1883).

25. Hardy, W. B., Proc. Roy. Soc. (London) 66:110(1900); A. Physik. Chem. 33:385(1900).

26. Matijevic, E., J. Colloid Interface Sci. 43(2):217(1973).

27. Matijevic, E., Broadhurst, D., and Kerker, J., J. Phys. Chem. 63:1552(1959).

28. Ruehrwein, R. A. and Ward, D. W., Soil Sci. 73:485(1952).

29. Kane, J. C., LaMer, V. K., and Linford, H. B., J. Phys. Chem. 67:1977 (1963).

30. Kane, J. C., LaMer, V. K., and Linford, H. B., J. Phys. Chem. 68:2273 (1964).

31. Kane, J. C., LaMer, V. K., and Linford, H. B., J. Phys. Chem. 68:3539 (1964).

32. Kane, J. C., LaMer, V. K., and Linford, H. B., J. Am. Chem. Soc. 86: 3450(1964).

33. Slater, R. W. and Kitchener, J. A., Disc. Faraday Soc. 42:267(1966).

34. Gregory, J., Trans. Faraday Soc. 65:2260(1969).

35. Dixon, J. K. and Zielyk, M. W., Environ. Sci. Technol. 3:551(1969).

36. Heller, W. and Pugh, T. L., J. Polymer Sci. 47:203, 219(1960).

37. Gregory, J., J. Colloid Interface Sci. 42:448(1973).

38. Gregory, J., J. Colloid Interface Sci. 55:35(1975).

39. Eggert, A. R. Role of particle size of colloidal polystyrene latex in flocculation studies by a cationic polymer. Doctor's Dissertation. Appleton, Wis., The Institute of Paper Chemistry, 1976. 190 p.

40. Einstein, A., Ann. Physik. 17:549(1905); 19:289, 371(1906); 34:591(1911).

41. Jeffrey, G. B., Proc. Roy. Soc. (London) A102:161(1922).

42. Taylor, G. I., Proc. Roy. Soc. (London) A103:58(1923).

43. Eirich, F., Bunzl, M., and Magaretha, H., Kolloid A. 75:20(1936).

44. Bairstow, L., Cave, B. M., and Lang, E. D., Proc. Roy. Soc. (London) 101A:383(1923).

45. Stokes, G. G. In Berry and Swain's Mathematical and physical papers. No. 3. p. 65. Proc. Roy. Soc. (London) 102A:766(1923).

46. Taylor, G. I., Proc. Roy. Soc. (London) 138A:41(1932).

47. Stimson, M. and Jeffrey, G. B., Proc. Roy. Soc. (London) 111A:110(1926).

48. Eisenschitz, R., A. Phys. Chem. A163:133(1933).

49. Guth E., Kolloid-Z. 74:147; 75:15(1936).

50. Sadron C. H. Dilute solutions of impenetrable rigid particles. p. 131-199. In Herman's Flow properties of disperse systems. New York, Interscience, 1953.

51. Vadas, E. B., Goldsmith, H. L., and Mason, S. G., J. Colloid Interface Sci. 43(3):630(1973).

52. Goldsmith, H. L. and Mason, S. G. The microrheology of dispersions. p. 85-251, In Eirich's Rheology. Vol. 4. New York, Academic, 1967. 522 p.

53. Rumscheidt, F. D. and Mason, S. G., J. Colloid Sci. 16:238(1961).

54. Mason, S. G. and Trevelyan B. J., J. Colloid Sci. 6:345(1951).

55. Bartok, W. and Mason, S. G., J. Colloid Sci. 12:243(1957).

56. Manley, R. S. J. and Mason, S. G., J. Colloid Sci. 7:354(1952).

57. Anczurowski, E. and Mason, S. G., J. Colloid Interface Sci. 23:522(1967).

58. Forgacs, O. L. and Mason, S. G., J. Colloid Sci. 14:457(1959).

59. Goldsmith, H. L. and Mason, S. G., J. Fluid Mech. 12:88(1952).

60. Bartok, W. and Mason, S. G., J. Colloid Sci. 7:354(1952).

61. Staudinger, H. and Heuer, W. Ber. 67:1159(1934).

62. Mark, H. and Simha, R., Trans. Faraday Soc. 36:611(1940).

63. Montroll E. and Simha, R., J. Chem. Phys. 8:721(1940).

64. Simha, R., J. Appl. Phys. 12:569(1941).

65. Jellinek, H. H. G., Trans. Faraday Soc. 40:266(1944).

66. Schmid, G. and Rommel, O., Z. Electrochem. 45:659(1939).

67. Schmid, G. and Rommel, O., Z. Physik. Chem. A185:97(1939).

68. Hess, K. and Steurer, E., A. Physik. Chem. 193:234(1944).

69. Schmid, G. and Beuttenmuller, E., Z. Electrochem. 50:209(1944).

70. Frenkel, J., Acta Physic. Chim. URSS 19(1):51(1944).

71. Morris, W. J. and Schnurmann, R., Nature 160:674(1947).

72. Bestul, A. B. and Belcher, H. V., J. Appl. Phys. 24:1011(1953).

73. Bestul, A. B., J. Chem. Phys. 32:350(1960).

74. Jellinek, H. H. G. Degradation of vinyl polymers. New York, Academic Press, 1955. 329 p.

75. Porter, R. S., Cantow, M. J. R., and Johnson, J. F., J. Polymer Sci. 16:1(1967).

76. Cavalieri, L. G., J. Am. Chem. Soc. 79:5319(1957).

77. Davison, P. F., Proc. Natl. Acad. Sci. (U.S.) 45:1560(1959).

78. Hershey, A. D. and Burgi, E., J. Mol. Biol. 2:143(1960).

79. Mandell, J. D. and Hershey, A. D., Anal. Biochem. 1:66(1960).

80. Burgi, E. and Hershey, A. D., J. Mol. Biol. 41:313(1962).

81. Rubenstein, I., Thomas, C. A., Jr., and Hershey, A. D., Proc. Natl. Acad. Sci. (U.S.) 47:113(1961).

82. Levinthal, C. and Davison, P. F., J. Mol. Biol. 3:674(1961).

83. Pauling, L. The nature of the chemical bond. Ithaca, New York, Cornell Univ. Press, 1960. 644 p.

84. Johnson, W. R. and Price, C. C., J. Polymer Sci. 45:217(1960).

85. Ott, R. L., J. Polymer Sci. A2:973(1964).

86. Harrington, R. E. and Zimm, G. H., J. Phys. Chem. 69:161(1965).

87. Harrington, R. E., J. Polymer Sci. A1, 4:489(1966).

88. Yew, F. F. H. and Davidson, N., Biopolymers 6:629(1968).

89. Hlavacek, F. and Schreiber, H. P., Polymer 17(5):435(1976).

90. Cottrell, F. R., Merrill, E. W., and Smith, K. A., J. Polymer Sci. A-2, 7:1415(1969).

91. Fukutomi, T., Tsukada, M., Kakurai, T., and Noguchi, T., Polymer J. 3(6): 717(1972).

92. Nakano, A. and Minoura, Y., Macromolecules 8(5):677(1975).

93. Adam, R. E. Shear degradation of DNA. Doctor's Dissertation. San Diego, California, University of California, 1976. 96 p.

94. Ovenall, D. W., Hastings, G. W., and Allen, P. E. M., J. Polymer Sci. 33: 207(1958).

95. Allen, P. E. M., Burnett, G. M., Hastings, G. W., Melville, H. W., and Ovenall, D. M., J. Polymer Sci. 33:213(1958).

96. Mostafa, M. A. K., J. Polymer Sci. 33:295(1958).

97. Mostafa, M. A. K., J. Polymer Sci. 33:311(1958).

98. Mostafa, M. A. K., J. Polymer Sci. 33:323(1958).

99. Glynn, P. A. R., Van der Hoff, B. M. E., and Reilly, P. M., J. Macromol. Sci.-Chem. A6(8):1653(1972).

100. Glynn, P. A. R. and Van der Hoff, B. M. D., J. Macromol. Sci.-Chem. A7(8):1695(1973).

101. Weissler, A., J. Appl. Phys. 21:171(1950).

102. Weissler, A., J. Chem. Phys. 18:1513(1950).

103. Prudhomme, R. O. and Grabar, P., J. Chim. Phys. 46:667(1949).

104. Melville, H. W. and Murray, A. J. R., Trans. Faraday Soc. 46:966(1950).

105. Brett, H. W. W. and Jellinek, H. H. G., J. Polymer Sci. 13:441(1954).

106. Taylor, G. I., Proc. Roy. Soc. (London) A146:501(1934).

107. Forgacs, O. L. and Mason, S. G., J. Colloid Sci. 14:473(1959).

108. Albers, W. and Overbeek, J. Th. G., J. Colloid Sci. 15:489(1960).

109. Mitin, B. A., Kolloid Zh. 28(6):852(1966).

110. McKenzie, A. W., Appita 21(4):104(1968).

111. Strazdins, E., ACS Cellulose, Wood and Fiber Chemistry Symposium, Minneapolis, Minn., April, 1969.

112. Zia, I. Y., Cox, R., and Mason, S. G., Proc. Roy. Soc. 300A:421(1967).

113. Argaman, Y. and Kaufman, W. J., J. Sanitary Eng. Div., ASCE 96(SA2):223 (1970).

114. Patterson, I. Deagglomeration in sheared viscous liquids. Doctor's Dissertation. Montreal, Canada, McGill University, 1973. 282 p.

115. Tomi, D. and Bagster, D. F., Chem. Eng. Sci. 30:269(1975).

116. Firth, B. A. and Hunter, R. J., J. Colloid Interface Sci. 57:226(1976).

117. Goosens, J. W. S. and Luner, P., Tappi 59(2):89(1976).

118. Beck, U., Muller, F., Goosens, J. W. S., Rohleff, E., and Tretter, H., Wochbl. Papierfabr. 105:391(1977). (Transl. IPC)

119. Hart, R., Bull. Soc. Chim. Belg. 65:291(1956); 66:229(1957); J. Polymer Sci. 29:629(1958); Makromol. Chem. 32:51(1959).

120. Bloys van Treslong, C. J. and Morra, D. F. H., Recuel, J. Roy. Neth. Chem. Soc. 94(5):101(1975).

121. Dawson, D. J., Gless, R. D., and Wingard, R. E., Jr., Polymer Preprints 17(2):779(1976); J. Am. Chem. Soc. 98(19):5996(1976).

122. Hawk, G. L., Cameron, J. A., and Dufault, L. B., Prep. Biochem. 2(2): 193(1972).

123. Ottewill, R. H. and Vincent, G., J. Chem. Soc., Faraday Trans. I, 68:1533 (1972).

124. Smitham, J. B., Gibson, D. V., and Napper, D. H., J. Colloid Interface Sci. 45(1):211(1973).

125. Van den Hul, H. J. and Vanderhoff, J. W., J. Colloid Interface Sci. 28(2):336(1968).

126. Bloyd, G. E. and Bunzl, K., J. Am. Chem. Soc. 89:1776(1967).

127. Hen, J., J. Colloid Interface Sci. 49(3):425(1974).

128. Kenchington, A. W. Analytical information from titration curves. Vol. 2. p. 353-88. In Alexander and Block's Laboratory manual of analytical methods of protein chemistry. New York, Pergamon Press, 1960.

129. Tanford, C. Hydrogen ion titration curves of proteins. p. 218-65. In Shedlovsky's Electrochemistry in biology and medicine. New York, Wiley, 1955.

130. Clapp, R. R. An investigation of the relations between carboxyl content and zeta potential. Doctor's Dissertation. Appleton, Wisconsin, The Institute of Paper Chemistry, 1972. 138 p.

131. Bloys van Treslong, C. J., Private communication, 1976.

132. Dawson, D. J., Private communication, 1976.

133. Amicon Scientific Systems Publication No. 427A. Lexington, Mass., 1976.

134. Yphantis, D. A., Biochem. 3(3):297(1964).

135. Scholte, Th. G., J. Polymer Sci. A-2, 6:91, 111(1968).

136. Scholte, Th. G., Eur. Polymer J. 6:51(1970).

137. Timell, T. E., Svensk Papperstid. 57:777(1954).

138. Perrine, T. D. and Landis, W. R., J. Polymer Sci. A-1, 5:1993(1967).

139. Kimura, K., Inaki, Y., and Takemoto, K., Makromol. Chem. 175:83(1974).

140. Skoog, D. A. and West, D. M. Principles of instrumental analysis. New York, Holt, Rinehart and Winston, 1971. 710 p.

141. Becker, R. S. Theory and interpretation of fluorescence and phosphorescence. New York, Interscience, 1969. 283 p.

142. Chang, R. Basic principles of spectroscopy. New York, McGraw-Hill, 1971. 304 p.

143. Price, J. M., Kaihara, M., and Howerton, H. K., Appl. Optics 1:521(1962).

144. Aminco-Bowman Instruction No. 768-E. American Instrument Co., Inc., 8030 Georgia Ave., Silver Springs, Maryland, 1964. 61 p.

145. Udenfriend, S., Stein, S., Bohlen, P., Dairman, W., Leimgruber, W., and Weigele, M., Science 178:871(1972).

146. Benson, J. R. and Hare, P. E., Proc. Natl. Acad. Sci. (U.S.A.) 72(2): 619(1975).

147. Roth, M., Anal. Chem. 43(7):880(1971).

148. Gregory, J. and Sheiham, I., Br. Polymer J. 6(1):47(1974).

149. LaMer, V. K., Smellie, R. H., Jr., and Lee, P. K., J. Colloid Sci. 12:230(1957).

150. Dupont, P. R. Private communication, 1977.

151. Connor, P. and Ottewill, R. H., J. Colloid Interface Sci. 37(3):642 (1971).

152. Ottewill, R. H. and Shaw, J. N., J. Colloid Interface Sci. 26(1):110 (1968).

153. Henry, D. C., Proc. Roy. Soc. (London) 133:106(1931).

154. Stokes, G., Trans. Cambridge Phil. Soc. 8:287(1847).

155. Katchalsky, A., Shavit, N., and Eisenberg, H., J. Polymer Sci. 13:69 (1954).

156. Nagasawa, M., Murase, T., and Kondo, K., J. Phys. Chem. 69:4005(1965).

157. Nagasawa, M. and Holtzer, A., J. Am. Chem. Soc. 86:538(1964).

158. Katchalsky, A., Mazur, J., and Spitnik, P., J. Polymer Sci. 23:513(1957).

159. Bloys van Treslong, C. J. and Staverman, A. J., Rec. Trav. Chim. 93(6): 171(1974).

160. Kitchener, J. A. and Shepherd, E. J., J. Chem. Soc. 1956:2448.

161. Katchalsky, A., J. Polymer Sci. 7:393(1951).

162. Dubin, P. L. and Strauss, U. P., J. Phys. Chem. 74(14):2842(1970).

163. Ising, E., Z. Physik. 31:253(1925).

164. Marcus, R. A., J. Phys. Chem. 58:62(1954).

165. Lifson, S., J. Chem. Phys. 26:727(1957); 29:89(1958).

166. Overbeek, J. Th., Bull. Soc. Chim. Belges 57:252(1948).

167. Katchalsky, A. and Gillis, J., Rec. Trav. Chim. 68:879(1949).

168. Alexandrowicz, Z. and Katchalsky, A., J. Polymer Sci. A1:3231(1963).

169. Tanford, C. Physical chemistry of macromolecules. New York, Wiley, 1961. 710 p.

170. Nagasawa, M., Pure Appl. Chem. 26:519(1971).

171. Kirkwood, J. G. and Riseman, J., J. Chem. Phys. 16:565(1948).

172. Fuoss, R. M., J. Polymer Sci. 3:603(1948).

173. Shyluk, W. P., J. Appl. Polymer Sci. 8:1063(1964).

174. Oth, A. and Doty, P., J. Phys. Chem. 56:43(1952).

175. Basu, S. and Das Gupta, P. C., J. Colloid Sci. 7:53(1952).

176. Alexander, P. and Hitch, S. F., Biochem. Biophys. Acta 9:229(1952).

177. Rosen, B., Kamath, P., and Eirich, F., Disc. Faraday Soc. 11:135(1951).

178. Kurucsev, T., Rev. Pure Appl. Chem. 14:147(1964).

179. Fujita, H., Mitsuhashi, H., and Homma, T., J. Colloid Sci. 9:466(1954).

180. Eisenberg, H. and Pouyet, J., J. Polymer Sci. 13:85(1954).

181. Mock, R. A. and Marshall, C. A., J. Polymer Sci. 13:263(1954).

182. Conway, B. E., J. Polymer Sci. 18:257(1954).

183. Strauss, U. P. and Fuoss, R. M., J. Polymer Sci. 8:593(1953).

184. Alfrey, T., Jr. and Morawetz, H., J. Am. Chem. Soc. 74:436(1952).

185. Butler, J. A., Robins, A. G., and Shooter, K. V., Proc. Roy. Soc. A241: 299(1957).

186. Heller, W., J. Colloid Sci. 9:547(1954).

187. Jordan, D. O. and Kurucsev, T., Polymer 1:185(1960).

188. Hermans, J. J. and Pals, D. T. F., J. Polymer Sci. 6:733(1950).

189. Darskus, R. L., Jordan, D. L., Kurucsev, T., and Martin, M. L., J. Polymer Sci. A3:1941(1965).

190. Katchalsky, A., J. Polymer Sci. 12:159(1954).

191. Fuoss, R. J. and Cathers, G. I., J. Polymer Sci. 4:97(1949).

192. Shore, P. A., Burkhalter, A., and Cohn, V. H., Jr., J. Pharm. Expt. Therap. 127:182(1959).

193. Marton, L. J., Private communication, 1977.

194. Seekles, L., Rec. Trav. Chim. 42:97(1924).

195. Thiele, J. and Winter, E., Ann. 311:341(1900).

196. Bird, R. G., Stewart, W. E., and Lightfoot, E. N. Transport phenomena. New York, Wiley, 1960. 780 p.

197. Einstein, A., Ann. Physik. 19:371(1906); as cited in Ref. 198.

198. Overbeek, J. Th. G. Kinetics of flocculation. p. Vol. I. p. 278. In Kruyt's Colloid science. New York, Elsevier, 1952. 389 p.

199. Smoluchowski, M. v., Physik. Z. 17:557, 585(1916); Z. Physik. Chem. 92: 129(1917); as cited in Ref. 198.

200. Uriarte, F. A. Kinetics of colloid aggregation. I. Coagulation rate constants by turbidimetry. II. Kinetics of colloid flocculation using polyelectrolytes. Doctor's Dissertation. Pittsburgh, Penn., Carnegie-Mellon University, 1971. 351 p.

201. Mie, G., Ann. Physik. 25:377(1908); as cited in Ref. 205.

202. Grumprecht, R. and Sliepcevich, --. Tables of scattering functions for spherical particles. Ann Arbor, Mich., Eng. Res. Inst., University of Michigan, 1951.

203. Lowan, A. N., Natl. Bur. Standards, AMS-4, Washington, D.C., 1948.

204. Meehan, E. J. and Hugus, A. A., J. Opt. Soc. Am. 51:260(1961).

205. Fair, G. M. and Gemmell, R. S., J. Colloid Sci. 19:360(1964).

206. Van Vliet, T. and Lyklema, J., J. Colloid Interface Sci. 63(1):97(1978).

207. Franco, R. P. and Stratton, R. A., to be published.

208. Parker, D. S., Kaufman, W. J. and Jenkins, D., J. Sanitary Eng. Div., ASCE, SAI:79(1972).

209. Mason, S. G. Plenary lecture presented at the IUPAC Conference on Colloids and Interfaces/50th Symposium of ACS Div. of Colloid and Surface Chemistry, San Juan, Porto Rico, June 21, 1976. Orthokinetic phenomena in disperse systems. p. 293-303. In Kerker, Zettlemoyer, and Rowell's Colloid and Interface Science. New York, Academic Press, 1977.

210. McCrackin, F. L., J. Appl. Polymer Sci. 21:191(1977).

211. Ring, G., Personal communication, 1978.

212. Abdel-Alim, A. H. and Hamielec, A. E., J. Appl. Polymer Sci. 17:3769 (1973).

213. Beckman Instruments, Inc., Scientific and Process Instruments Division, Instructions 1553-D, 1967.

214. Eirich, F. R., J. Colloid Interface Sci. 58:423(1977).

215. Chan, D., Mitchell, D. J., Ninham, B. W. and White, L. R., J. Chem. Soc., Faraday Trans. II, 71:235(1975).

216. Healy, T. W. Adsorption-flocculation reactions of macromolecules at the solid-liquid interface. Doctor's Dissertation. New York, Columbia University, 1963. 75 p.

217. Brandrup, J. and Immergut, E. H., eds. Polymer Handbook. p. iv-64. New York, Wiley, 1975.

218. Bauer, N. and Lewin, S. Z. In Weissberger's Techniques of chemistry. Vol. I. Part IV. New York, Wiley, 1972. 561 p.

219. Kindler, W. A. Adsorption kinetics in the polyethylenimine-cellulose fiber system. Doctor's Dissertation. Appleton, Wis., The Institute of Paper Chemistry, Jan. 1971. 136 p.

220. Gosting, L. J. Measurement and interpretation of diffusion coefficients of proteins. Vol. XI. p. 429. In Advances in protein chemistry. New York, Academic Press, 1956.

APPENDIX I

MOLECULAR WEIGHT DETERMINATION

The weight-average molecular weights of several PVAm fractions were determined by sedimentation equilibrium analyses (134-136). All samples were analyzed in 0.1N NaCl at pH 8.0, using a Beckman Spinco Model E ultracentrifuge with Rayleigh optics.

Weight-averaged molecular weight may be determined from the concentration distribution of polymer in a centrifugal field using the following classical equation:

$$M(w) = [2RT/\omega^2(1 - \bar{v}\rho)][d(\ln C)/d(r^2)], \qquad (60)$$

where ω = angular velocity of the rotor

$\bar{v}$ = partial specific volume of the solute (Appendix II)

ρ = solvent density

C = solute concentration at a distance r from the axis of rotation

A plot of ln C versus r^2 produces a slope proportional to molecular weight. For an ideal monodispersed system this plot will be perfectly linear. A nonideal monodispersed system produces a line of decreasing slope, while a polydispersed system exhibits a line of increasing slope with respect to r^2.

APPENDIX II

PARTIAL SPECIFIC VOLUME OF POLYVINYLAMINE

The partial specific volume, $\bar{v}_2$, of a polymer is required for calculating molecular weights from ultracentrifugation data. The most convenient way to evaluate $\bar{v}$ is by first determining

$$\bar{v}_2^* = 1/g_2 \frac{\rho_1 - g_1 \rho_{12}}{\rho_1 \rho_{12}} , \tag{61}$$

where ρ_1 and ρ_{12} are the densities of solvent and solution, respectively

$g_1 = m_1/(m_1 + m_2)$

$g_2 = m_2/(m_1 + m_2)$

m_1 and m_2 = respective masses of solvent and polymer (217)

From Equation (61) it can be seen the $\bar{v}_2^*$ can be determined directly from measurements of ρ_1 and ρ_{12}. Densities were determined pycnometrically according to the method described by Bauer and Lewin (218). Measurements were made in a 5.5 mL Lipkin pycnometer at the same solvent conditions and temperature used for the sedimentation experiment. Calibration of the pycnometer was performed with triply-distilled water, assuming a density of 0.99707 g/cm^3. The density of 0.1N NaCl at 25.00° was determined to be 1.0010 g/cm^3, agreeing with that determined by Kindler (219).

Expressing the total volume of the polymer-salt solution as

$$v_{12} = m_1 \bar{v}_1 + m_2 \bar{v}_2^* , \tag{62}$$

where $\bar{v}_1$ is the partial specific volume of solvent, and the quantity $\bar{v}_2^*$ contains the parameters of nonideal mixing of both solvent and polymer (217). Partial specific volume may be determined from apparent specific volume by (217)

$$\bar{v}_2 = \bar{v}_2^* + g_1 g_2 \frac{\partial \bar{v}_2^*}{\partial g_2} \tag{63}$$

The apparent specific volume of PVAm at infinite dilution was determined to be 0.561 cm^3/g.

APPENDIX III

DIFFUSION COEFFICIENT OF POLYVINYLAMINE

The diffusion coefficient of PVAm in 0.1N NaCl was calculated with data obtained from a free-diffusion experiment. A boundary was created between two solutions having different concentrations of the polymer. The concentration of solute as a function of distance from the initial boundary was observed over a period of time. Calculation of the diffusion coefficient was performed with the aid of a computer program written by Kindler (219). A comprehensive review of the analysis of diffusion coefficients is given by Gosting (220).

A Beckman Spinco Model E ultracentrifuge was used for the diffusion coefficient determination. The difference in refractive index between solute and solvent produced an interference fringe pattern related to the solute distribution in the triple-sector cell.

The information gathered from the photographic plates included the total number of fringes, the horizontal position of each fringe, and the suitable base-line correction. Recording of these data was performed on an X-Y micro-comparator.

APPENDIX IV

SYNTHESIS OF N,N,N-TRIMETHYLDODECYLAMMONIUM IODIDE

Preparation of N,N,N-trimethyldodecylammonium iodide (DTA) was carried out in two batches, tagged and untagged. In the first batch, ^{12}C-methyl iodide (Aldrich Chemical Co.) was used as the quaternizing agent for the dimethyl amine (DDA), obtained from K and K Laboratories, Inc. In the second batch, ^{14}C-labeled surface active agent was prepared using ^{14}C-methyl iodide with an activity of 0.1 mCi, obtained from International Chemical and Nuclear Corporation in a sealed ampul.

Nonradioactive DTA was prepared by reacting a 5% (molar) excess of DDA with methyl iodide in acetone for 4 hours at room temperature. Precipitation of the quaternary salt commenced within a few minutes of the initiation of the reaction. The mixture was then poured onto petroleum ether (30-60°) and centrifuged at 15,000 rpm for 15 min. The precipitate was washed an additional three times with petroleum ether before drying *in vacuo* at room temperature for 8-12 hours.

Radioactive DTA was prepared by cooling all components to 3°C before introducing DDA in acetone to the ^{14}C-methyl iodide. Mixing was initiated after the amine-acetone solution was placed above the seal, which was subsequently perforated. Contents were transferred to a 15 mL beaker with three 2-mL washings of the ampul. The mixture was stirred magnetically for 48 hours at 3°C and an additional 2 hours at room temperature. The mixture was then centrifuged for 15 min at 15°C. The supernatant was removed by heating gently (60°C). Three petroleum ether washings were then performed before drying *in vacuo* at room temperature for 24 hours. Yield was 98.5%.

APPENDIX V

LIQUID SCINTILLATION COUNTING

Concentration of dilute solutions of labeled TDA were determined by liquid scintillation counting. A Beckman Liquid Scintillation System, LS-100, was used for this work. An advantage of the Beckman instrument is that there is no need to cool samples, thus eliminating the need for an antifreeze agent in the scintillation counting cocktail. Samples were counted in low-^{40}K glass vials.

The scintillation cocktail used was described in the LS-100 operation manual. It consisted of 5 g of PPO (2,5-diphenyloxazole) and 100 g of naphthalene per liter of 1,4-dioxane. 0.5 mL of sample was mixed with 10 mL of this fluor.

Because ionic strength was essentially constant for all experiments, a calibration curve for counting efficiency was unnecessary. A direct data readout (DDR) module allowed for automatic computation of the counting efficiency of each sample.

Samples were each counted for a total of 1,000,000 counts, providing a number statistically required to obtain an error of no more than 0.2%.